

**BINDING KINETICS OF MONOCLONAL ANTIBODIES  
AND FLUOROQUINOLONE DERIVATIVES**



A Thesis Submitted in Partial Fulfillment of the Requirements  
for the Degree of Master of Science in Biotechnology  
Common Course  
FACULTY OF SCIENCE  
Chulalongkorn University  
Academic Year 2019  
Copyright of Chulalongkorn University

จลนพลศาสตร์ของโมโนโคลนอลแอนติบอดีและอนุพันธ์ของฟลูออโรควิโนโลน



วิทยานิพนธ์นี้เป็นส่วนหนึ่งของการศึกษาตามหลักสูตรปริญญาวิทยาศาสตรมหาบัณฑิต

สาขาวิชาเทคโนโลยีชีวภาพ ไม่สังกัดภาควิชา/เทียบเท่า

คณะวิทยาศาสตร์ จุฬาลงกรณ์มหาวิทยาลัย

ปีการศึกษา 2562

ลิขสิทธิ์ของจุฬาลงกรณ์มหาวิทยาลัย

Thesis Title	BINDING KINETICS OF MONOCLONAL ANTIBODIES AND FLUOROQUINOLONE DERIVATIVES
By	Miss Patamalai Boonserm
Field of Study	Biotechnology
Thesis Advisor	Assistant Professor SARINTIP SOOKSAI, Ph.D.
Thesis Co Advisor	Associate Professor KITTINAN KOMOLPIS, Ph.D. Assistant Professor Pongsak Khunrae, Ph.D.

---

Accepted by the FACULTY OF SCIENCE, Chulalongkorn University in  
Partial Fulfillment of the Requirement for the Master of Science

..... Dean of the FACULTY OF  
SCIENCE  
(Professor POLKIT SANGVANICH, Ph.D.)

THESIS COMMITTEE

..... Chairman  
(Associate Professor NATTAYA  
NGAMROJANAVANICH, Ph.D.)

..... Thesis Advisor  
(Assistant Professor SARINTIP SOOKSAI, Ph.D.)

..... Thesis Co-Advisor  
(Associate Professor KITTINAN KOMOLPIS, Ph.D.)

..... Thesis Co-Advisor  
(Assistant Professor Pongsak Khunrae, Ph.D.)

..... Examiner  
(Associate Professor APHICHART KARNCHANATAT,  
Ph.D.)

..... External Examiner  
(Ratthaphol Charlermroj, Ph.D.)

บัทมาลัย บุญเสริม : จลนพลศาสตร์ของโมโนโคลนอลแอนติบอดีและอนุพันธ์ของฟลูออโรควิโนโลน. ( BINDING KINETICS OF MONOCLONAL ANTIBODIES AND FLUOROQUINOLONE DERIVATIVES) อ.ที่ปรึกษาหลัก : ผศ. ดร.ศรินทร์พ สุกใส, อ.ที่ปรึกษาร่วม : รศ. ดร.กิตตินันท์ โกมลภิส, ผศ. ดร.พงศ์ศักดิ์ ขุนแร่

ฟลูออโรควิโนโลน (FQs) เป็นยาปฏิชีวนะที่ใช้กันอย่างแพร่หลายในการยับยั้งเชื้อแบคทีเรียแกรมบวกและแกรมลบ ยาปฏิชีวนะในกลุ่มฟลูออโรควิโนโลนที่นิยมใช้ในทางปศุสัตว์และการประมง ได้แก่ นอร์ฟลอกซาซิน เอนโรฟลอกซาซิน ซิโอฟลอกซาซิน และโอฟลอกซาซิน เป็นต้น อย่างไรก็ตาม การใช้อย่างไม่ถูกวิธีอาจทำให้เกิดการดื้อยาในเนื้อสัตว์ที่นำมาบริโภค ดังนั้นเพื่อป้องกันผู้บริโภคจากการได้รับยาปฏิชีวนะที่ตกค้างในอาหาร และป้องกันการเกิดการดื้อยาของเชื้อก่อโรคนั้น จึงได้มีการกำหนดปริมาณสารตกค้างในอาหารในหลายประเทศ ซึ่งโดยทั่วไป วิธีเอนไซม์ลิงค์อิมมูโนซอร์เบนต์แอสเสย์ (ELISA) เป็นที่ยอมรับและถูกนำมาใช้กันอย่างกว้างขวางในการตรวจคัดกรองเพื่อตรวจสอบหาสารตกค้างในเนื้อสัตว์ ในการศึกษาครั้งนี้ โมโนโคลนอลแอนติบอดี ที่จำเพาะต่อเอนโรฟลอกซาซิน (mAb Nor132 และ mAb Nor155) และเอนโรฟลอกซาซิน (mAb Enro44 และ mAb Enro48) โดยโมโนโคลนอลแอนติบอดีทั้ง 4 โคลน ถูกนำมาตรวจสอบความไวด้วย antigen-captured indirect competitive ELISA โดยมีค่าความเข้มข้นที่ทำให้ค่าการดูดกลืนแสงลดลง 50 เปอร์เซ็นต์ ( $IC_{50}$ ) ที่ 0.1388 ไมโครกรัมต่อมิลลิลิตร, 0.0511 ไมโครกรัมต่อมิลลิลิตร, 0.2369 ไมโครกรัมต่อมิลลิลิตร และ 0.3320 ไมโครกรัมต่อมิลลิลิตร ตามลำดับ ในส่วนความจำเพาะได้ถูกศึกษาและแสดงค่าในรูปของร้อยละการทำปฏิกิริยาข้าม พบว่า mAb Nor132 และ mAb Nor155 สามารถเกิดปฏิกิริยาข้ามกับยาในกลุ่ม FQs มีค่าอยู่ในช่วงร้อยละ 21.79-89.34 แต่ mAb Enro44 และ mAb Enro48 มีความจำเพาะต่อเอนโรฟลอกซาซินเท่านั้น นอกจากนี้ จลนพลศาสตร์ของอันตรกิริยาการจับระหว่างโมโนโคลนอลแอนติบอดีต่อยาที่จำเพาะในกลุ่ม FQs ( $K_D$ ) ถูกศึกษาโดยใช้หลักการตรวจวัดด้วยเซอร์เฟสพลาสมอนเรโซแนนซ์ (SPR) พบว่า mAb Nor132 และ mAb Nor155 มีความสามารถในการจับต่อเอนโรฟลอกซาซินดีกว่าซิโอฟลอกซาซิน ส่วน ประสิทธิภาพการจับของ mAb Enro44 ต่อเอนโรฟลอกซาซินต่อ ดีกว่า mAb Enro48 จากการศึกษาการจำลองรูปแบบการเข้าจับระหว่างยา FQs กับโมโนโคลนอลแอนติบอดีด้วยเทคนิค antigen-antibody docking โดยใช้ Autodock vina ผลการศึกษาพบว่า FQs มีอันตรกิริยาที่สำคัญกับโมโนโคลนอลแอนติบอดีทั้ง 4 โคลน โดยเฉพาะที่กรดอะมิโน บริเวณ pocket site และบริเวณใกล้เคียง ของ CDRs ซึ่งเป็นบริเวณที่เกี่ยวข้องกับการจับจำเพาะของแอนติบอดีและแอนติเจน ด้วยพันธะไฮโดรเจน จากผลการทดลอง ความไวและความสามารถในการจับของ mAb Nor155 สูงกว่า mAb Nor132 เช่นเดียวกับ mAb Enro44 เมื่อเปรียบเทียบกับ mAb Enro48 ดังนั้น mAb Nor155 และ mAb Enro44 มีความเหมาะสมสำหรับใช้ตรวจหา นอร์ฟลอกซาซิน และ เอนโรฟลอกซาซิน ในผลิตภัณฑ์อาหาร ตามลำดับ

จุฬาลงกรณ์มหาวิทยาลัย  
CHULALONGKORN UNIVERSITY

สาขาวิชา เทคโนโลยีชีวภาพ  
ปีการศึกษา 2562

ลายมือชื่อนิสิต .....  
ลายมือชื่อ อ.ที่ปรึกษาหลัก .....  
ลายมือชื่อ อ.ที่ปรึกษาร่วม .....  
ลายมือชื่อ อ.ที่ปรึกษาร่วม .....

## 6071962023 : MAJOR BIOTECHNOLOGY

KEYWORD: fluoroquinolones, surface plasmon resonance, monoclonal antibody

Patamalai Boonserm : BINDING KINETICS OF MONOCLONAL ANTIBODIES AND FLUOROQUINOLONE DERIVATIVES. Advisor: Asst. Prof. SARINTIP SOOKSAI, Ph.D. Co-advisor: Assoc. Prof. KITTINAN KOMOLPIS, Ph.D., Asst. Prof. Pongsak Khunrae, Ph.D.

Fluoroquinolones (FQs) are a group of antibiotics which have been extensively used against both Gram-negative and Gram-positive bacteria. Some of FQs antibiotics commonly used in livestock and fishery include norfloxacin, enrofloxacin, ciprofloxacin, and ofloxacin. However, misuse of these antibiotics may cause drug residues in food products. Therefore, to prevent consumers from getting residual antibiotics in food and the drug resistance of pathogens in humans. As a result, surveillance detection program of these drug residues must be in practice to ensure safety of the consumers in many countries. In general, detections based on immunological method include enzyme-linked immunosorbent assay (ELISA) has been widely used as a screening tool in food safety applications. In this research, sensitivity of four monoclonal antibodies, mAbs against norfloxacin (mAb Nor132 and mAb Nor155), and mAbs against enrofloxacin (mAb Enro44 and Enro48) were quantified by an antigen-captured indirect competitive ELISA. The sensitivity in term of 50% inhibition concentration ( $IC_{50}$ ) of mAb Nor132, mAb Nor155, mAb Enro44, and mAb Enro48 were found to be 0.1388  $\mu\text{g/ml}$ , 0.0511  $\mu\text{g/ml}$ , 0.2369  $\mu\text{g/ml}$ , and 0.3320  $\mu\text{g/ml}$  respectively. Moreover, the specificity of mAbs were examined in term of % cross-reactivity. The mAb Nor132 and mAb Nor155 are highly specificity for norfloxacin and several drugs in FQs group in range of 21.79-89.34% but mAb Enro44 and mAb Enro48 are highly specificity only enrofloxacin. Then, the kinetic binding ( $K_D$ ) of four mAbs and drugs were studied by surface plasmon resonance (SPR). The result showed that mAb Nor155 bound to norfloxacin and ciprofloxacin better than mAb Nor132 did. As mAb Enro44 bound to enrofloxacin better than mAb Enro48. To investigate *In silico* binding between FQ drugs and mAbs by using antigen-antibody docking technique, Autodock vina program. The docking results expose significant interactions between the FQ dugs and four mAbs, especially with amino acid residues at the pocket site or nearby the area CDRs of mAbs, the region of mAb recognizes the antigen, with hydrogen bonds. The results indicated that sensitivity and affinity of mAb Nor155 were higher than those of mAb Nor132 as the mAb Enro44 compared to the mAb Enro48. These suggested that mAb Nor155 and mAb Enro44 were suitable for using in the development of norfloxacin and enrofloxacin detection in food products, respectively.

Field of Study: Biotechnology  
Academic Year: 2019

Student's Signature .....  
Advisor's Signature .....  
Co-advisor's Signature .....  
Co-advisor's Signature .....

## ACKNOWLEDGEMENTS

I would like to express my special thanks of gratitude to my advisor Assistant Professor Dr. Sarintip Sooksai as well as my co-advisors Associated Professor Dr. Kittinan Komolpis and Assistant Professor Pongsak Khunrae who gave me the golden opportunity to do this wonderful project on the topic “Binding Kinetics of Monoclonal Antibodies and Fluoroquinolone Derivatives”. Whenever I ran into a trouble spot or had a question about my research or writing, they always helped me in solving the problems. I have learnt so many new things from them.

I also would like to thank Associated Professor Dr. Nattaya Ngamrojanavanich, Associated Professor Dr. Aphichart Karnchanatat, and Dr. Rattaphol Charlermroj for serving as the committee and their careful reviews of the master thesis.

I would also like to thank the experts, researchers, staffs, especially Songchan Puthong, Thanaporn Wichai, and Sajee Noitang at the Institute of Biotechnology and Genetic Engineering, and the Program in Biotechnology, Faculty of Science, Chulalongkorn University who were involved in the validation survey for this research project. Without their passionate participation and input, the validation survey could not have been successfully conducted.

I would like to thank the Systems Biology Research Center, Faculty of Medicine, Chulalongkorn University and the Laboratory for Protein Research, Department of Microbiology, King Mongkut's University of Technology Thonburi for permission to use their SPR-instrument and I am thankful to Thittaya Audomsun, Tossapon Wongtangprasert, Nichapha Chinprasit, Harit Boonyaputthikul, and Apichet Ngenyoung. I am grateful to them for very valuable comments and help on this thesis.

I would like to thank Ratchadaphiseksomphot Endowment Fund of Chulalongkorn University and The National Research University Development Project (CUGR\_62\_33\_61\_01), The Office of the Higher Education Commission, Thailand for their financial support of this research.

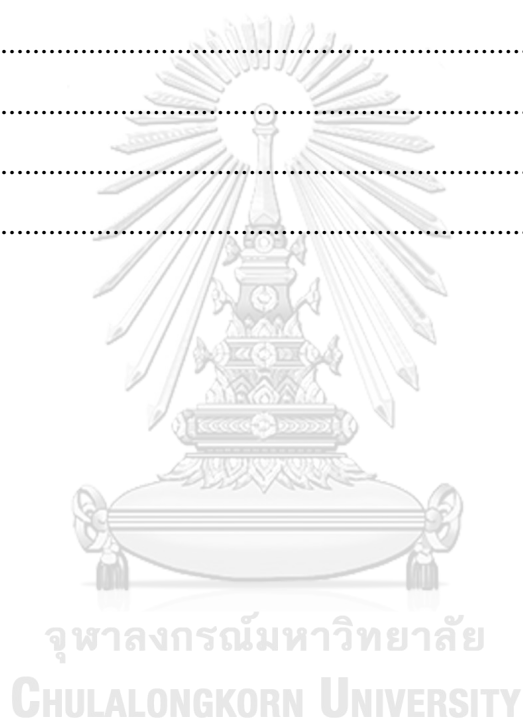
Finally, I must express my very profound gratitude to my parents and beloved friends for providing me with endless support and continuous encouragement. This accomplishment would not have been possible without them. Thank you.

Patamalai Boonserm

## TABLE OF CONTENTS

	<b>Page</b>
ABSTRACT (THAI) .....	iii
ABSTRACT (ENGLISH).....	iv
ACKNOWLEDGEMENTS.....	v
TABLE OF CONTENTS.....	vi
LIST OF TABLES.....	viii
LIST OF FIGURES .....	ix
LIST OF ABBREVIATIONS.....	xii
CHAPTER I INTRODUCTION.....	1
1.1 Importance and Rationale.....	1
1.2 Objectives .....	2
1.3 Expected Beneficial Outcomes.....	3
CHAPTER II THEORETICAL BACKGROUND AND LITERATURE REVIEWS..	4
2.1 Antibody.....	4
2.2 Fluoroquinolone .....	6
2.3 Enzyme-Linked Immunosorbent Assay (ELISA) .....	9
2.4 Surface Plasmon Resonance .....	13
2.5 Circular Dichroism Spectroscopy.....	15
CHAPTER III MATERIALS AND METHODS .....	19
3.1 Chemicals and Reagents .....	19
3.2 Equipment and Supplies .....	20
3.3 Methods .....	21
CHAPTER IV RESULTS AND DISCUSSION.....	27
4.1 Conjugation of Drug-OVA .....	27
4.2 Production and Purification of MAb .....	27

4.3 Sensitivity and Specificity of The Monoclonal Antibody.....	29
4.4 Binding Affinities and Kinetic Analysis of Drug-mAbs Using SPR .....	33
4.5 Conformational Analysis of MAbs Using CD Spectroscopy .....	44
4.7 Molecular Docking .....	48
CHAPTER V CONCLUSIONS AND SUGGESTION.....	59
5.1 Conclusion .....	59
5.2 Suggestions .....	59
REFERENCES .....	60
APPENDICES .....	67
APPENDIX A.....	68
APPENDIX B .....	73
VITA.....	81





## LIST OF TABLES

Table		Page
4.1	Protein concentration of drugs by BCA assay.....	27
4.2	Protein concentrations of purified mAbs by BCA assaylll.....	28
4.3	IC <sub>50</sub> and Cross-reactivity of monoclonal antibody with variou.s competitors by ELISA.....	32
4.4	Equilibrium dissociation constants and rate constants (ka and k <sub>d</sub> ) measured for mAbs and drug-OVA by Biacore.....	44
4.5	Secondary structure analysis of mAb Nor155 in different buffer.....	46
4.6	Prediction of the mAbs structure with SWISS-MODEL program.....	48
4.7	Docking scoring function and interaction bonds of mAbs and target fluoroquinolone molecules.....	58
B-1	Concentration of standard BSA and absorbance at 560 nm for determination for NOR-OVA and ENRO-OVA concentration.....	67
B-2	Concentration of standard BSA and absorbance at 560 nm for determination for CIPRO-OVA and OFLOX-OVA concentration.....	68
B-3	Concentration and absorbance at 560 nm of BSA standard for the determination of mAbs concentration.....	69

## LIST OF FIGURES

Figure		Page
2.1	This diagram illustrates the process for harvesting polyclonal antibodies produced in response to an antigen.....	5
2.2	Illustrates the principle of direct ELISA format.....	10
2.3	Illustrates the principle of indirect ELISA format.....	11
2.4	Illustrates the principle of a sandwich ELISA format.....	11
2.5	Illustrates the principle of competitive ELISA format.....	12
2.6	Illustration of Surface Plasmon Resonance. The binding of analyte shifts the SPR angle.....	14
2.7	The sensograms of analyte-ligand binding.....	15
2.8	The circular dichroism (CD) for various secondary structures: $\alpha$ -helix (solid line), antiparallel $\beta$ -sheet (bold dashed line), $\beta$ -turn (dotted line), and random coil (dashed line).....	16
2.9	Components in molecular docking.....	17
2.10	A typical docking workflow for protein-ligand docking.....	18
4.1	15% SDS-PAGE analysis of purified mAbs were loaded 20 $\mu$ l/well at a constant current of 25 mA per gel with 1 $\times$ Tris-glycine-SDS running buffer; standard protein marker (lane1), mAb Nor132 (lane2), mAb Nor155 (lane3), mAb Enro44 (lane4), and mAb Enro48 (lane5).....	28
4.2	Affinity Constant curves of mAbs binding with drugs-OVA immobilize on surface of ELISA plate 3 $\mu$ g/ml; a) NOR-OVA, b) ENRO-OVA, c) CIPRO-OVA, and d) OFLOX-OVA.....	29
4.3	Some of fluoroquinolone Chemical structure of norfloxacin, ciprofloxacin enrofloxacin and ofloxacin.....	30
4.4	Calibration curves of icELISA base on NOR-OVA or ENRO-OVA for 4FQs. B is the absorbance of a tested free drugs; norfloxacin: enrofloxacin: ciprofloxacin: ofloxacin and B <sub>0</sub> is the absorbance of buffer without free drugs. The standard curve was established by different concentrations of norfloxacin or enrofloxacin versus the values of B/B <sub>0</sub> .....	31

4.5	Illustrated data sets (color lines) for the SPR kinetic analysis of NOR-OVA with mAb Nor132 interactions. Different concentrations of mAb Nor132 were flow over the immobilized NOR-OVA. The association and dissociation times were 400 and 600 s, respectively, at a constant flow rate of 30 $\mu$ l/min. Black lines show the global fits of the data to a) 1:1 binding model and b) Bivalent binding model.....	37
4.6	Kinetic analysis of NOR-OVA with mAb Nor155. Different concentrations of mAb Nor155 were flow over the immobilized NOR-OVA. The association and dissociation times were 400 and 600 s at a constant flow rate of 10 $\mu$ l/min. The response data were fit to Bivalent binding model (black lines).....	38
4.7	SPR sensorgrams of mAbs at two fold concentrations 15.625-500 nM; a) mAb Nor132 and b) mAb Nor155 on CM5 sensor chip which CIPRO-OVA was immobilized, and the association and dissociation times were 400 and 600 s at a constant flow rate of 10 $\mu$ l/min. Data fitted using Bivalent binding model (black lines).....	40
4.8	Kinetic analysis of a) mAb Enro44 and b) mAb Enro48 with ENRO-OVA using HBS-EP+ buffer, the association and dissociation times were 400 and 600 s at a constant flow rate of 10 $\mu$ l/min. Data fitted using Bivalent binding model (black lines).....	41
4.9	Buffer scouting for binding of ENRO-OVA with mAb Enro44 (left) and mAb Enro48 (right). The mAbs at concentration 1 $\mu$ M was diluted in different buffers; 150 mM NaCl+P20 (red), HBS-EP+ (green), PBS (blue), and PBS+P20 (pink). The association and dissociation times were 400 and 120 s at a constant flow rate of 10 $\mu$ l/min.....	42
4.10	Kinetic analysis of a) mAb Enro44 and b) mAb Enro48 with ENRO-OVA using PBS+P20 buffer, the association and dissociation times were 400 and 600 s at a constant flow rate of 10 $\mu$ l/min. Data fitted using Bivalent binding model (black lines).....	43
4.11	The far-UV CD spectra at 4 $^{\circ}$ C for mAb Nor155 in different buffers...	45

4.12	Sequence alignment of VH and VL of mAbs with the template; Nor132 (VH:1a0q.1.B, VL:2y6s.1.A), Nor155 (VH:5do2.1.B, VL:4qnp.1.C) (VH:2aab.1.B, VL:4amk.1.B), Enro48 (VH:2r29.1.B, VL:2y6s.1.A), and the CDR1 (orange), CDR2 (yellow) and CDR3 (pink).....	47
4.13	The structure of a typical antibody is composed of two heavy chains and two light chains linked by disulfide bonds which each heavy chain is linked to a light chain and the two heavy chains are linked together.....	49
4.14	Showing the docked FQ molecules include norfloxacin (cyan), enrofloxacin (magenta), ciprofloxacin (yellow), and ofloxacin (salmon pink) with mAbs; a) mAb Nor132, b) mAb Nor155, c) mAb Enro44, and d) mAb Enro48. Image created in PyMOL.....	50
4.15	Schematic diagram of the binding for mAb Nor132 and a target FQ molecule; a) norfloxacin, b) enrofloxacin, c) ciprofloxacin, and d) ofloxacin.....	52
4.16	Schematic diagram of the binding for mAb Nor155 and a target FQ molecule; a) norfloxacin, b) enrofloxacin, c) ciprofloxacin, and d) ofloxacin.....	53
4.17	Schematic diagram of the binding for mAb Enro44 and a target FQ molecule; a) norfloxacin, b) enrofloxacin, c) ciprofloxacin, and d) ofloxacin.....	56
4.18	Schematic diagram of the binding for mAb Enro48 and a target FQ molecule; a) norfloxacin, b) enrofloxacin, c) ciprofloxacin, and d) ofloxacin.....	57
B-1	Standard curve of BSA by BCA protein assay for detection NOR- OVA and ENRO-OVA concentration.....	67
B-2	Standard curve of BSA by BCA protein assay for detection CIPRO- OVA and OFLOX-OVA concentration.....	68
B-3	Standard curve of BSA by BCA protein assay for detection mAbs concentration.....	69

## LIST OF ABBREVIATIONS

%	Percentage
%CR	Percentage of cross-reactivity
°C	Degree Celsius
µg	Microgram
µl	Microliter
A	Absorbance
Ab	Antibody
Ag	Antigen
BCA assay	Bicinchonic acid assay
BSA	Bovine serum albumin
CDR	Complementarity-determining region
CH	Constance region of heavy chain
CL	Constance region of light chain
Da	Dalton
DMF	Dimethylformamide
DMSO	Dimethyl sulfoxide
EDC	1-Ethyl-3-(3-dimethylaminopropyl)-carbodiimide hydrochloride
ELISA	Enzyme-linked immunosorbent assay
FCS	Fetal calf serum
g	Gram
GAM	Goat anti mouse IgG
HCDR	Heavy chain complementarity-determining region
hr	Hour
HRP	Horseradish peroxidase
IC50	50% Inhibition concentration
icELISA-GAM	Indirect competitive ELISA using GAM-HRP
iELISA	Indirect ELISA
IgG	Immunoglobulin G
ka	Association rate constant (M <sup>-1</sup> s <sup>-1</sup> )
kd	Dissociation rate constant (s <sup>-1</sup> )

KD	Equilibrium dissociation constant (M)
kDa	Kilo Dalton
LCDR	Light chain complementarity-determining region
LOD	Limit of detection
M	Molar
mAb	Monoclonal antibody
mg	Milligram
MRLS	Maximum residue limits
NHS	N-hydroxysuccinimide
OVA	Ovalbumin
PBS	Phosphate buffer saline
PBST	Phosphate buffer saline with 0.05% Tween 20
RIU	Refractive index unit
SDS-PAGE	Sodium dodecyl sulfate polyacrylamide gel electrophoresis
SPR	Surface plasmon resonance
TMB	3,3',5,5'-tetramethylbenzidine
VH	Variable region of heavy chain
VL	Variable region of light chain

# CHAPTER I

## INTRODUCTION

### 1.1 Importance and Rationale

Fluoroquinolones (FQs) are a group of antibiotics extensively used against both Gram-negative and Gram-positive bacteria due to their inhibition activities of DNA gyrase, topoisomerase and other enzymes essential for bacterial DNA replication. However, misuse of these antibiotics such as overdose treatment and long term use to prevent infection could lead to problems of drug residues in animal products for human consumption<sup>1</sup>. Unintentionally long-term consumption of these contaminated products could result in a more severe problem of antibiotic resistance in human. Therefore, Food and Drug Administration of many countries had set the maximum residue limit (MRL) and developed the surveillance program for these drug residues in foods. The most widely used method for drug residue screening detection is based on immunological method such as enzyme-linked immunosorbent assay (ELISA) and lateral flow immunoassay (strip test). In both methods, capability of antibody for detecting and binding to a very low amount of antigen or drug residue is crucial for the assay. Besides sensitivity, specificity which is the ability of any antibody to bind with a specific antigen is also equally important. If the antibody used in the assay could bind to many antigens, the assay might give a false positive result, thus reducing the effectiveness and reliability of the tests. In general, sensitivity and specificity of the antibodies are analyzed and compared in order to select the most suitable antibody for the assay development. However, sometimes this information is not enough for the selection. Binding affinity of each antibody to different antigens also comes into considerations. The information of affinity such as association constant and dissociation constant can be obtained by investigation of the binding kinetics between antibodies and antigens using surface plasmon resonance (SPR) technique. SPR biosensors have been used to characterize antibody-antigen interactions for approximately three decades<sup>2</sup>. SPR measurement was performed on Biacore instrument which has been widely used to analyze the interaction of high affinity antibodies<sup>3</sup>. Affinity and kinetics of molecular interaction determined by SPR

is important to understand protein interactions<sup>4</sup>. Furthermore, molecular docking approach has been used as a powerful tool for drug discoveries and studies of protein binding. Currently, several molecular docking software and servers including both commercial and free formats based on different algorithms are available for uses in many applications<sup>5</sup> such as AutoDock<sup>6</sup>, SwissDock<sup>7</sup>, GOLD (Genetic Optimization for Ligand Docking<sup>8</sup>, HADDOCK<sup>9</sup>, and MVD<sup>10</sup>. These programs can predict structure-base of ligand conformation and position within a binding site of the targeted protein. In the immunological field, the interaction of antibody-antigen was important because antibody has specificity epitope binding with its target. This data can use to detect residue drug in food. So, molecular docking was used to determine the binding site between antibody and drug.

The Institute of Biotechnology and Genetic Engineering has produced monoclonal antibodies (mAbs) against norfloxacin and enrofloxacin which have similar structures. In order to select a suitable mAb for further development of immunoassay, understanding of binding kinetics of the mAbs and those antibiotics are important. Consequently, in this study, binding kinetics of mAbs against norfloxacin, mAb Nor132 and mAb Nor155 and mAbs against enrofloxacin, mAb Enro44 and mAb Enro48 to some fluoroquinolones such as norfloxacin, enrofloxacin, ciprofloxacin and ofloxacin were studied. It has been known that amino acid sequence of any mAb greatly affects their binding characteristics to the antigens. Therefore, three-dimensional (3D) modeling analysis was performed using program AutoDock vina to investigate the amino acid residues of the mAbs that played an important role in the binding to different antibiotic antigens.

## **1.2 Objectives**

1.2.1 To analyze kinetics of binding interaction between the four mAbs and norfloxacin, enrofloxacin, ciprofloxacin and ofloxacin

1.2.2 To find relationship between kinetic information and sensitivity or specificity of the mAbs

1.2.3 To determine the major amino acid sequence or residues that played an important role in the binding between the mAbs and norfloxacin, enrofloxacin, ciprofloxacin and ofloxacin



### 1.3 Expected Beneficial Outcomes

1.3.1 The obtained information of binding kinetics of mAb-antigen interaction could be useful for antibody selection and further development of immunoassay for fluoroquinolone detection or other applications.

1.3.2 Information from molecular modeling analysis and results of indirect enzyme-linked immunosorbent assay between the four mAbs and fluoroquinolones probably indicate the possible major sites or specific amino acid sequences that govern the binding characteristics of the mAbs.



## CHAPTER II

### THEORETICAL BACKGROUND AND LITERATURE REVIEWS

#### 2.1 Antibody

Antibodies, known as immunoglobulins, are produced by the immune system to help protect the host against foreign invasion. Basically, antibody is glycoproteins that bind specifically to single antigens. Antigens recognized and bound by antibodies can be proteins such as receptors expressed on cancer cells, sugars on bacterial and viral cell surfaces, hormones, chemical compounds, or nucleic acid structures. The region of an antigen that interacts with an antibody is called the epitope. An antibody is Y shaped immunoglobulin (Ig) that consists of two heavy chains (H) and two light chains (L). The amino-terminal ends of the polypeptide chains show considerable variation in amino acid composition and refer to as the variable (V) regions to distinguish them from the relatively constant (C) regions. Each L chain consists of one variable domain, VL, and one constant domain, CL. The H chains consist of a variable domain, VH, and three constant domains CH1, CH2 and CH3. Each heavy chain has about twice the number of amino acids and molecular weight (~50,000) as each light chain (~25,000), resulting in a total immunoglobulin monomer molecular weight of approximately 150,000. Immunoglobulins can group into five different classes: IgA, IgD, IgE, IgG, and IgM. Individual classes of immunoglobulins have distinctive structural and biological properties. The class of an immunoglobulin molecule is determined by its heavy chains. Thus IgM, IgD, IgG, IgE, and IgA possess  $\mu$ ,  $\delta$ ,  $\gamma$ ,  $\epsilon$ , and  $\alpha$  heavy chains, respectively<sup>11-13</sup>. The most common type of antibody used for immunoassays is the IgG class of immunoglobulins. The antigen-binding fragments (Fabs) of the IgG immunoglobulins, which are the sites of antibody-antigen interaction. The interactions of the antibody molecule with specific antigen are non-covalent and reversible, dependent on hydrogen bonds, hydrophobic interactions, electrostatic forces, and Van der Waals forces.

### 2.1.1 Polyclonal Antibody

Polyclonal antibodies (pAbs) are a mixture of heterogeneous which are usually produced by different B cell clones in the body which can recognize and bind to many different epitopes of a single antigen. Production of polyclonal antibodies by injecting an immunogen into an animal. After injected with a specific antigen to elicit a primary immune response, the animal is given a secondary even tertiary immunization to produce higher titers of antibodies against the particular antigen. After immunization, polyclonal antibodies can be obtained straight from the serum or purified to obtain a solution that is free from other serum proteins<sup>14</sup>. To identify and handle specific epitopes, polyclonal antibodies are effortless to store, bind faster to the antigen and allow powerful protection. The performance of polyclonal antibodies is superior to monoclonal antibodies in a specific situation as they are able to attach greater than one antigen. Even if there is low intensity, they are capable of expelling the target by spreading the signal. Polyclonal antibodies exceptionally perform when it comes to chromatin immunoprecipitation since they have a wider target area while a protein can be picked up even if the resonance is at the lowest<sup>15</sup>.

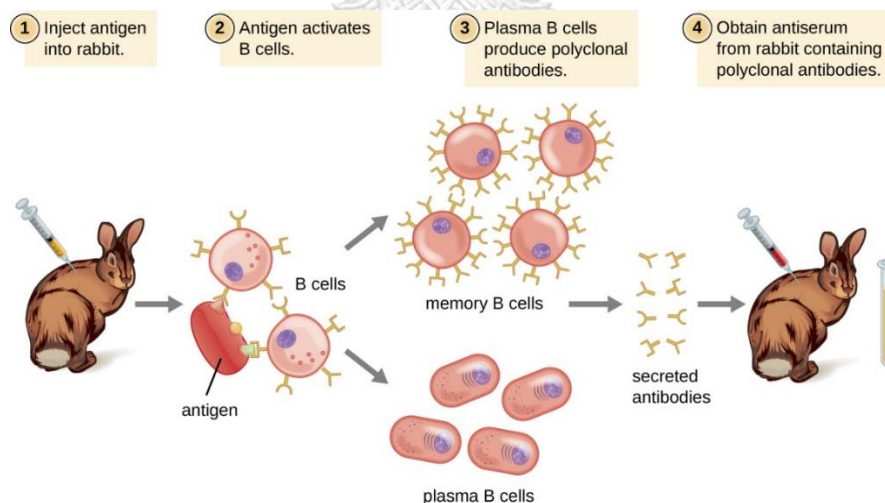


Figure 2.1 This diagram illustrates the process for harvesting polyclonal antibodies produced in response to an antigen. From: <https://bio.libretexts.org>

### 2.1.2 Monoclonal Antibody

Monoclonal antibodies are single antibodies derived from fuse antibody-producing cells with an immortalized cell line. As a result, the cell line is called hybridoma. Individual antibodies generate distinguish cell reaching the pure cell line that produce single antibody that hybridomas are divided. Given that cell lines can be produced completely the same antibody on and on since they are eternal. Generally, monoclonal antibodies were solely produced by mouse cells even though their immune responses are not the best. Nevertheless, recent technology has come up with rabbit monoclonal antibodies. Furthermore, rabbits' immune responses are more exceptional than mice<sup>16</sup>.

Monoclonal antibodies surpass these entire issues, enabling absolutely precise region not just for the immune protein. Additionally, the antigen degree of purity is disparate as originally described by Köhler and Milstein (1975, 1976). When the antibody-forming cells become immortal, the immune response is broken into its component parts. The antigen does not need to be purified as soon as the targeted clone is divided. Additionally, the specificity will be endlessly conserved where between animals, there is no variation. Thereby, monoclonal antibodies have yielded resolution to a number of biological problems<sup>17</sup>.

### 2.2 Fluoroquinolone

The fluoroquinolones are a set of broad spectrums, systemic antibacterial agents that have been commonly utilized as respiratory and urinary tract infections therapy, which against in a various range of both aerobic gram-positive and gram-negative organisms. Gram-positive coverage consists of penicillinase- and non-penicillinase producing *Staphylococci*, *Streptococcus pneumoniae* and *viridans*, *Enterococcus faecalis*, *Listeria monocytogenes*, and *Nocardia* species. Gram negative coverage comprises *Neisseria meningitidis* and *gonorrhoeae*, *Haemophilus influenzae*, and most clinically important *Enterobacteriaceae* species, *Pseudomonas aeruginosa* and *Vibrio* species. The fluoroquinolones are considered to react by the inhibition of type II DNA gyrases that are required for synthesis of bacterial mRNAs and DNA replication. They illustrate a few inhibitions of human, host enzymes and

provide exceptional safety evidence. The fluoroquinolones are signified as remedy for several bacterial infections.

Nowadays, the fluoroquinolones are accessible in the US including ciprofloxacin, gemifloxacin, levofloxacin, moxifloxacin, norfloxacin, and ofloxacin. With a low rate of harmful effects, these agents are perfect for oral absorption as well as high tolerance. However, with the instinctive reports of fatal circumstances, multiple quinolones and fluoroquinolones were removed, for example, hepatotoxicity: temafloxacin (1992), gatifloxacin (2006), and trovafloxacin (1999). Lately, a contemplation of 1:100,000 people-exposed having the idiosyncratic liver injury caused by fluoroquinolones. There is a pattern of this symptom owing to fluoroquinolones where it is acute and frequently serious hepatocellular rising in 1-4 weeks after a treatment. It might be a class effect which pattern of injury is alike. The fluoroquinolones are usually related to liver injury which are ciprofloxacin and levofloxacin. Although these two agents are commonly used. Only 1%-3% of patients obtaining ciprofloxacin, norfloxacin or ofloxacin in liver enzymes. The typical fluoroquinolones' side effects could be gastrointestinal disturbances, headaches, skin rash and allergic reactions. Barely occur but giving dreadful impact comprises of QT prolongation, seizures, hallucinations, tendon rupture, angioedema and photosensitivity<sup>18-20</sup>.

### **2.2.1 Norfloxacin**

Norfloxacin is one of fluoroquinolone antibacterial agents with a fluorine at position 6 and a piperazine ring at position 7<sup>21</sup>. Nevertheless, it is lacked indications and barely used these days. Like other fluoroquinolones, norfloxacin is activated in broad range for aerobic both gram positive and negative organisms. Moreover, it is perceived as inhibition of type II DNA topoisomerases that needed for bacterial mRNAs synthesis as well as DNA duplication. In 1986, the United States authorized norfloxacin for usage. Nowadays, its purpose is for urinary tract infections, sexually transmitted diseases and prostatitis. Furthermore, it plays a role in fighting serious bacteria peritonitis in cirrhosis and ascites patients. Under trademark Noroxin, norfloxacin comes in the form of 400 mg tablets. Normal doses of 400 mg are taken every 12 hours from 3 days to 10 days. Still, chronic treatment is used for antibacterial prophylaxis. Side effects that can be typically found are gastrointestinal

upset, headaches, skin rash and allergic reactions. However, there are more drastic side effects: prolongation of the QT interval, seizures, hallucinations, tendon rupture, angioedema, hypersensitivity reactions, photosensitivity and peripheral neuropathy<sup>21-23</sup>.

### **2.2.2 Enrofloxacin**

Alike other fluoroquinolones, enrofloxacin plays its role in treating vulnerable bacteria in a wide range of species. The remedy consists of urinary tract infections in dogs and cats and infections of skin as well as tissue. Crucially, enrofloxacin demonstrates effectiveness in curing dogs Rickettsia infections. Nevertheless, treating Ehrlichia, enrofloxacin does not work well. In horses, it heals soft tissues and respiratory infections. Though, it is mainly used on anecdotal experience. The approval of enrofloxacin is for the medication and swine respiratory disease (SRD) related to *Actinobacillus pleuropneumoniae*, *Pasteurella multocida*, *Haemophilus parasuis*, and *Streptococcus suis*<sup>24</sup>. Furthermore, enrofloxacin is used in exotic creatures due to its safety and defense of numerous pathogens.

### **2.2.3 Ciprofloxacin**

Ciprofloxacin acts as oral fluoroquinolone which aims to cure light-to-medium diarrhea, typhoid fever, uncomplicated gonorrhoea and respiratory tract and urinary infections. Like other fluoroquinolones, ciprofloxacin is activated in broad range for aerobic both gram positive and negative organisms. Additionally, it is perceived as inhibition of type II DNA topoisomerases that needed for bacterial mRNAs synthesis as well as DNA duplication. Ciprofloxacin has been utilized in the US since 1990 where every year it is prescribed around 20 million times. It is in several oral formulas of 100, 250, 500 to 700 mg tablets. It also broadens to 500 and 1000 mg tablets. Proquin and Cipro, for instance, are the trademark of ciprofloxacin. The typical dose of ciprofloxacin is every 12 hours for 250 and 500 mg. For medium to drastic infections, intravenous formula is more appropriate by obtaining 200 to 400 mg IV every 8 hours. Oral remedy normally lasts from 7 to 10 days for both longer and shorter courses. Typical side effects are skin rash, headache and allergic reactions. Still, serious side one is hallucinations, tendon rupture and QT interval<sup>25, 26</sup>.

#### 2.2.4 Ofloxacin

Ofloxacin is the second group of fluoroquinolones. It was formerly used to cure light-to-medium valuable organisms causing respiratory and urinary tract infections. Ofloxacin is a mixture of race and semisynthetic antibiotic. Like other fluoroquinolones, ofloxacin is activated in broad range for aerobic both gram positive and negative organisms. In addition, it is perceived as inhibition of type II DNA topoisomerases that needed for bacterial mRNAs synthesis as well as DNA duplication. There was approval of ofloxacin in 1990 in the Unites States. However, it was suspended since several terrible sides' effects happened from its earlier 2009 sponsor. Nonetheless, ofloxacin still exists in form of 200, 300 and 400 mg tablets which can be taken every 12 hours for 3 to 10 days. Yet, for persistent and complex infections, longer courses are used from time to time. Typical side effects can be found are headaches, skin rash and gastrointestinal upset. Anyhow, rarely occur but bring serious side effects are photosensitivity, QT interval and tendon rupture<sup>27, 28</sup>.

### 2.3 Enzyme-Linked Immunosorbent Assay (ELISA)

The enzyme-linked immunosorbent assay (ELISA) is the most widely used immunoassays available for detecting and quantifying substances such as antibodies, antigen, proteins and hormones in biological sample. ELISA can be divided into four major types: direct, indirect, sandwich, and competitive.

#### 2.3.1 Direct ELISA

In a direct ELISA, reporting molecule is conjugated to either antigen or antibody in order to directly detect the binding between the antigen and the antibody. This method is the simplest one because it required only a few steps in the preparation and the assay. However, it usually gives low sensitivity because the signal is not amplified. In this method, either antigen or antibody can be immobilized on the solid surface and then the labelled antibody or antigen is added. The binding between the antigen and the antibody is detected from the labelled molecule as shown in Figure 2.2. The reporting molecule can be an enzyme (such as horse-radish peroxidase which requires the addition of substrate to give the detectable product) or other molecules such as fluorophore or nanoparticles.

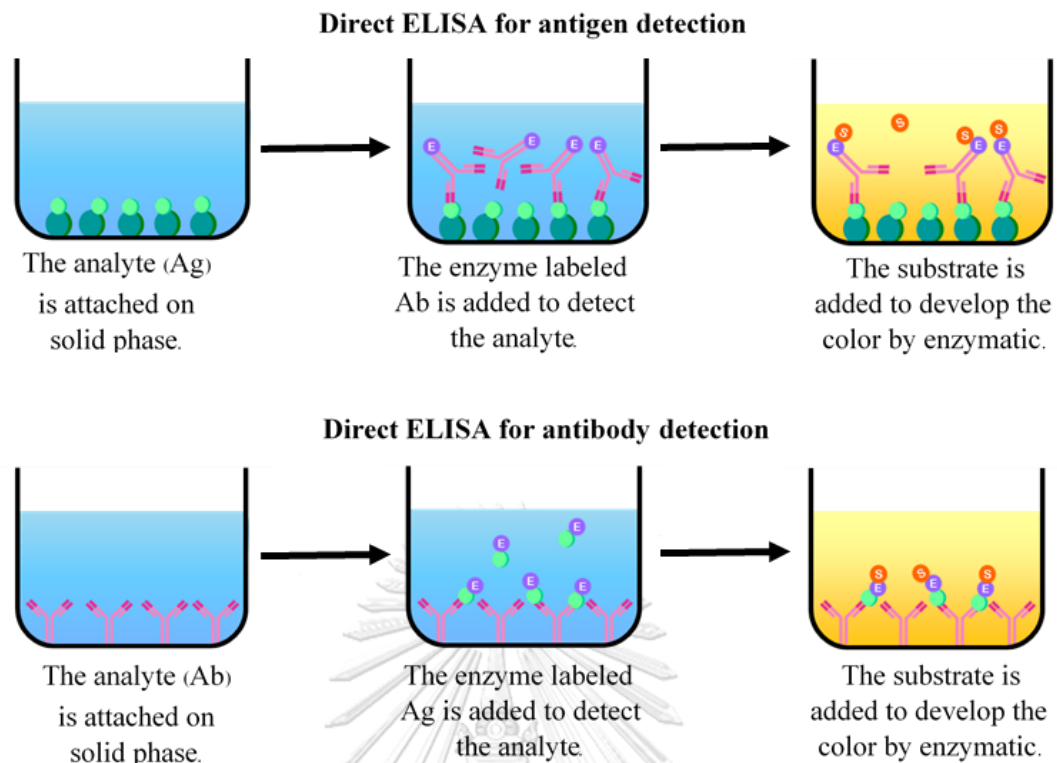


Figure 2.2 Illustrates the principle of direct ELISA format.

### 2.3.2 Indirect ELISA

In an indirect ELISA, the binding between the antigen and the antibody of interest is not directly detected. But it requires another labelled molecule which can bind to the antigen or the antibody. For example, in the case that the antigen is coated on to the surface of a micro titer plate, then the primary antibody is added into the wells, which specifically bind to the antigen. The binding between the antigen and the primary antibody is then detected by the addition of the labelled secondary antibody which can bind with the primary antibody as shown in Figure 2.3. In another case that the antibody is coated on the surface, the biotin-labelled antigen is added to bind with the antibody. The binding between the antibody and the antigen can be detect by using horse radish peroxidase-labelled streptavidin which can bind with the biotin labelled on the antigen. Although, this method is more complex that the direct ELISA, its sensitivity can be improved by signal amplification.



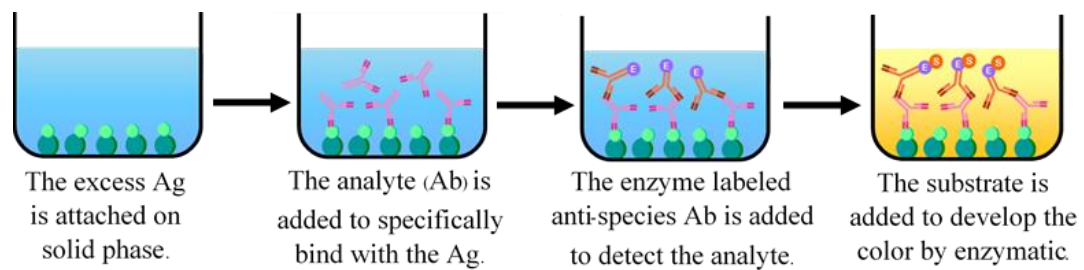


Figure 2.3 Illustrates the principle of indirect ELISA format.

### 2.3.3 Sandwich ELISA

In a sandwich ELISA, two antibodies which can bind to different epitope on the molecule of antigen are required. This method does not suitable for a small antigen molecule because it usually has only single epitope for antibody binding. To perform the assay, the first antibody is coated on the surface of ELISA plate. After the antigen is added to bind with the first antibody, the second antibody is added to bind with the same antigen but at the different site or epitope of the antigen. The binding between the antigen and the antibody in the sandwich ELISA can be detected using the direct (Figure 2.4a) or indirect method (Figure 2.4b).

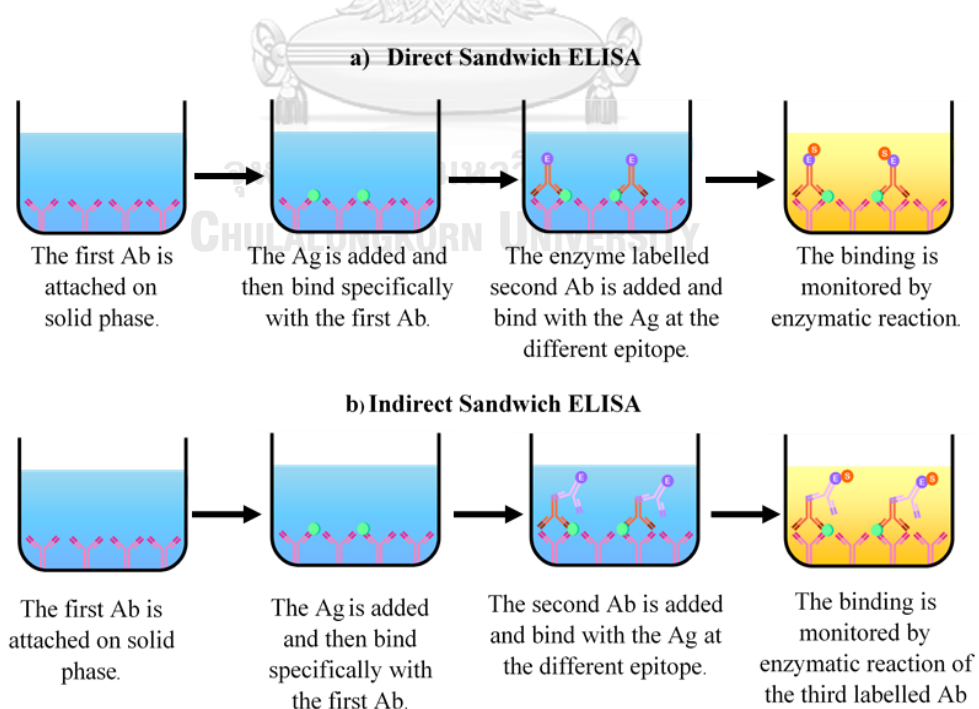


Figure 2.4 Illustrates the principle of a sandwich ELISA format.

### 2.3.4 Competitive ELISA

In previous types of ELISA described above, the signal intensity of the reporting molecule is varied with respect to the number of binding between the antibody and the antigen. In the competitive format, the competitor is added into the system in order to compete in binding with the antigen and antibody of interest. As a result, the signal intensity of the reporting molecule is varied inversely with respect to the number of binding as shown in Figure 2.5. For example, in the case of an antibody labelled direct competitive ELISA, the antigen is first attached onto the surface. Then the labelled antibody and the Ag competitor (usually analyte) are added. The Ag competitor and the attached antigen compete to bind with the labelled antibody. The higher the amount of the competitor, the lower the amount of the antibody which can bind with the attached antigen.

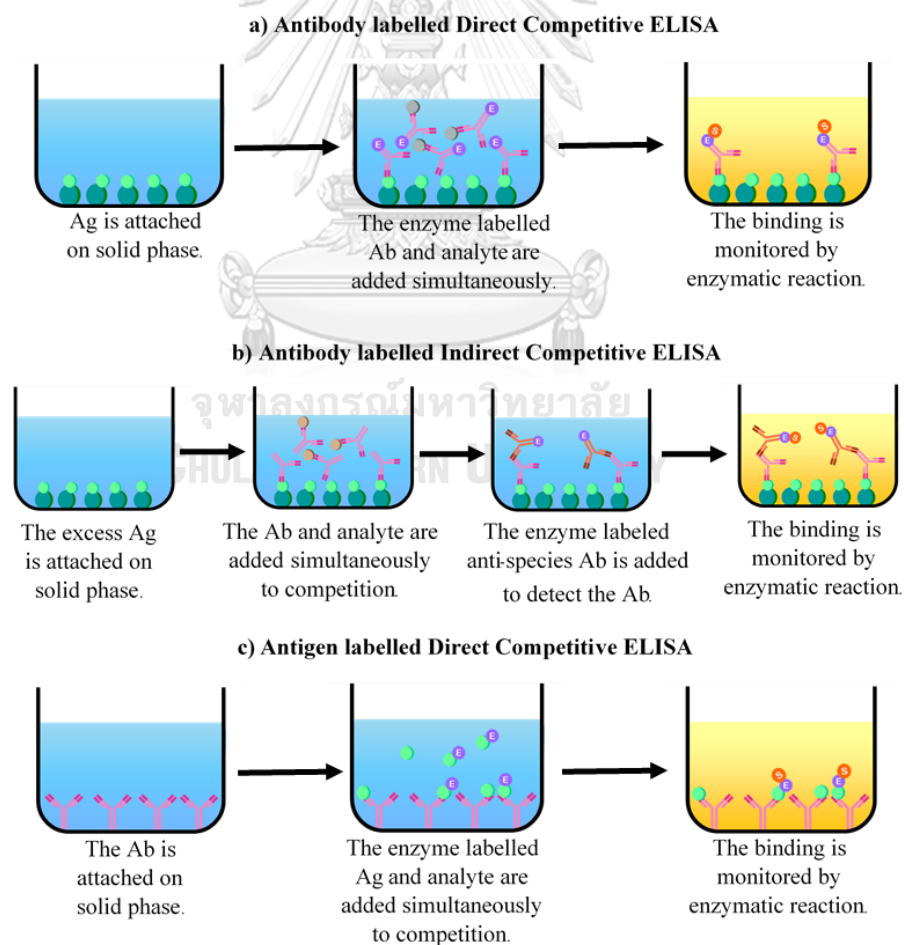


Figure 2.5 Illustrates the principle of competitive ELISA format.

## 2.4 Surface Plasmon Resonance

SPR is a label-free biosensor technique for studying interactions between all classes of biomolecules and biochemical mechanisms in real time<sup>29</sup>. This is done in a label free environment, while the ligand of interest is immobilized on the surface of the sensor chip and solutions with different concentrations of the analyte can flow over it. The increase in mass associated with a binding event causes a proportional increase in the refractive index, which is observed as a change in response<sup>30</sup>. The association and dissociation rate are measured in resonance units (RU) and plotted as a sensogram.

### 2.4.1 Principle of SPR

SPR is a phenomenon when the light is bent towards the plane of interface between media of different refractive indices. The incidence angle ( $\Theta$ ) will change the reflect light until it reaches a critical angle. At this point, all the incoming light reflects within the circular prism. This is called total internal reflection (TIR), an electric field intensity known as an evanescent wave is generated. At a specific wavelength, the incident light excites plasmon in the gold film and the intensity of reflected light was dropped due to the resonance transfer between evanescent wave and surface plasmons<sup>31</sup>. The material absorbed onto the thin metal film influence on the resonance. In general, gold is widely used because it gives a SPR signal at convenient combinations of reflectance angle and wavelength. In addition, gold is chemically inert to solutions and solutes typically used in biochemical contexts. Moreover, SPR signal depends on the refractive index of solution when contact with the surface of sensor chip (Figure 2.6).

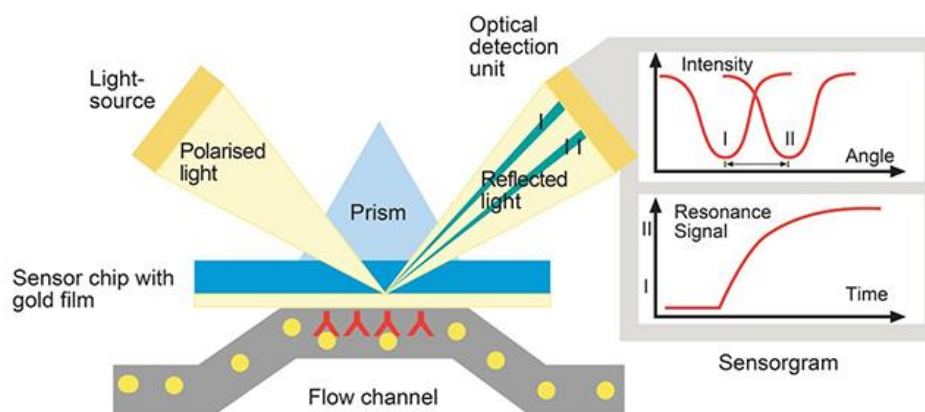


Figure 2.6 Illustration of Surface Plasmon Resonance. The binding of analyte shifts the SPR angle. From: <https://phoenixmed.arizona.edu/mcd/instrumentation/pioneer>

#### 2.4.2 Biacore Instrument

Biacore is an SPR biosensor instrument for studying interactions between all classes of biomolecules and biochemical mechanisms in real time. The detection principle based on surface plasmon resonance (SPR) for studying the interaction between two binding partners, one partner is immobilized on the surface (ligand) and other is flow over the surface in sample solution (analyte). When analyte binds to the ligand, the accumulation of protein on the surface of the sensor chip increases, leading to an increasing refractive index. Changing refractive index is measured in real time and plotted to a sensorgram between response unit (RU) and time. These sensorgrams provide information on binding specificity, affinity, concentration profiles, and kinetics as shown in Figure 2.7.

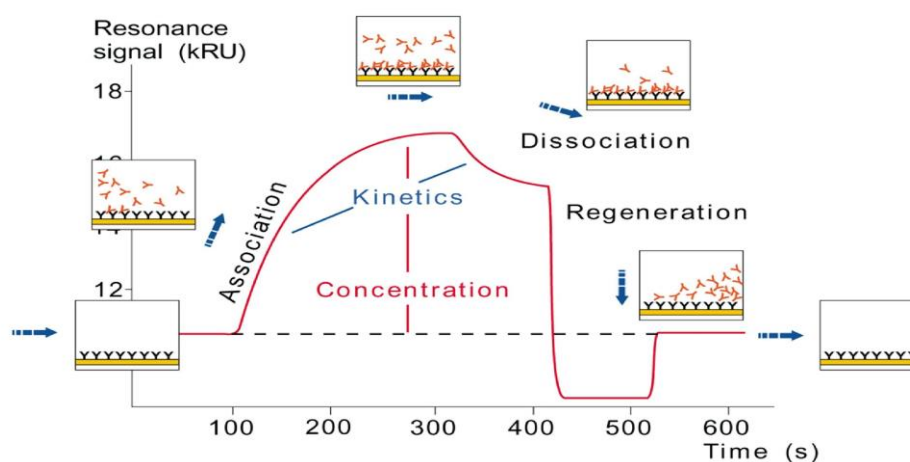


Figure 2.7 The sensograms of analyte-ligand binding.

## 2.5 Circular Dichroism Spectroscopy

Circular dichroism (CD) is a fast and powerful spectroscopic method for studying macromolecules that differential absorption of clockwise (right-handed) or counterclockwise (left-handed) circularly polarized light as the result of structural asymmetry. CD spectroscopy has been applied to study the control of protein stability in different situations such as changes in thermal, pH and ionic strength or solvent conditions. Moreover, different protein conformational were compared from various expression systems or species. Other advantages for observed changing in structure of protein-protein or protein-ligand interactions and to confirm suitable folding during purification processes<sup>32-34</sup>. CD is measured with a CD spectropolarimeter that measures in the far-UV spectral region from 190 to 250 nm and near-UV spectral region from 250 to 350 nm. Specific CD signals, the chromophores of peptide bonds at 190-250 nm wavelengths as the aromatic amino acids and disulfide bonds at 250-350 nm wavelengths<sup>35</sup>. CD in the far UV region from approximately 190 to 240 nm gives the secondary structure of a protein information because of the arrangement of peptide bonds into distinct constrained structures<sup>36</sup>. The CD spectrum of proteins in far-UV range has distinct spectra for  $\alpha$ -helix,  $\beta$ -sheet, and random coil (Figure 2.8)<sup>37</sup>. The CD spectra show the  $\alpha$ -helix dominates with a strong positive band at  $\sim$ 192 nm, and negative bands at  $\sim$ 208 and  $\sim$ 222 nm, while the  $\beta$ -sheet has an intense negative peak at  $\sim$ 216 nm, and positive peak at  $\sim$ 200 nm consist of  $\beta$ -sheet and  $\beta$ -turn components, and any  $\alpha$ -helix contribution. Random coil structure can exhibit a strong

negative band at  $\sim 195\text{--}200\text{ nm}$ <sup>38</sup>. The near-UV CD spectra at  $250\text{--}350\text{ nm}$  reflects the chiral environment around the aromatic amino acid residues including Phe, Tyr, and Trp, and around disulfide bonds. When the solution condition such as pH, ionic strength, and temperature are changed causing the changed tertiary structure of the protein.

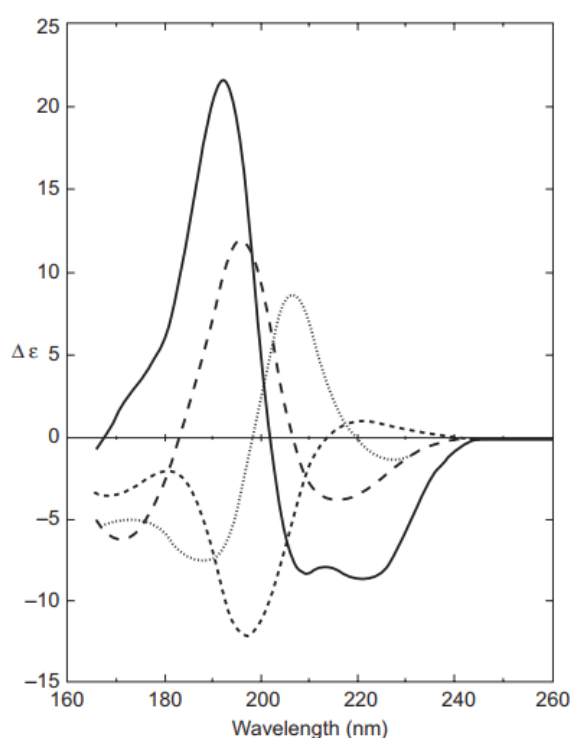


Figure 2.8 The circular dichroism (CD) for various secondary structures:  $\alpha$ -helix (solid line), antiparallel ( $\beta$ -sheet (bold dashed line), ( $\beta$ -turn (dotted line), and random coil (dashed line). From: Johnson (1990)

## 2.6 Molecular Docking

Molecular interaction such as protein-protein, protein-ligand, enzyme-substrate, and drug-protein present significant function in many biological processes including cell regulation, gene expression control, enzyme inhibition, and antibody-antigen recognition<sup>39</sup>. The complex protein structures, which obtain from X-ray crystallography or NMR, are crucial to understand the binding and affinity between molecule interaction, but these methods are difficult, take a long time, and expensive.

Therefore, the docking computation is a key tool for understanding the protein-protein or protein-ligand interaction<sup>40</sup>. In antibody-antigen docking study, computational docking has been used to design antibodies with improved binding properties<sup>41</sup>. Lippow et al. (2007) generated higher affinity variants for 3 antibody targets by computationally selecting mutations that improved antibody– antigen interaction energy. Similarly, Poosarla et al. (2017) developed a computational framework for the de novo design of fully human antibody variable domains to bind any specified antigen by assembling the six best-scored modular antibody parts<sup>42</sup>. In addition, a fundamental characteristic of the immune system is its ability to continuously generate novel protein recognition sites, Ab-Ag interaction<sup>43</sup>. For example, Keskin, O (2007) used X-ray crystallographic structures of Ab-Ag complexes to explain principles of the molecular of protein–protein interaction.

Molecular docking is a widely use computer simulation to predict the conformation of protein- ligand complex and binding modes of ligand with a three-dimensional protein (Figure 2.9).

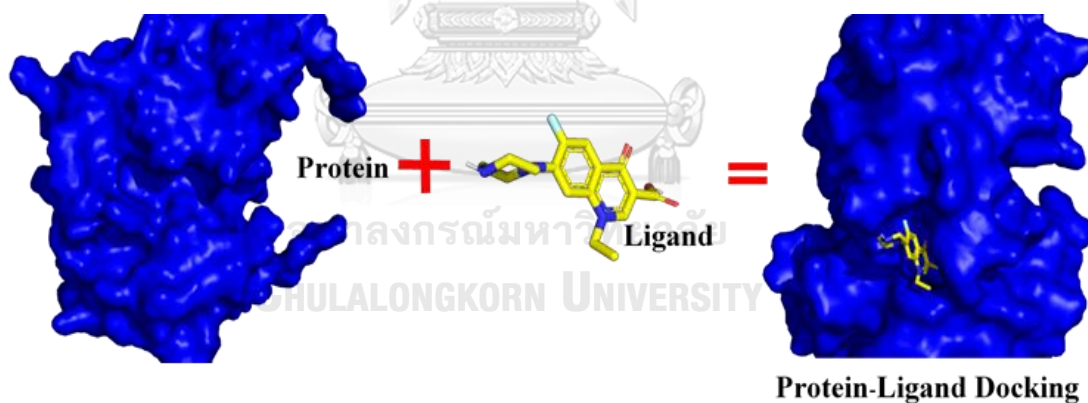


Figure 2.9 Components in molecular docking.

The predicted binding of the protein and ligand should be accurate as best as possible. The significant of docking software is the visual screening, where the interesting molecules are select from database. Moreover, the prediction must be fast and reliable. There are several docking software and algorithms that have been used in crucial process in predicting binding pose of ligand into protein by making use biochemical and biophysical combination with bioinformatics. Examples of docking

tool are AutoDock <sup>44, 45</sup><http://autodock.scripps.edu>, DOCK <sup>46</sup><http://dock.compbio.ucsf.edu>, FlexX <sup>47</sup><https://www.biosolveit.de/FlexX>, GOLD <sup>48</sup><https://www.ccdc.cam.ac.uk>, and ICM <sup>49</sup>[http://www.molsoft.com/icm\\_pro.html](http://www.molsoft.com/icm_pro.html). Figure 2.10 shows the common major step of all docking protocols.

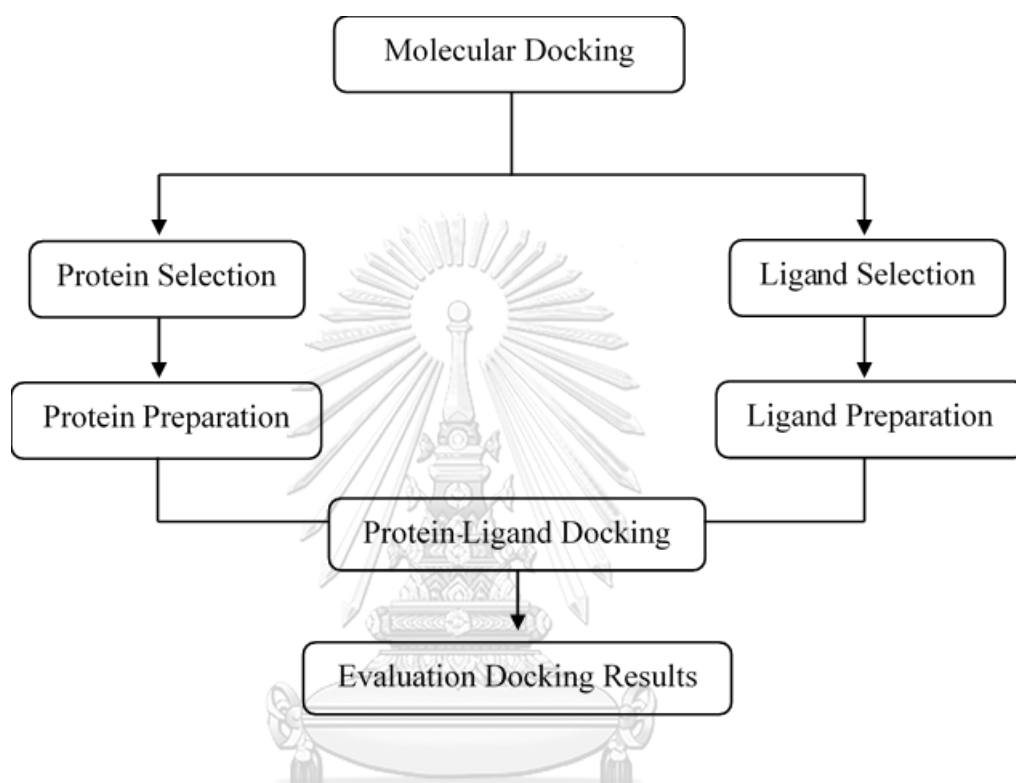


Figure 2.10 A typical docking workflow for protein-ligand docking.



**CHAPTER III**  
**MATERIALS AND METHODS**

**3.1 Chemicals and Reagents**

<b>Chemicals and Reagent</b>	<b>Company, country</b>
Absolute ethanol	Merk, United States of America
Absolute methanol	Merk, United States of America
Acetic acid (glacial) 100% anhydrous	Merk, Germany
Acrylamide	Bio-Rad, California
Agar (Microbiology grade)	Merk, Germany
Agarose (Molecular biology grade)	Research organics, Inc., United States of America
Albumin, from bovine serum (BSA)	Sigma-Aldrich, Missouri
Albumin, from chicken egg white (OVA)	Sigma-Aldrich, Missouri
Bacto™ Peptone powder	Becton, Dickinson and company, France
BCA Protein Assay kit	Thermo Scientific, Illinois
Biotin	Fluka, Germany
Ciprofloxacin hydrochloride monohydrate	Sigma-Aldrich, Missouri
Coomassie brilliant blue G	Pierce, Illinois
Dimethylformamide (DMF)	Merck, Germany
Dimethylsulfoxide (DMSO)	Merck, Germany
Enrofloxacin	Sigma-Aldrich, Missouri
Ethidium bromide	Bio basic, Inc., Canada
Fetal calf serum (FCA)	PAA lab, Austria
Glycerol	Ajax Chemicals, Australia
Goat anti mouse IgG-Horseradish peroxidase conjugate (GAM-HRP)	Jackson Immuno, Pennsylvania
HBS-EP <sup>+</sup> Buffer	GE Healthcare Lifescience™, Sweden
Hydrochloric acid (HCL)	Merck, Germany
30% Hydrogen peroxide (H <sub>2</sub> O <sub>2</sub> )	Merck, Germany
Methanol	Merck, Germany
Norfloxacin	Sigma-Aldrich, Missouri
Ofloxacin	Sigma-Aldrich, Missouri
RPMI 1640 medium	Biochrom, Germany
Skim milk	Difco, United States of America
Sodium chloride	Ajax Chemicals, Australia
Sodium dodecyl sulfate (SDS)	Bio basic, Inc., Canada
Sodium hydroxide	Ajax Chemicals, Australia
Sulfuric acid (H <sub>2</sub> SO <sub>4</sub> )	Merck, Germany
Surfactant P20	GE Healthcare Lifescience™, Sweden
TAE buffer premix powder	Bio basic, Inc., Canada
TMB (3,3',5,5'-tetramethylbenzidine)	Sigma Aldrich, Germany

N,N,N',N'-tetramethylethylenediamine (TEMED)	Pierce, Illinois
Tris (Molecular biology grade)	Research organics, Inc., United States of America
Tween-20	Sigma Aldrich, United Kingdom
Yeast nitrogen base powder	Bio basic, Inc., Canada
Yeast extract powder	Bio Springer, France
Zeocin™	Invitrogen, United States of America

### 3.2 Equipment and Supplies

Equipment and Supplies	Company, country
Autoclave (HV-50)	Hirayama manufacturing Corp., Japan
Balance (Adventurer™, ARC 120)	Ohaus Corp., United States of America
Balance (Adventurer™, AR 2140)	Ohaus Corp., United States of America
Bench-top centrifuge, WiseSpin® (CF-10)	Dihan scientific Co., Ltd., South Korea
Biacore T200	GE Healthcare Lifescience™, Sweden
Biological safety cabinet (Heal force®, HFsafe-1200)	Shanghai Lishen
1-Ethyl-3-(3-dimethylaminopropyl) carbodiimide (EDC)	GE Healthcare Lifescience™, Sweden
E.Z.N.A.® Gel extraction kit	Omega Bio-Tek, Inc., United States of America
Freezer (-20°C) (SF-C697)	Sanyo Commercial Solution, Ltd, Thailand
Gene Pulser® Cuvette, 0.2 cm.	Bio Rad Laboratories, Inc., China
High speed micro refrigerated centrifuge (MTX-150)	Tomy Seiko Co., Ltd., Japan
High speed refrigerated centrifuge (6500)	Kubota Corp., Japan
Hot plate (PC-101)	Corning, United States of America
Incubator (MIR 152)	Sanyo Electric Co., Ltd. Japan
Laminar flow	Lab Survice Ltd., Thailand
Liquid Nitrogen Tank	Harsco Corp., Camp Hill, Pennsylvania
Microplate reader, model: MCC/340	Titertek multiskan, Helsinki, Finland
Microwave oven (National®)	Matsushita Electric Co.Ltd., Japan
Multichannel autopipette	HTL, Warsaw, Poland
Mupid® -EXU Submarine electrophoresis system	Advance Co, Ltd., Japan
N-hydroxysuccinimide (NHS)	GE Healthcare Lifescience™, Sweden
Petri dish, 90 mm	Sterilin Ltd., Newport, United Kingdom
pH meter (Accumet® AB15)	Fisher Scientific, Singapore
Precision weighting balance, model: AG204 and PG402S	Mettler Toledo, Greifensee, Switzerland

Protein G sepharose 4 fast flow	GE healthcare, Cardiff, United Kingdom
Sensor Chip CM5	GE Healthcare Lifescience™, Sweden
Syring filter, Nylon membrane	Whatman, United Kingdom
Vacuum pump	Iwaki pump, Japan
Vortex mixer	Scientific Industries, Colorado
Water bath	Memmert, Germany

### 3.3 Methods

#### 3.3.1 Production and Purification of MABs

##### 3.3.1.1 Recovery Hybridoma Cells from Stock

The hybridoma cells, Nor132 and Nor155 (mAb against norfloxacin) and Enro44 and Enro48 (mAb against enrofloxacin) were obtained from Institute of Biotechnology and Genetic Engineering (IBGE), Chulalongkorn University. The cryotube of hybridoma cell was taken from liquid nitrogen storage and immediately placed into a 37°C water bath until a small bit of ice left in the vial. Cells were suspended in RPMI 1640 medium and centrifuged at 1,500 rpm for 5 min to remove DMSO. Cell pellet was resuspended in RPMI 1640 medium supplemented with 20% FCS and cultured in 5% CO<sub>2</sub> incubator at 37 °C until the color medium changed to turbid yellow.

##### 3.3.1.2 Protein Purification

Culture medium was centrifuged and mAb in the supernatant was purified using an ÄKTA affinity chromatography with HiTrap Protein G HP antibody purification column (GE Healthcare). The column was pre-equilibrated with 2 mM phosphate buffer (pH 7.0), flow rate 1.0 ml/min. Prior to media loading (1 liter), unbound protein was washed out with 30 ml equilibrated buffer. MAb was eluted with 0.1 M glycine-HCl buffer (pH 2.7) then each fraction (1ml/fraction) was collected into 70 µl of 1M Tris-HCl buffer (pH 9.0). Finally, the purify mAb was dialyzed to desalting and remove undesired low-molecular weight components and stored at -20 °C.

##### 3.3.1.3 Determination of Protein by BCA Protein Assay

Protein concentration was quantified by BCA Protein Assay kit. The assay procedure was employed according to the manufacturer's instructions. Briefly, 25 µl of bovine serum albumin (BSA) at different concentrations of 0, 0.1, 0.2, 0.4,

0.6, 0.8 and 1 mg/ml and diluted protein samples were separately transferred into each well of microtiter plate. The BCA working reagent (WR) was prepared by mixing reagent A with reagent B (50:1, Reagent A: B) and added (200  $\mu$ l) to each well. The microplate was incubated at 37 °C for 30 min and measured the absorbance at 560 nm using microplate reader.

#### **3.3.1.4 Protein Analysis by SDS-PAGE**

The gel solutions for 15% separating gel and 5% stacking gel were prepared. Antibody samples were diluted and mixed with Next Gel<sup>®</sup> Sample Loading buffer, 4X (AMRESCO, USA) then the samples were boiled for 10 min. After that the samples and molecular weight standards were loaded (20  $\mu$ l/well) onto the gels. Electrophoresis was carried out at a constant current of 25 mA per gel with 1 $\times$ Tris-glycine-SDS running buffer. Following electrophoresis, gels were stained with coomassie blue and de-stained with a destaining solution.

#### **3.3.2 Determination of Monoclonal Antibody by ELISA**

##### **3.3.2.1 Conjugation of Drug-OVA**

The 4 drugs of FQs; norfloxacin, enrofloxacin, ciprofloxacin, and ofloxacin were conjugated to OVA by a modified method of carbodiimide active ester method from Watanabe, H., et al. (2002). Each drug (20 mg), N-hydroxysuccinimide (NHS) (10 mg) and 1-Ethyl-3-(3-dimethylaminopropyl) carbodiimide (EDC) (10 mg) were dissolved in dimethylformamide (DMF, 1 ml) and the solution was stirred for 30 min at room temperature. The reactant solution was added dropwise to the OVA solution (50 mg in 3 ml PBS). The solution was stirred at room temperature for 2 h and dialyzed 3 times in PBS at 4 °C. Finally, the drug-OVA solution was filtrated with 0.2  $\mu$ m cellulose acetate membrane and kept -20 °C until use.

##### **3.3.2.2 Antibody-captured iELISA**

The 96-well plates were coated with NOR-OVA (2.3464 mg/ml) or ENRO-OVA (3.0436 mg/ml) (100  $\mu$ l/well) at 4 °C overnight. The plates were washed three times with 10 mM phosphate buffer saline, pH 7.4 containing 0.05% Tween<sup>®</sup> 20 (washing buffer or PBST) then blocked with 5% skim milk (300  $\mu$ l/ well) at 37 °C for 1 h. The plates were washed three times with washing buffer. The monoclonal antibody of interest was added (100  $\mu$ l/well) into the plates and incubated at 37 °C for 2 h. After three washing times with PBST, goat anti-mouse IgG was added at

concentration 230 ng/ml into the plates and the plate was incubated at 37 °C for 1 h. After another three washing times, tetramethylbenzidine substrate solution (TMB) was added (100µl/well) and the reaction could occur for 15 min in the dark at room temperature. The enzymatic reaction was stopped by adding 1 N H<sub>2</sub>SO<sub>4</sub> (100 µl/well) and the absorbance was measured at 450 nm using microplate reader.

### **3.3.2.3 Antibody-captured icELISA**

The general ELISA protocol was used. The 96-well plates were coated with NOR-OVA for detect mAb Nor132 and mAb Nor155 as well as ENRO-OVA for detect mAb Enro44 and mAb Enro48 (100 µl/well) at 4 °C overnight. The plates were washed three times with PBST then blocked with skim milk (300 µl/ well) at 37 °C for 1 h. The plates were washed three times with washing buffer. Various concentrations of unconjugated free drug (norfloxacin, enrofloxacin, ciprofloxacin, and ofloxacin) and the monoclonal antibody of interest were added 50 µl/well and 100 µl/well, respectively into each well and the plates were incubated at 37 °C for 2 h. After three washing steps, goat anti-mouse IgG-HRP was added (1:10,000 in PBS, 100 µl/well) into each well and the plates were incubated at 37 °C for 1 h. After another three washing steps, tetramethylbenzidine substrate solution (TMB) was added (100 µl/well) and the reaction was allowed to occur for 15 min in the dark at room temperature. The enzymatic reaction was stopped by adding 1 N H<sub>2</sub>SO<sub>4</sub> (100 µl/well) and the absorbance was measured at 450 nm using microplate reader.

### **3.3.2.4 Evaluation of Prototype ELISA**

#### **3.3.2.4.1 Sensitivity of ELISA**

Sensitivity of the mAb was quantified in terms of both 50% inhibition concentration (IC<sub>50</sub>) and limit of detection (LOD). The IC<sub>50</sub> of each compound was determined using the following formula:

$$IC_{50} = 50\% (B/B_0) \quad \text{Eq.1}$$

where B<sub>0</sub> and B are the average absorbance obtained from the icELISA with different concentrations of the competitors (B) and without the competitors (B<sub>0</sub>).

LOD was calculated from the average concentration (n=10) of B<sub>0</sub> in the icELISA plus three times of its standard deviation value.

### 3.3.2.4.2 Specificity of ELISA

To evaluate the specificity of icELISA for mAbs was evaluated in terms of the cross-reactivity. The percentage of cross-reactivity is calculated using the formula:

$$\% \text{ cross reactivity} = \frac{\text{IC50 of norfloxacin or enrofloxacin}}{\text{IC50 of other interested compound}} \times 100 \quad \text{Eq.2}$$

The competitors in this study were some of fluoroquinolones group including norfloxacin, enrofloxacin, ciprofloxacin, and ofloxacin.

### 3.3.3 SPR study of Antigens-mAbs Kinetics

#### 3.3.3.1 Immobilizing Drug-OVA on CM5 sensor chip

The amine coupling kit from Biacore was used for procedure. Sensor chip was activated with a freshly NHS and EDC solution at 1:1 mixture. Antigen (NOR-OVA, CIPRO-OVA, and ENRO-OVA) at 0.1 M in sodium acetate buffer (pH 4.5) were injected into the one flow cell for immobilization onto the surface of CM5 chip at 30 min. The ligand level was calculated using the formula as:

$$R_{\max} = (\text{analyte MW} / \text{ligand MW}) \times \text{Stoichiometry} \times R_L \quad \text{Eq.3}$$

Then, ethanolamine was used to deactivate of remaining active esters on the surface. The sensor chip has four flow cells which immobilized ligand on flow cell 2 or 4 using flow cell 1 or 3 as reference accordingly.

#### 3.3.3.2 Kinetic Analysis of Antigens-mAbs Interactions

Binding kinetics of mAb Nor132, mAb Nor155, mAb Enro44 and mAb Enro48 were measured by Biacore T200. MAb Nor132 and mAb Nor155 were diluted in HBS-EP<sup>+</sup> buffer at concentration ranged from 70 to 400 nM for binding with NOR-OVA while CIPRO-OVA binding, both of mAb Nor132 and mAb Nor155 were diluted in PBS+P20 buffer to a series of concentrations at 15.625-500 nM. MAb Enro44 and mAb Enro48 were diluted in PBS+P20 buffer at concentration ranged from 150 to 1100 nM for binding with ENRO-OVA. All of analytes were injected with a contact time of 400 s at 10-30  $\mu$ l/min and a dissociation time of 600 s. The

surface was regenerated each cycle with 50 mM NaOH (contact time 30 s at 30  $\mu$ l/min). Equilibrium binding constant ( $K_D$ ) was calculated as follow:

$$K_D = [A][B]/[AB] = k_d/k_a. \quad \text{Eq.4}$$

Where  $K_D$  = Equilibrium binding constant

$k_d$  = dissociation constant obtained from the analysis

$k_a$  = association constant obtained from the analysis

### 3.3.4 Circular Dichroism Spectroscopy Analysis

The secondary structures of mAb Nor155 were determined using a CD spectropolarimeter (Model J-810, Jasco, Japan) at the Salaya Central Instrument Facility, Mahidol university. Far-UV CD spectra were recorded at wavelengths between 190 and 240 nm using a 0.1 cm path length cell at 25 °C with a protein concentration of 0.2 mg/ml in various buffer include 150 mM NaCl+P20, HBS-EP<sup>+</sup>, PBS, and PBS+ P20 buffer. Each spectrum was a representative of three scans. The CD spectra were corrected for buffer contributions.

### 3.3.5 Generation of 3D mAbs and Homology Modeling

Homology modeling is a method for building a three-dimensional structures (3D) of a target protein which its amino-acid sequence of target protein was aligned with a similar protein with known structure as a template<sup>50</sup>. The amino acid sequence of the mAb Nor132, mAb Nor155, mAb Enro44, and mAb Enro48 were submitted to the SWISS-MODEL in the Automated Protein Modeling Server which automated sequence alignments are sufficiently dependable when target and template share more than 50% same residues<sup>51</sup>. Therefore, the molecular structure template of V<sub>H</sub> and V<sub>L</sub> of mAbs were chosen from the highest sequence identities from the PDB Data Bank. Then, the percentage identity of amino acid sequence V<sub>H</sub> and V<sub>L</sub> of mAbs with the template were aligned using CLUSTALW server. To generate 3D Fab fragment of mAbs, V<sub>H</sub> and V<sub>L</sub> were superimposed with the crystal structure template of 5e0q, which structure of the murine Fab 1G6 bound to the vaccinia virus A27 peptide 31-40

### 3.3.6 Docking Analysis using AutoDock vina

The 3D structure of ligands including norfloxacin (CID: 4539), enrofloxacin (CID: 71188), ciprofloxacin (CID: 2764) and ofloxacin (CID: 4583) were obtained from PubChem web site. Docking simulations of mAbs with the ligands were performed using the molecular docking and visual screening program AutoDock vina by a modified method from Al Qaraghuli, M.M., et al. (2015). Structure of mAbs were added with polar hydrogen atoms and the generated models were saved as pdbqt files. The ligands (free drug) were investigated and saved in pdbqt format. The AutoDock vina could determine the docking position of the mAbs by setting the X, Y, and Z dimensions of the docking grid box to cover the binding site of the mAb , which the complementarity-determining regions (CDRs) of both the heavy and light chains of mAb are probably the active site. The coordinates and size of the grid boxes are given in Appendix B. The docking process was achieved using the command prompt into Windows 10. The command script below:

```
C:\Users\ (file name)>cd...
C:\Users>cd...
C:\>cd vina
C:\Vina>vina --config config.txt --log log.txt
C:\Vina>vina_split --input out.pdbqt
```

After the docking process finished, Vina score showed as Gibbs free binding energies were obtained from docking calculation. Finally, and the models were exported and analyzed by Discovery Studio 2019 and PyMOL Stereo 3D Quad-buffer, respectively.



## CHAPTER IV

### RESULTS AND DISCUSSION

#### 4.1 Conjugation of Drug-OVA

Norfloxacin (319.33 Da), enrofloxacin (359.40 Da), ciprofloxacin (331.34 Da), and ofloxacin (361.40 Da) are small molecules which are not suitable to be immobilized on the surface of ELISA plate. Therefore, these antibiotics must be conjugated to a carrier protein such as ovalbumin (OVA) and bovine serum albumin (BSA) to enlarge their sizes and expose their molecules in order to increase accessibility for binding. In this study, the antibiotics were conjugated to OVA (42.7 kDa) using carbodimide active ester method. In this method, peptide bond was formed between the carboxyl group of the antibiotics and the amino group of OVA. Protein concentrations of the conjugates were determined by BCA assay as shown in Table 4.1.

Table 4.1 Protein concentration of drugs by BCA assay.

Drug-OVA	Concentration of protein (mg/ml)
Norfloxacin-OVA	2.3464
Enrofloxacin-OVA	3.0436
Ciprofloxacin-OVA	3.6227
Ofloxacin-OVA	3.8979

Remark: The standard curve was shown in Appendix A.

#### 4.2 Production and Purification of MAb

After thawing from liquid nitrogen, anti-norfloxacin producing clone Nor132 and Nor155, and anti-enrofloxacin producing clone Enro44 and Enro48 were cultured in RPMI 1640 medium supplemented with 20% FCS. After expansion, monoclonal antibodies (mAbs) in culture media were purified using an ÄKTA affinity chromatography with HiTrap Protein G HP antibody purification column. The purified mAbs were harvested, diluted in PBS and quantified their concentrations based on the protein concentration. The protein concentrations were shown in table 4.2.

Table 4.2 Protein concentrations of purified mAbs by BCA assay.

Monoclonal antibody	Concentration of protein (mg/ml)
mAb Nor132	2.1200
mAb Nor155	4.7947
mAb Enro44	4.4930
mAb Enro48	3.7840

Remark: The standard curve was shown in Appendix A.

Molecular weight and purity of the mAb were checked by SDS-PAGE as shown in Figure 4.1. The result showed that only two-protein bands were found at approximately 25 kDa and 50 kDa which were in an agreement as found in findings of other reports<sup>53, 54</sup> that an mAb is made up of a heavy chain of approximately 50 kDa and a light chain of approximately 25 kDa. In addition, any minor band was clearly observed, thus indicating that the obtained mAbs were pure enough for uses in further study.

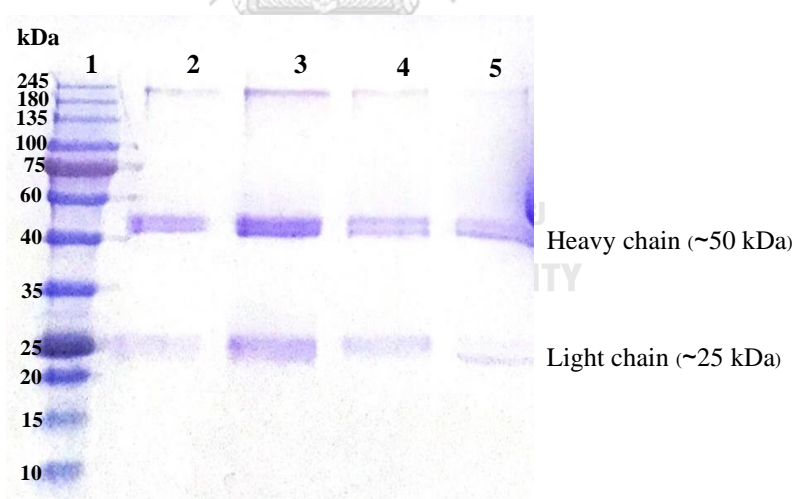


Figure 4.1 15% SDS-PAGE analysis of purified mAbs were loaded 20  $\mu$ l/well at a constant current of 25 mA per gel with 1 $\times$ Tris-glycine-SDS running buffer; standard protein marker (lane1), mAb Nor132 (lane2), mAb Nor155 (lane3), mAb Enro44 (lane4), and mAb Enro48 (lane5).

### 4.3 Sensitivity and Specificity of The Monoclonal Antibody

#### 4.3.1 Indirect ELISA

The binding capability of the mAbs with the antigens was analyzed by as antibody-captured indirect ELISA. Dose response curves of the assays were shown in Figure 4.2. The results showed that mAb Nor132 and mAb Nor155 can bind with both norfloxacin and ciprofloxacin but cannot bind with enrofloxacin and ofloxacin. On the contrary, mAb Enro44 and mAb Enro48 can bind with enrofloxacin and ofloxacin but cannot bind with norfloxacin and ciprofloxacin. It could be explained by the reason that Mab Nor132 and mAb Nor155 were raised by norfloxacin-ovalbumin (OVA) conjugate which was prepared by carbodiimide reaction. In this reaction, the carboxylic group of norfloxacin reacted with amino group of OVA to form the peptide bond, thus exposing the opposite side of the molecule for antibody recognition. Therefore, it is possible that the pyrazine ring is more susceptible to expose for antibody to recognize the antibiotics than the cyclopropane moiety<sup>55-57</sup> (Figure 4.3).

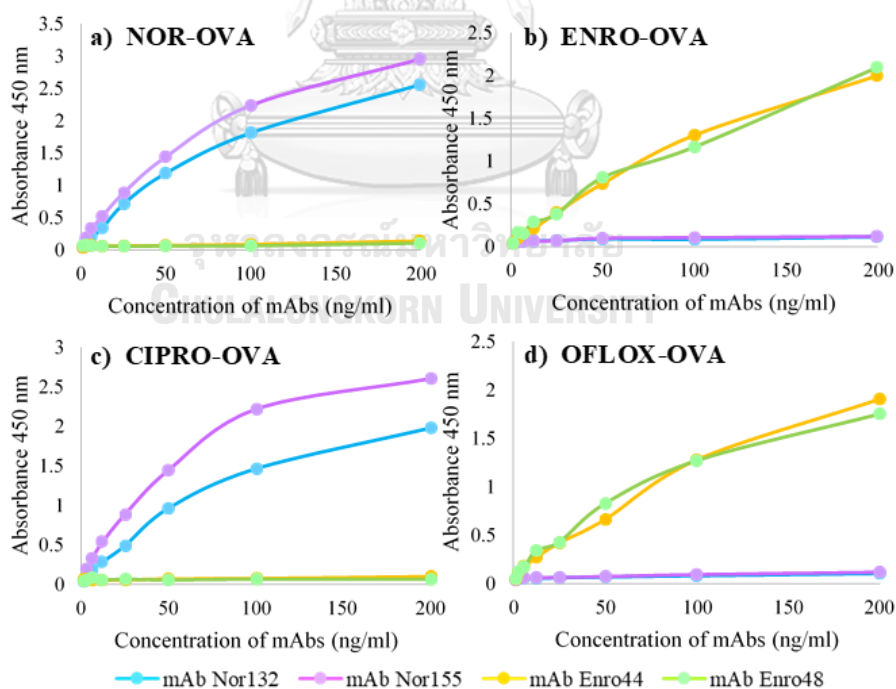


Figure 4.2 Affinity Constant curves of mAbs binding with drugs-OVA immobilized on surface of ELISA plate 3  $\mu\text{g/ml}$ ; a) NOR-OVA, b) ENRO-OVA, c) CIPRO-OVA, and d) OFLOX-OVA.

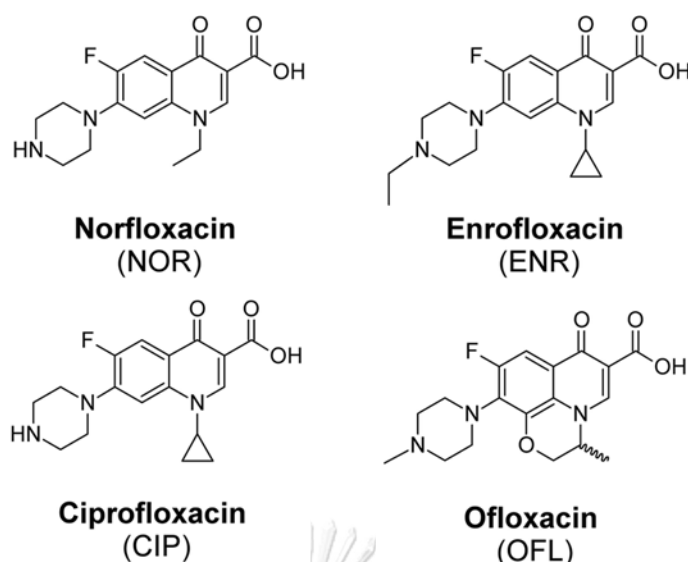


Figure 4.3 Some of fluoroquinolone Chemical structure of norfloxacin, ciprofloxacin enrofloxacin and ofloxacin. Modified from: Marina Rusch et al. (2019)

#### 4.3.2 Competitive Indirect ELISA

In the competitive indirect ELISA, norfloxacin, enrofloxacin, ciprofloxacin, and ofloxacin were separately added to the system in order to compete with the immobilized NOR-OVA or ENRO-OVA for binding with the mAbs. If the mAb can bind to the added competitor, a lower number of the mAb molecules are free to bind with immobilized antibiotic-protein conjugate, thus yielding the lower absorbance value. The dose response curves from the competitive indirect ELISA of all mAb were shown in Figure 4.4. The limit of detection (LOD) and the  $IC_{50}$  values obtained from the curves were summarized in Table 4.3. In term of the LOD value, mAb Nor132 ( $0.0086 \mu\text{g/ml}$ ) had high sensitivity than mAb Nor155 ( $0.0166\mu\text{g/ml}$ ) in binding with norfloxacin. But, in term of the  $IC_{50}$  value, mAb Nor155 ( $0.0511 \mu\text{g/ml}$ ) was more sensitive than the mAb Nor132 ( $0.1388 \mu\text{g/ml}$ ). These could be due to the different in the characteristics of the dose response curves where were used in the calculation. However, both mAbs were sensitive enough to be used in the detection of norfloxacin of which the MRL value was set at  $0.02 \text{ mg/ml}$ . In case of mAb Enro44 and mAb Enro48, the sensitivities in term of both LOD and  $IC_{50}$  were not so different.

The percentage of cross-reactivity (% CR) was calculated from the percentage ratio of the  $IC_{50}$  of norfloxacin or enrofloxacin to the  $IC_{50}$  of other interested compounds. The %CR of all tested competitors were also summarized in Table 4.3. It could be clearly seen that mAb Nor132 and mAb Nor155 could bind with the four FQs but mAb Enro 44 and Enro 48 rarely bound with other tested FQs except enrofloxacin. Moreover, previous studies reported that these mAbs did not cross-react with other compounds unrelated to the FQs group (Puthong S., unpublished data) and <sup>58</sup>. These indicated that mAb Nor132 and mAb Nor155 were suitable for the development of a generic or broad specificity test while mAb Enro44 and mAb Enro48 were suitable for use in a specific test.

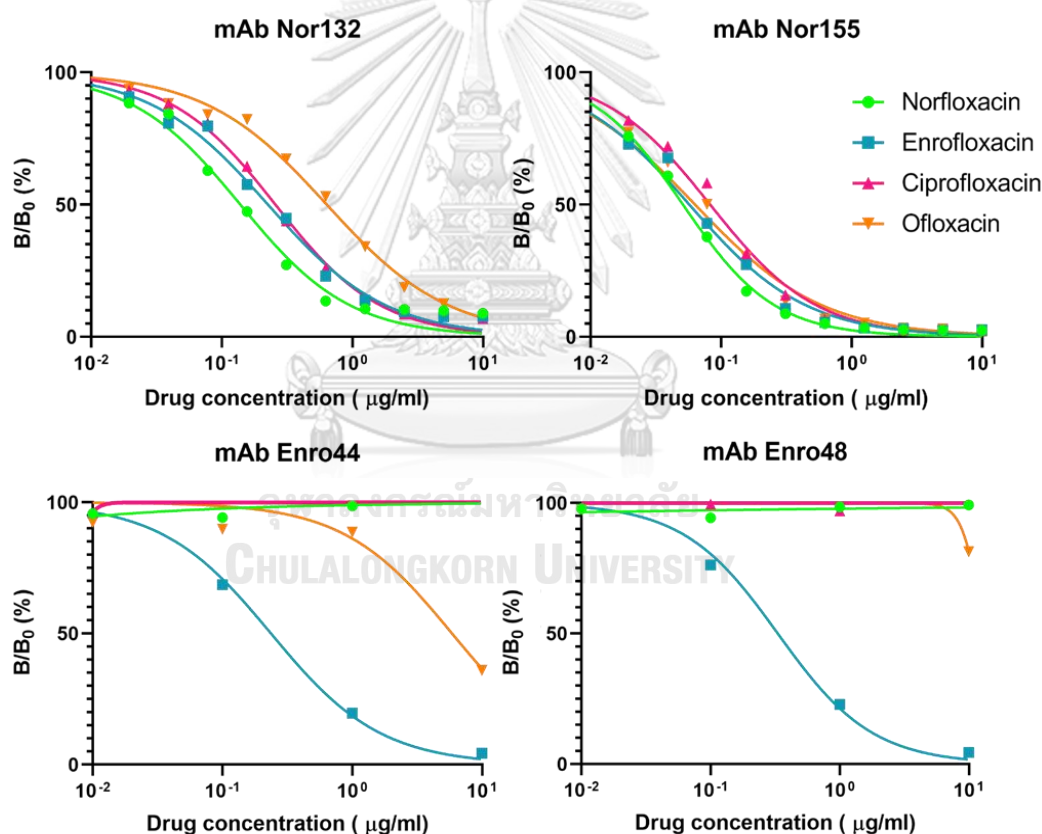


Figure 4.4 Calibration curves of icELISA base on NOR-OVA or ENRO-OVA for 4FQs. B is the absorbance of a tested free drugs; norfloxacin: enrofloxacin: ciprofloxacin: ofloxacin and  $B_0$  is the absorbance of buffer without free drugs. The standard curve was established by different concentrations of norfloxacin or enrofloxacin versus the values of  $B/B_0$ .

Table 4.3 IC<sub>50</sub> and Cross-reactivity of monoclonal antibody with various competitors by ELISA.

Competitors	LOD(µg/ml)				IC <sub>50</sub> (µg/ml)				Cross-reactivity (%)			
	mAb Nor132	mAb Nor155	mAb Enro44	mAb Enro48	mAb Nor132	mAb Nor155	mAb Enro44	mAb Enro48	mAb Nor132	mAb Nor155	mAb Enro44	mAb Enro48
Norfloracin	0.0086	0.0166	nd	nd	0.1388	0.0511	>10	>10	100%	<0.01%	<0.01%	<0.01%
Enrofloxacin	0.0060	0.0230	2.015	2.126	0.2257	0.0572	0.2369	0.3320	61.50%	89.34%	100%	100%
Ciprofloxacin	0.0105	0.0338	nd	nd	0.2576	0.0826	>10	>10	54.28%	61.86%	<0.01%	<0.01%
Ofloxacin	0.0054	0.0604	49.10	nd	0.6369	0.0633	5.883	>10	21.79%	80.73%	4.03%	<0.01%

\*nd = non determine

#### 4.4 Binding Affinities and Kinetic Analysis of Drug-mAbs Using SPR

SPR technology is capable provide information about the affinity value and the kinetic interaction between the mAbs and drugs. Moreover, it has become extensive technique in antibody-antigen interaction studies. Determination of kinetic association rate constant ( $k_a$ ), dissociation rate constant ( $k_d$ ), and the equilibrium dissociation constant ( $K_D$ ) of mAb Nor132, mAb Nor155, mAb Enro44, and mAb Enro48 were performed by SPR using Biacore T200, and the data was calculated by Biaevaluation software for chosen the suitable model fitting. In this study, the direct assay format was used for SPR, which used for determining the kinetic constant for binding of mAbs to FQ drugs were as follows: Drugs conjugate OVA (ligand) were immobilized onto the CM5 sensor chip, followed by injected mAbs (analyte) pass over the immobilized sensor chip. Due to nonspecific binding of drugs, the assay format whereby mAbs (ligand) were immobilized onto the CM5 chip, followed by binding drugs (analyte), were unsuccessful (result not shown). This format of SPR is like iELISA technique. As the previous results of iELISA shown that mAb Nor132 and mAb Nor155 specifically bind to norfloxacin and ciprofloxacin while mAb Enro44 and mAb Enro48 specifically bind to enrofloxacin and slightly ofloxacin. Thus, these binding affinities and kinetic between mAbs and drugs-OVA were examined. Generally, the kinetic of protein-protein will be 1:1 interaction, which one antibody bind to one antigen (Eq.5). Nevertheless, the data fitting for antigen-mAbs interaction in this research were done by bivalent model analysis since mAbs are bivalent monoclonal antibody. In SPR studies by Dagmar et al. (2017), reported that the bivalent antibodies can specifically bind to immobilized antigen with one binding site (1:1 bond) or both binding sites (bivalent bond). The binding of mAb to the immobilized surface has two steps when data was fitted by bivalent binding (Eq.6). First step, the bivalent antibody in solution bind to a surface bond ligand, while the second step can only occur when the remaining binding site of antibody bind a second ligand on the immobilized surface <sup>59</sup>.



where A is the analyte  
 B is the ligand  
 $k_a$  is the association rate constant  
 $k_d$  is the dissociation rate constant



where  $k_{a1}$  and  $k_{d1}$  are the association and dissociation rate constants for the first site  
 $k_{a2}$  and  $k_{d2}$  are the association and dissociation rate constants for the second site

#### 4.4.1 Comparing Binding Affinity of Immobilized NOR-OVA with MAb Nor132 and MAb Nor155

The immobilization of NOR-OVA at concentration 0.1  $\mu\text{M}$  on CM5 sensor chip was done using amine coupling. The NOR-OVA immobilization for mAb Nor132 and mAb Nor155 interaction studies was 50.9 RU. The NOR-OVA ligand was immobilized on flow cell 2 using flow cell 1 as reference (chip No.1). For kinetic analysis, different concentrations of mAb Nor132 were passed over the sensor surface in order of increasing slope from the lowest concentration to the highest concentration. The running buffer was HBS-EP<sup>+</sup> and the injected concentrations of mAb Nor132 were 240, 300, 320, 380, and 400 nM. The association time was from 0-400 s with flow rate 30  $\mu\text{l}/\text{min}$ , then the dissociation time was started when the injection was stopped, and only buffer was flowing. When finished all cycles, these data were calculated by Biaevaluation software. As the rate constant ( $k_a$ ,  $k_d$ ) and equilibrium binding constants ( $K_D$ ) were fitted globally, which all curves of the rate constant are fitted concurrently and give one value per parameter<sup>60</sup>. The representative sensograms of evaluated data are presented in Figure 4.5.



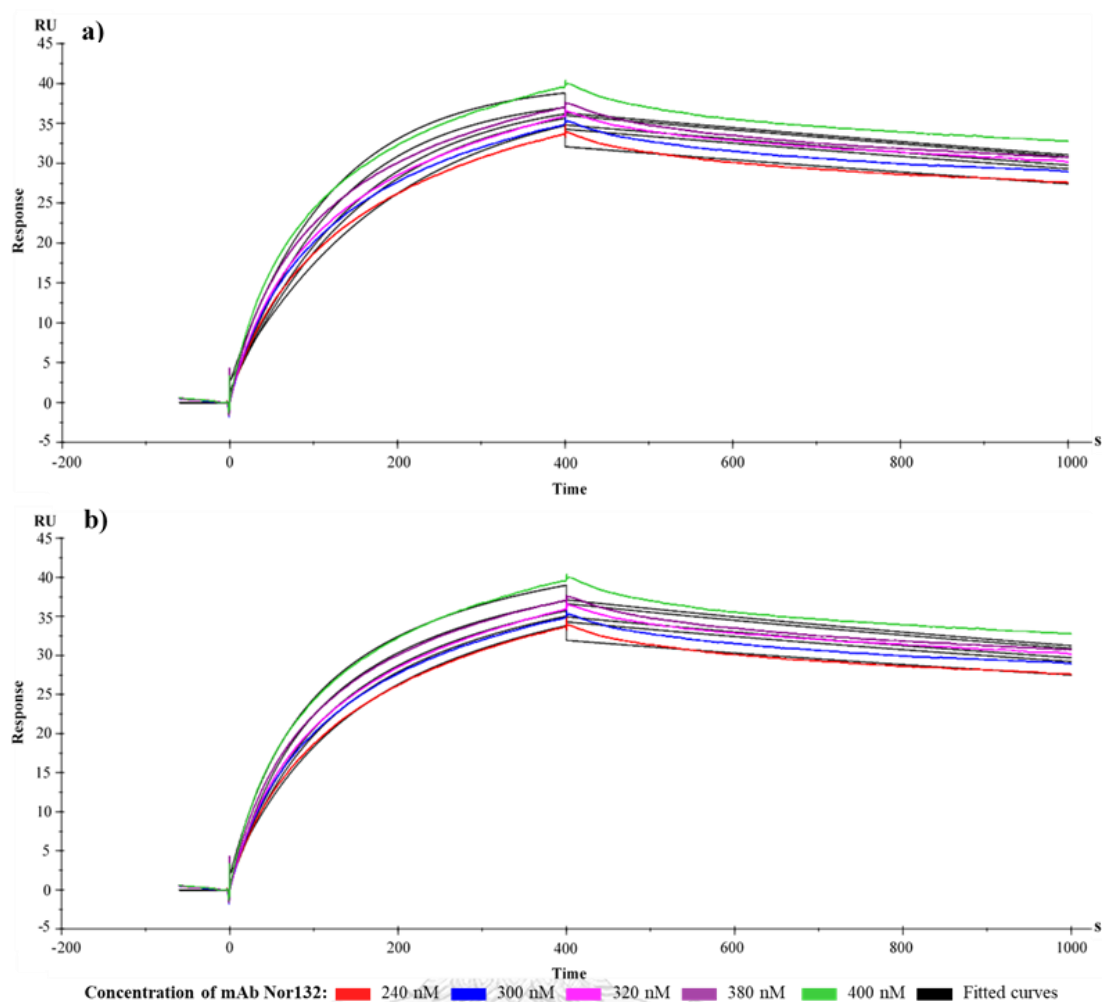


Figure 4.5 Illustrated data sets (color lines) for the SPR kinetic analysis of NOR-OVA with mAb Nor132 interactions. Different concentrations of mAb Nor132 were flow over the immobilized NOR-OVA. The association and dissociation times were 400 and 600 s, respectively, at a constant flow rate of 30  $\mu\text{l}/\text{min}$ . Black lines show the global fits of the data to a) 1:1 binding model and b) Bivalent binding model.

Figure 4.5.a shows the 1:1 fitted curves do not follow the data curves, especially in association rate while the Bivalent fitted quite follows the data curves (Figure 4.5. b). Thus, Bivalent binding model seems better fit than 1:1 binding model. Moreover, the  $\chi^2$  of Bivalent model was 0.368 while 1:1 model was 0.760, which the lowest  $\chi^2$  value shows a good fitting. From the result indicated that the Bivalent binding model was selected to the curve fitting. According to this analysis, mAb Nor132 showed  $k_a$  of  $9.904 \times 10^3 \text{ M}^{-1}\text{s}^{-1}$  and  $k_d$  of  $4.010 \times 10^{-4} \text{ s}^{-1}$ , resulting in a

calculated  $K_D$  of  $4.049 \times 10^{-8}$  M. As for mAb Nor155, it also used HBS-EP<sup>+</sup> buffer to dilute mAb concentrations of 70, 90, 100, 110, and 140 nM for 400 s at a constant flow rate of 10  $\mu\text{l}/\text{min}$ . The kinetic of mAb Nor155 was calculated by the Biaevaluation software using a Bivalent binding model in Figure 4.6.

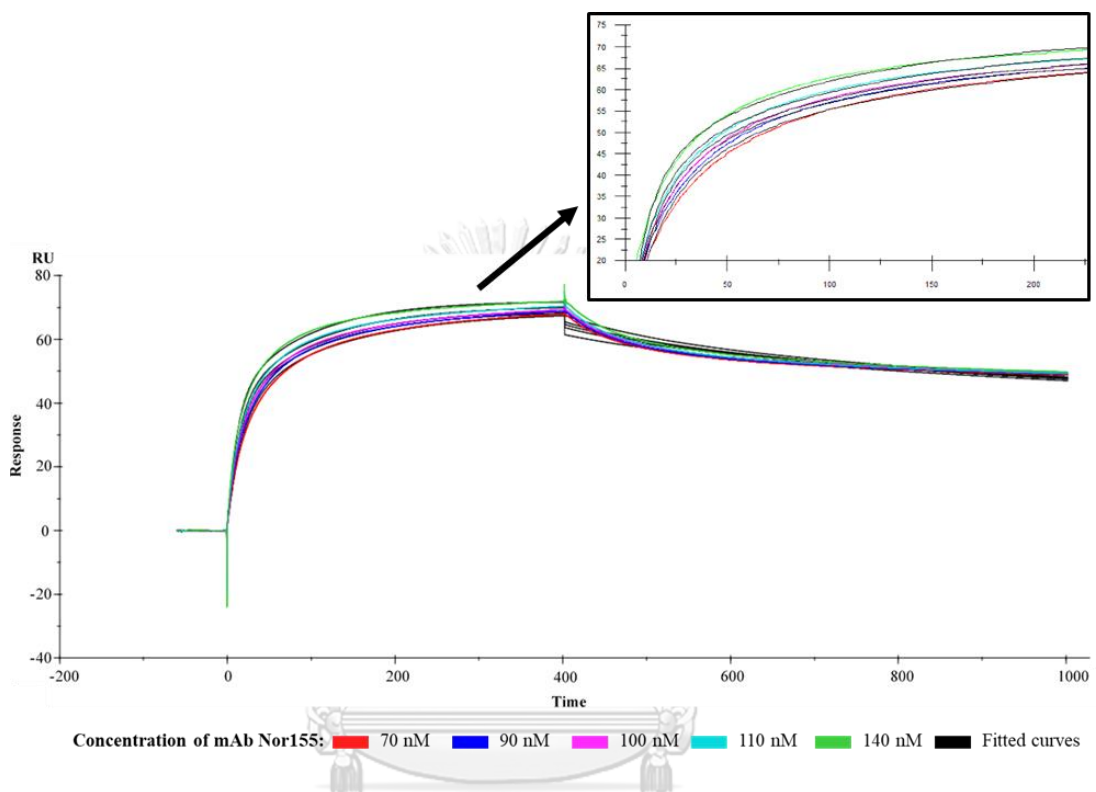


Figure 4.6 Kinetic analysis of NOR-OVA with mAb Nor155. Different concentrations of mAb Nor155 were flow over the immobilized NOR-OVA. The association and dissociation times were 400 and 600 s at a constant flow rate of 10  $\mu\text{l}/\text{min}$ . The response data were fit to Bivalent binding model (black lines)

The sensorgrams fitted using Bivalent binding model since this model showed a better fit than 1:1 Langmuir binding model (data not shown). From the data probably indicated that the analyte to bind first with one site to the ligand. The other site is closer contact with other ligand molecules and can bind to a second ligand site. The curves showed a slow dissociation with apparent  $k_a$  of  $2.773 \times 10^5 \text{ M}^{-1}\text{s}^{-1}$  and  $k_d$  of  $6.359 \times 10^{-3} \text{ s}^{-1}$ , resulting in a calculated  $K_D$   $2.293 \times 10^{-8}$  M. It has been reported that low  $K_D$  value indicates high affinity between the analyte and the ligand [16] which the

$K_D$  value of NOR-OVA with mAb Nor155 less than mAb Nor132. Therefore, the result suggested that mAb Nor155 bound to norfloxacin better than mAb Nor132 did.

#### **4.4.2 Comparing Binding Affinity of Immobilized CIPRO-OVA with MAb Nor132 and MAb Nor155**

The CIPRO-OVA was immobilized on flow cell 4 using flow cell 3 as reference (chip No.1) using amine coupling. The CIPRO-OVA immobilization for mAb Nor132 and mAb Nor155 interaction studies was 165.1 RU. The running buffer was PBS supplement with P20 (PBS+P20) buffer. The measuring kinetic interaction, the varying concentration of both mAbs were injected in PBS+P20 buffer, two-fold serial dilutions from 500 nM to 15.625 nM, over the immobilized CIPRO-OVA sensor chip for 400 s at a constant flow rate of 10  $\mu$ l/min (Figure 4.7). Kinetic parameters were determined by global fitting using Bivalent binding model. The kinetic affinity,  $k_a$  of  $2.931 \times 10^4 \text{ M}^{-1}\text{s}^{-1}$  and  $k_d$  of  $2.153 \times 10^{-2} \text{ s}^{-1}$ , and equilibrium dissociation constant,  $K_D$ , for ciprofloxacin and mAb Nor132 was determined as  $7.346 \times 10^{-7} \text{ M}$ . Kinetic experiments to determine the interaction between ciprofloxacin and mAb Nor155 were executed. Considering the dissociation rate constant ( $k_d$ ) to be  $5.597 \times 10^{-3} \text{ s}^{-1}$ , data was fitted for an association constant  $k_a$  of  $4.897 \times 10^4 \text{ M}^{-1}\text{s}^{-1}$  and a corresponding  $K_D$  of  $1.143 \times 10^{-7} \text{ M}$  was observed. From the result, mAb Nor155 bond to ciprofloxacin better than mAb Nor132. However, when compare the  $K_D$  values between norfloxacin and ciprofloxacin to mAb Nor155, mAb Nor155 could bond to norfloxacin better than ciprofloxacin. Therefore, these results have been related to sensitivity values from icELISA.

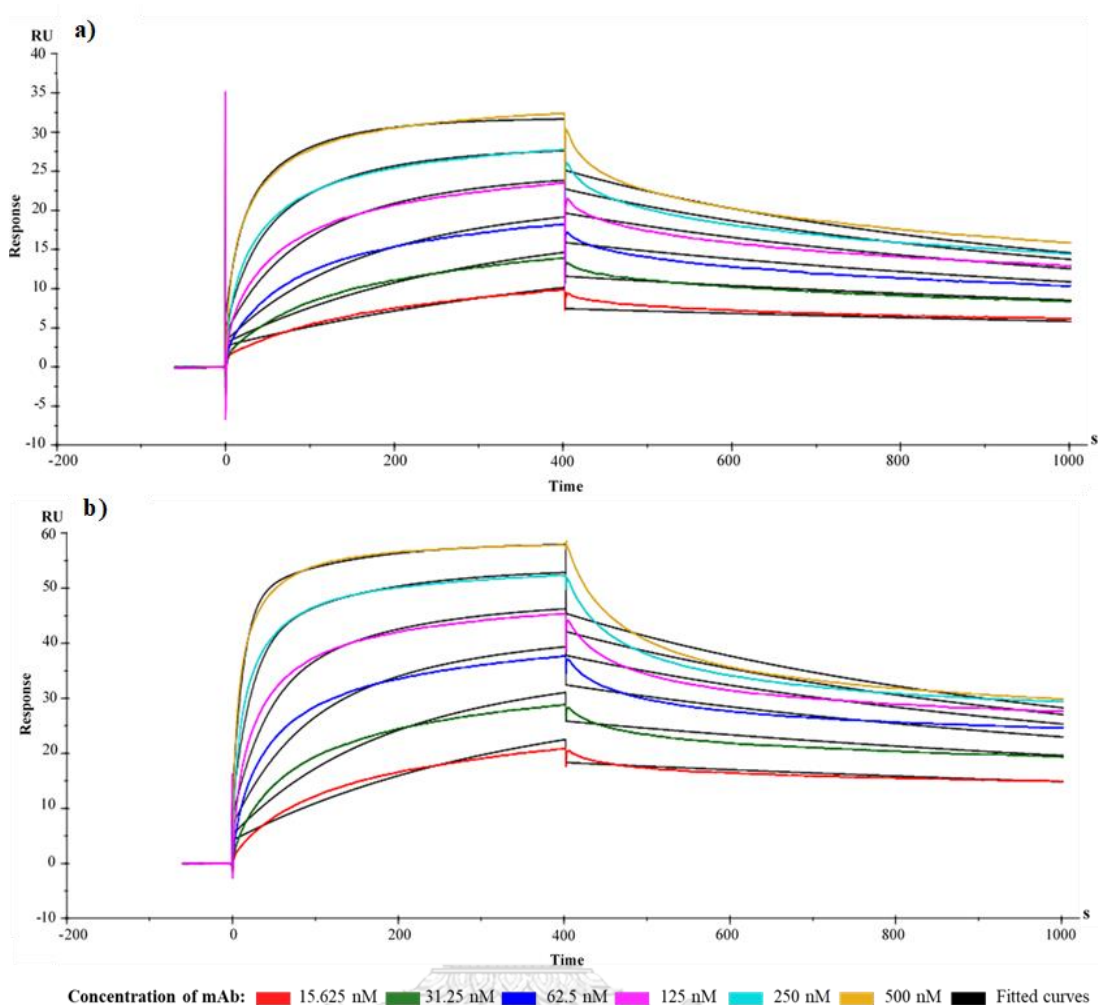


Figure 4.7 SPR sensorgrams of mAbs at two fold concentrations 15.625-500 nM; a) mAb Nor132 and b) mAb Nor155 on CM5 sensor chip which CIPRO-OVA was immobilized, and the association and dissociation times were 400 and 600 s at a constant flow rate of 10  $\mu$ l/min. Data fitted using Bivalent binding model (black lines).

#### 4.4.3 Comparing Binding Affinity of Immobilized ENRO-OVA with MAb Enro44 and MAb Enro48

The immobilization of ENRO-OVA on CM5 sensor chip was done using amine coupling. The ENRO-OVA immobilization for mAb Enro44 and mAb Enro48 interaction studies was 98.4 RU. The ENRO-OVA ligand was immobilized on flow cell 3 using flow cell 1 as reference (chip No.2). MAb Enro44 was used in increasing concentrations run from low to high order using kinetic analysis. HBS-EP<sup>+</sup> buffer was

used to make dilutions and the concentrations injected were 700, 800, 900, 1000, an 1100 nM. While mAb Enro48 was used at concentrations of 150, 200, 250, 350, and 400 nM. The representative sensorgrams of evaluated data are shown in Figure 4.8.

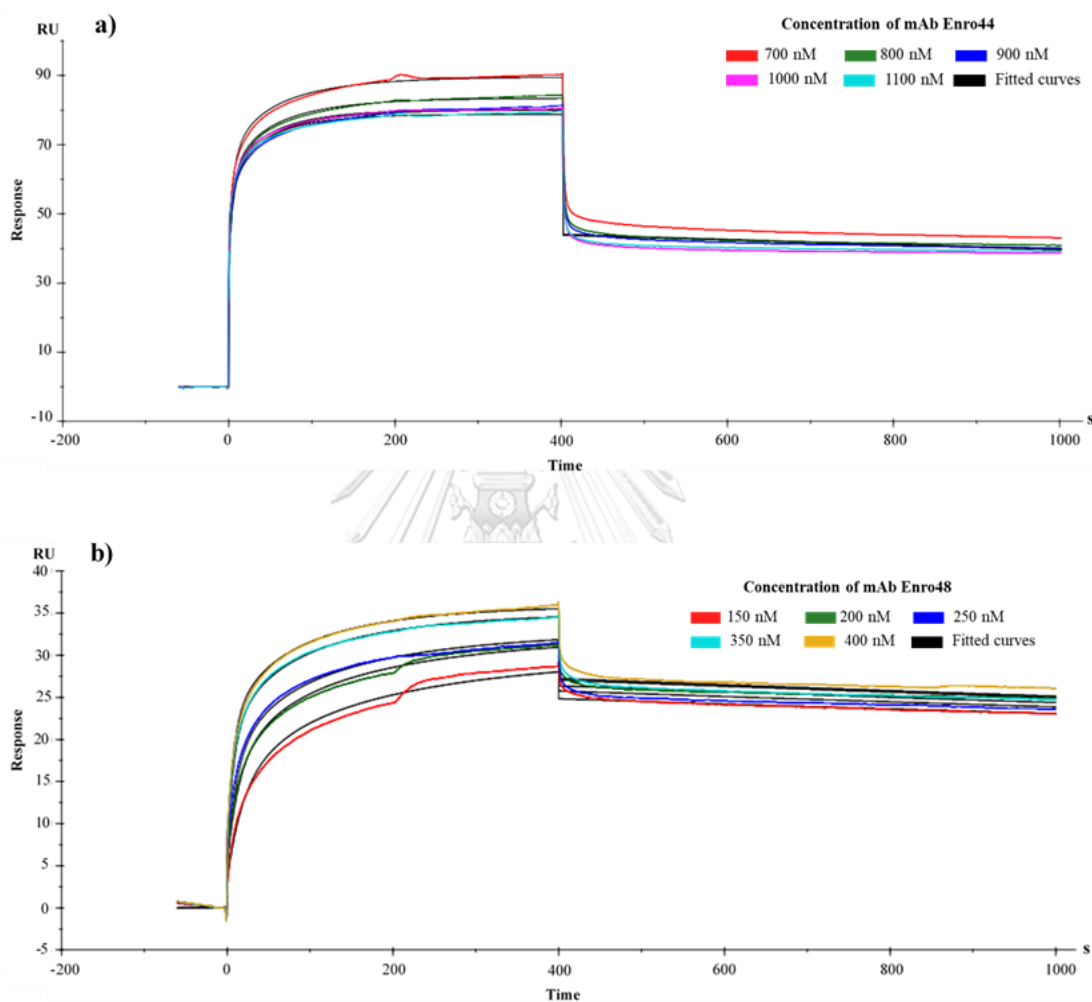


Figure 4.8 Kinetic analysis of a) mAb Enro44 and b) mAb Enro48 with ENRO-OVA using HBS-EP<sup>+</sup> buffer, the association and dissociation times were 400 and 600 s at a constant flow rate of 10  $\mu$ l/min. Data fitted using Bivalent binding model (black lines).

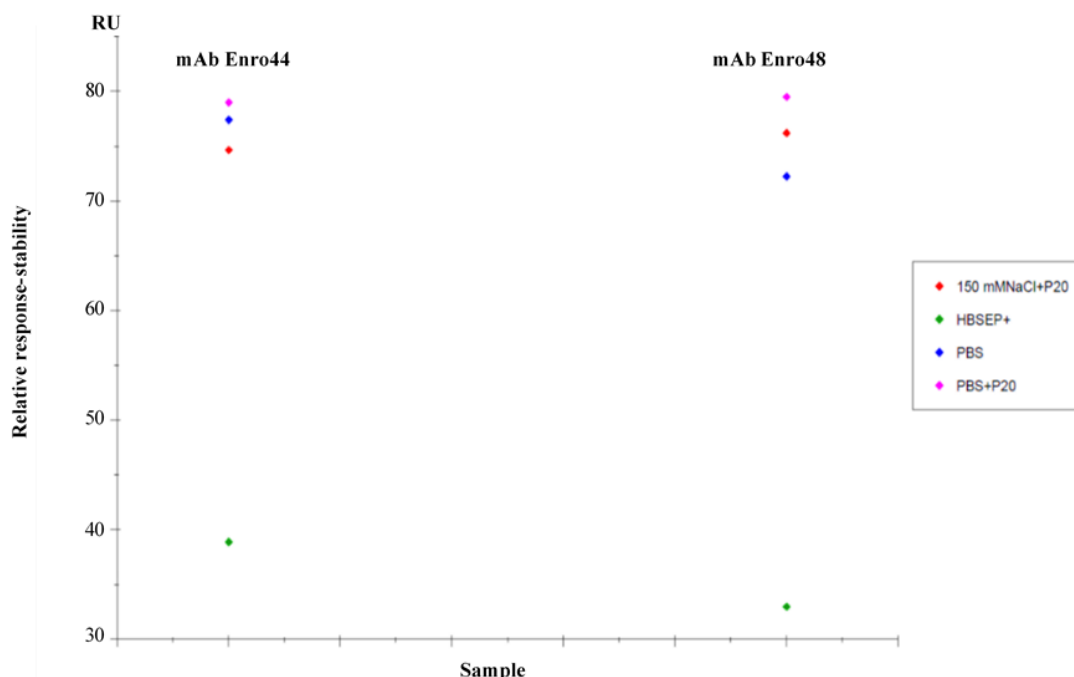


Figure 4.9 Buffer scouting for binding of ENRO-OVA with mAb Enro44 (left) and mAb Enro48 (right). The mAbs at concentration 1  $\mu$ M was diluted in different buffers; 150 mM NaCl+P20 (red), HBS-EP<sup>+</sup> (green), PBS (blue), and PBS+P20 (pink). The association and dissociation times were 400 and 120 s at a constant flow rate of 10  $\mu$ l/min.

The sensorgrams showed fast dissociation and couldn't use to evaluate kinetic which probably caused by the buffer mismatches (Figure 4.8). Thus, solving this problem was done by buffer scouting. The chosen buffers were 150 mM of NaCl+P20, HBS-EP<sup>+</sup>, PBS, and PBS+P20<sup>61</sup>. The data of buffer scouting are presented in Figure 4.9, PBS+P20 buffer shown the highest relative response compared with another buffer. Therefore, PBS+P20 was used to evaluate kinetic studies of mAb Enro44 and mAb Enro48 at the same concentrations. Mingfei Pan, et al. (2017) also used PBS containing 0.5% P20 for the detection of enrofloxacin residue in animal-derived food products. The fitted data for association and dissociation binding is shown in the Figure 4.10. The sensograms fitted using Bivalent analyte model, since this model had the lower  $\chi^2$  and closest fitting than 1:1 model. Considering the dissociation rate constant ( $k_d$ ) of mAb Enro44 and mAb Enro48 were

$1.614 \times 10^{-4} \text{ s}^{-1}$  and  $2.243 \times 10^{-4} \text{ s}^{-1}$ , respectively, while the association constant ( $k_a$ ) were  $3.745 \times 10^4 \text{ M}^{-1}\text{s}^{-1}$  and  $1.611 \times 10^4 \text{ M}^{-1}\text{s}^{-1}$ , respectively. Resulting in a calculated  $K_D$  of mAb Enro44 and mAb Enro48 were  $4.31 \times 10^{-9} \text{ M}$  and  $1.3923 \times 10^{-8} \text{ M}$ , respectively. Comparing mAb Enro44 and mAb Enro48 binding to ENRO-OVA, these results indicated that the mAb Enro44 is a stronger binding to ENRO-OVA than mAb Enro48. However, both mAbs show  $K_D$  values in the nanomolar range, indicating high binding interactions.

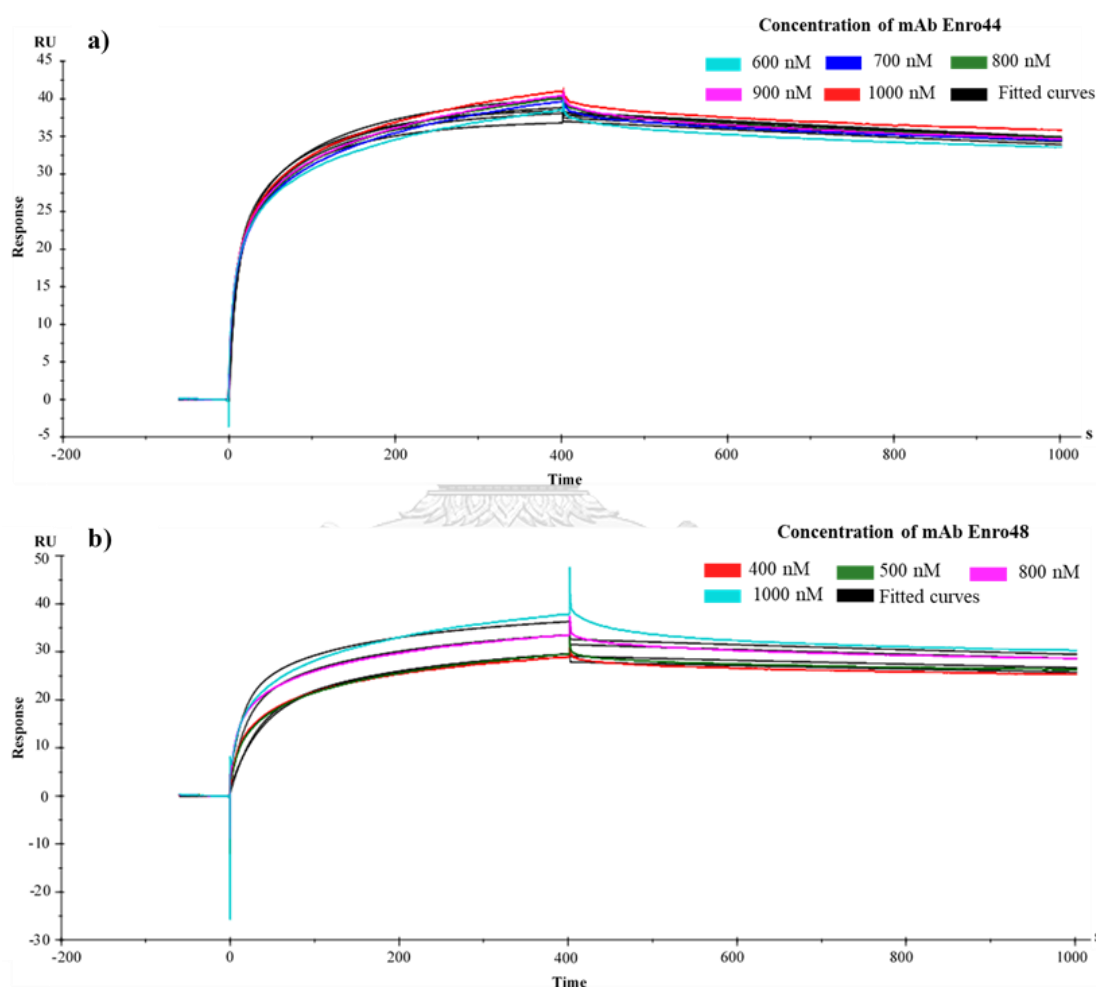


Figure 4.10 Kinetic analysis of a) mAb Enro44 and b) mAb Enro48 with ENRO-OVA using PBS+P20 buffer, the association and dissociation times were 400 and 600 s at a constant flow rate of  $10 \mu\text{l}/\text{min}$ . Data fitted using Bivalent binding model (black lines).

The kinetic result of mAbs by the Biaevaluation software using bivalent binding model were summarized in Table 4.4. When comparing our results to those of previous studies, it must be pointed out that the estimated kinetic constant value of mAbs were  $10^{-8}$ - $10^{-12}$   $M^{62-64}$ , signifying the acceptable capacity of antibody and antigen binding.

Table 4.4 Equilibrium dissociation constants and rate constants ( $k_a$  and  $k_d$ ) measured for mAbs and drug-OVA by Biacore.

Analyte	Ligand	$k_a$ ( $M^{-1}s^{-1}$ )	$k_d$ ( $s^{-1}$ )	$K_D$ (nM)
<b>mAb Nor132</b>	NOR-OVA	$9.904 \times 10^3$	$4.010 \times 10^{-4}$	40.49
	CIPRO-OVA	$2.931 \times 10^4$	$2.153 \times 10^{-2}$	734.60
<b>mAb Nor155</b>	NOR-OVA	$2.773 \times 10^5$	$6.359 \times 10^{-3}$	22.93
	CIPRO-OVA	$4.897 \times 10^4$	$5.597 \times 10^{-3}$	114.30
<b>mAb Enro44</b>	ENRO-OVA	$3.745 \times 10^4$	$1.614 \times 10^{-4}$	4.31
<b>mAb Enro48</b>	ENRO-OVA	$1.611 \times 10^4$	$2.243 \times 10^{-4}$	13.92

#### 4.5 Conformational Analysis of MABs Using CD Spectroscopy

The frequently technique for estimate of protein conformation in solution is CD spectroscopy. Far-UV CD spectra were recorded at wavelengths between 190 and 240 nm are directly related to the asymmetrical packing of the intrinsically chiral peptide bond groups of the secondary structure of the protein<sup>65</sup>. Different buffers for CD spectroscopy affect sample conformation data. Appropriate buffer for dissolved protein should be as transparent as possible such as water, which has the highest transparency and not contain any material<sup>66</sup>. However, some proteins denature in water include mAbs in this research. The far UV CD data of mAb Nor155 dissolve in different buffer (Fig 4.11). The secondary structure analysis of mAb Nor155 in different buffers (Table 4.5) were analyzed by the CDNN software<sup>67</sup>, which predicted secondary structure elements for the mAb Nor155 in phosphate buffered saline pH 7.4 (PBS) consist of  $\alpha$ -helix 19.6%,  $\beta$ -sheet 40.6%, and random coil 39.8%. Comparison secondary structure conformations of mAb Nor155 in PBS from another buffer, in PBS supplement P20 (PBS+P20),  $\alpha$ -helix and random coil conformations reduced



with an increase in  $\beta$ -sheet and  $\beta$ -turn conformations;  $\beta$ -sheet 63%,  $\beta$ -turn 35.2%, and random coil 1.7%. The CD spectra of mAb Nor155 in NaCl supplement P20 (NaCl+P20) increases the percentage of  $\alpha$ -helix from 19.6% to 73.1% and followed by decrease  $\beta$ -sheet from 40.6% to 26.9%. The increment of  $\beta$ -sheet could find in HBSEP<sup>+</sup> 62.5%, like the PBS+P20 buffer. These results are resemble with catumaxomab include  $\alpha$  helical 6.2%,  $\beta$ -sheet 37.5%,  $\beta$ -parallel 5.4%,  $\beta$ -turn 18%, and random coil 34.9%<sup>68</sup>. According to Joshi, et al. (2014), the secondary structure elements in IgGs consist of the antiparallel  $\beta$ - sheet,  $\beta$ -turns and random coil conformations. Moreover,  $\alpha$ -helices are found in some bends of mAb. For kinetic binding, buffer influences on antibody-antigen binding. So, indicating that percentage of  $\beta$ -sheet when mAb Nor155 was diluted in PBS+P20 and HBSEP<sup>+</sup> quite the same, which both buffers present  $\beta$ -sheet more than another buffer. As these results related to SPR analysis, which proper buffer for determining the kinetic constant of mAb Nor155 with norfloxacin are HBSEP<sup>+</sup> while used PBS+P20 for ciprofloxacin.

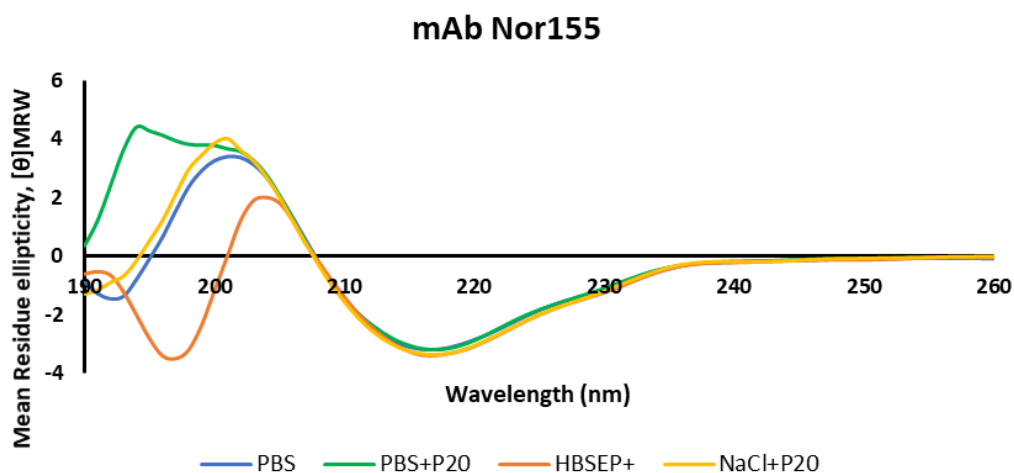


Figure 4.11 The far-UV CD spectra at 4 °C for mAb Nor155 in different buffers.

Table 4.5 Secondary structure analysis of mAb Nor155 in different buffer.

<b>Results</b>	<b>%Helix</b>	<b>%Strand (Beta sheet)</b>	<b>%Turn</b>	<b>%Unordered (Random coil)</b>	<b>Total (%)</b>
<b>PBS</b>	19.6	40.6	0	39.8	100
<b>PBS+P20</b>	0	63	35.2	1.7	100
<b>NaCl+P20</b>	73.1	26.9	0	0	100
<b>HBSEP<sup>+</sup></b>	0	62.5	0	37.5	100

#### 4.6 Amino Acid Sequence Analysis and 3D Structure Prediction of MAbs

To explain binding of mAbs-antigen interaction, the homology modelling of mAbs 3D structure with the ligand was regenerated based on template from SWISS-MODEL server (<https://swissmodel.expasy.org/>) that shown in Figure 4.12. As mAb Nor132 shown the percentage of sequence identity with the template of heavy chain (VH) (PDB ID: 1a0q.1.B) and light chain variable (VL) (PDB ID: 2y6s.1.A) are 83.87% and 87.72%, respectively. The mAb Nor155 has 87.10% and 94.23% sequence identity with the template of VH (PDB ID: 5do2.1.B) and VL (PDB ID: 4qnp.1.C), respectively. The identity of mAb Enro44 with template; 80.17% VH (PDB ID: 2aab.1.B) and 95.28% VL (PDB ID: 4amk.1.B). While the sequence identity of mAb Enro48 with the VH (PDB ID: 2R29) and VL (PDB ID: 2y6S) template are 82.93% and 94.23%, respectively. Moreover, in determining whether the model is reliable and accurate, GMQE and QMEAN score were also considered which the result showed in Table 4.6. GMQE (Global Model Quality Estimation) provided expected accuracy of a model built with that alignment and template and the coverage of the target when the score high closer to 1 indicate higher reliability. While QMEAN score uses statistical potentials of mean force to provide global and local absolute quality estimates when the score around zero indicate good agreement between the model structure and target structures of similar size. In case of score -4.0 or below indicated low quality<sup>69</sup>. After superimposed x-ray structure with PyMOL, which V<sub>H</sub> and V<sub>L</sub> of each mAbs were combined. The mAbs were composed of two chains (H and L) and interacting with all CDRs; CDR1, CDR2, and CDR3. The mAbs fold consists of a pair of  $\beta$  sheets, each built of antiparallel  $\beta$  strands, and surrounding a central hydrophobic core.

```

Nor132VH  NVELKESDAEWVKPGASVKISCKAFGYTFDHTIHWMKQKPEQGLEWIGYISPGNGDIQY
1a0q.1.B  -VQLQESDAELVKPGASVKISCKASGYTFDHIHVVWVKQKPEQGLEWIGYISPGNGDIKY
*.*****
Nor132VH  NEKFKGKATLTADKSSNTAYMQLNSLTSEDSALYFCN---YYDSEGDYWGQGTSLTVSSA
1a0q.1.B  NEKFKGKATLTADKSSNTAYMQLNSLTSEDSAVYLCKRGYYGRSNVDYWGQGTTLTVSSA
*****
Nor132VH  KTTPPSVY
1a0q.1.B  KTTPPSVY
*****

Nor132VL  DIVITQSPASLAVSLGORATISYRASKSVSTSGYSYMHWNQOKPGOPRLLIYLVSNLES
2y6s.1.A  DIVLTQSPASLAVSLGORATISCRASKSVSTSGYSYMHWNQOKPGOPRLLIYLVSNLES
***.*****
Nor132VL  GVPARFSGSGSGTDFTLNIHPVEEEDAATYYCOHIRELTRSEGGPSWK
2y6s.1.A  GVPARFSGSGSGTDFTLNIAPVEEEDAATYYCQHIAELTRTFGG----
*****
Nor155VH  EVELEESGGGLVKPGGSLKLSCAASGFPSFDYMYVWVROTPKRWLVVAITISEGASYTY
5do2.1.B  DVKLVESGGGLVKPGGSLKLSCAASGFTFSSYTMWVROTPKRWLVVATISSGGSYTY
*.*****
Nor155VH  SDSVKGRFTISRDNARNTLYLQMSLSKSEDTAIYYCTRAYNNYVSKYFDVWGAGTTVTVS
5do2.1.B  PDSVKGRFTISRDNARNTLYLQMSLSKSEDTAMYYCTRDGN----DYDYWGQGTTLTVS
*****
Nor155VH  SAKTTPPSVY
5do2.1.B  SAKTTPPSV-
*****

Nor155VL  DIVMTQSTAILSASPGEKVTMTCRASSRVNYIHWFOOKAGSSPKPWIYATSNLASGVPDR
4qnp.1.C  -IVLSQSPAILSASPGEKVTMTCRTSSSVSYMHVYQOKPGSSPKPWIYATSNLASGVPFR
*.*****
Nor155VL  FSGRSGTSYSLTISRVEAEDAATYYCOOWSNPNPWFVGGGKLEIKRADAAPTVS
4qnp.1.C  FSGSGGTSYSLTISRVEAEDAATYYCQOWNSNPPTFGGGKLEIKRADAAPTVS
***.*****

Enro44VH  EVELKKSGGGLVOPGGRKLSCAASGFTFSSFGMHVWVROAPEKGLEWVAYISSGSSLHY
2aab.1.B  DVQLVESGGGLVOPGGRKLSCAASGFTFSSFGMHVWVROAPEKGLEWVAYISSDSSNIYY
*.*****
Enro44VH  ADTVKGRFTISRDNPKNQIFLQNSVTAEDTATYYCTREFIT--TSTWYFDVWGAGTTVT
2aab.1.B  ADTVKGRFTISRDNPKNTLFLQMTSLRSEDTAMYYCARSNYVGYHVRWYFDVWGAGTTVT
*****
Enro44VH  VSS
2aab.1.B  VSS
***

Enro44VL  RAVVTQESALTTSPGDTVLTICRSSTGAVTTSNYANWVQEKPDHLFTDLIGGTSNRVPGV
4amk.1.B  QAVVTQESALTTSPGETVLTICRSSTGAVTTSNYANWVQEKPDHLFTGLIGGTNNRAPGV
*.*****
Enro44VL  PARFSGSLIGDKAALTTITGAQTEDEAIYFCALWYSNHLVFGGGTKL
4amk.1.B  PARFSGSLIGDKAALTTITGAQTEDEAIYFCALWYSNHLVFGGGTKL
*****

Enro48VH  EVELEKSGAELVKPGASVKLSCTASGFNIKDTYIHWVRLRPEQGLEWIGRT--ANGNTRY
2r29.1.B  EVQLQSGAELVKPGASVKLSCTASGFNIKDTYMHVWVKQRPEQGLEWIGRIDPANGYSKY
*.*****
Enro48VH  DPKFQVEATITDTSNTAYLQLSRLTSEDTALYYCARSEGIYYSYAWFAYWGQGLTVT
2r29.1.B  DPKFQKATITADTSSNAYLQLSSLTSEDTAVYFCAR----DYEGFAYWGQGLTVT
*****
Enro48VH  SAAKTTPPSVY
2r29.1.B  SAAKTTPPSVY
*.*****

Enro48VL  DIVMTQSPASLAVSLGORATISYRASKSVSTSGYSYMHWNQOKPGOPRLLIYLVSNLES
2y6s.1.A  DIVLTQSPASLAVSLGORATISCRASKSVSTSGYSYMHWNQOKPGOPRLLIYLVSNLES
***.*****
Enro48VL  GVPARFSGSGSGTDFTLNIHPVEEEDAATYYCOHIRELTRSEGGPSWK
2y6s.1.A  GVPARFSGSGSGTDFTLNIAPVEEEDAATYYCQHIAELTRTFGG----
*****

```

Figure 4.12 Sequence alignment of V<sub>H</sub> and V<sub>L</sub> of mAbs with the template; Nor132 (V<sub>H</sub>:1a0q.1.B, V<sub>L</sub>:2y6s.1.A), Nor155 (V<sub>H</sub>:5do2.1.B, V<sub>L</sub>:4qnp.1.C), Enro44 (V<sub>H</sub>:2aab.1.B, V<sub>L</sub>:4amk.1.B), Enro48 (V<sub>H</sub>:2r29.1.B, V<sub>L</sub>:2y6s.1.A), and the CDR1 (orange), CDR2 (yellow) and CDR3 (pink).

Table 4.6 Prediction of the mAbs structure with SWISS-MODEL program.

Model		Template	Organism	GMQE	QMEAN
mAb Nor132	V <sub>H</sub>	1a0q.1.B	Mus musculus	0.97	0.39
	V <sub>L</sub>	2y6s.1.A	Mus musculus	0.96	-1.81
mAb Nor155	V <sub>H</sub>	5do2.1. B	Mus musculus	0.84	0.02
	V <sub>L</sub>	4qnp.1.C	Mus musculus	0.96	-0.6
mAb Enro44	V <sub>H</sub>	2aab.1. B	Mus musculus	0.92	-1.42
	V <sub>L</sub>	4amk.1. B	Mus musculus	0.99	-0.52
mAb Enro48	V <sub>H</sub>	2r69.1. B	Mus musculus	0.81	-2.52
	V <sub>L</sub>	2y6s.1.A	Mus musculus	0.97	-1.76

#### 4.7 Molecular Docking

Theoretically, mAb structure consist of four polypeptide chains, comprising two heavy chains (H chain) and two light chains (L chain). Each of heavy chains and Light chains has constant region (C), which identifies the isotype of antibody, and the amino-terminal variable or variable region (V) at the tip of the arms of antibody, which conduces to the antigen-binding site (Figure 4.13). The crucial part of variable regions is complementarity determining regions (CDRs), which are the high diversity of antigen specificities. For this reason, predicting antigen-antibody interaction will focus on the antigen binding site (V<sub>H</sub> and V<sub>L</sub>) region.

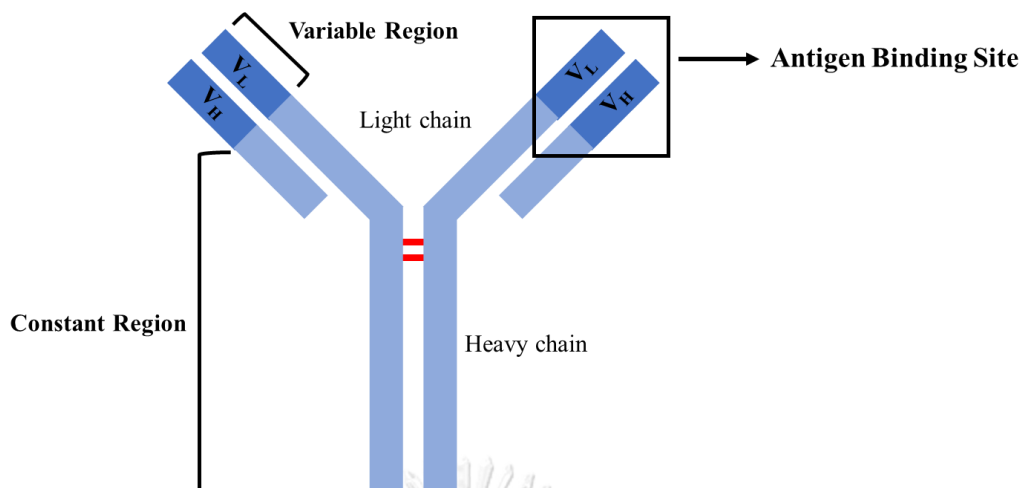


Figure 4.13 Structure of a typical antibody is composed of two heavy chains and two light chains linked by disulfide bonds which each heavy chain is linked to a light chain and the two heavy chains are linked together.

The best molecular docking by placing ligand into the active site of the mAbs using AutoDock vina, which uses global optimizer to provide repeated docking results for ligands with approximately 20 flexible bonds<sup>70, 71</sup>. This program would give the various snapshots when the protein dock with ligands. In this study, mAb-drug docking was done by blind docking method because the binding pocket of mAbs were unknown. Therefore, whole mAb was enclosed into grid box. Besides the energy binding, the proper lowest binding energy of ligand poses was selected since the score was calculated based on the negative of the sum component in term of energy, which the best-fitted ligand binding position has the least energy. Figure 4.14a shows that most of the ligands posed into CDRs area. Therefore, the area of ligand poses was significantly considered which mAb subdomains of HCDR1, HCDR2, HCDR3, LCDR1, LCDR2, and LCDR3 are favorable for interaction with targeted fluoroquinolone molecules (Figure 4.14). The apposition of complementary shapes results in numerous contacts between amino acids at the binding surfaces of both molecules. Principally, numerous hydrogen bonds, electrostatic interactions, and van der Waals interactions, reinforced by hydrophobic interactions, combine to give specific and strong binding<sup>72, 73</sup>. Furthermore, the binding models were examined by PyMOL Stereo 3D Quad-buffer, and the prediction of different amino acid residues

interacts with the homology modeling of mAbs using Discovery Studio 2019 client (BIOVIA Inc, Shenzhen, China).

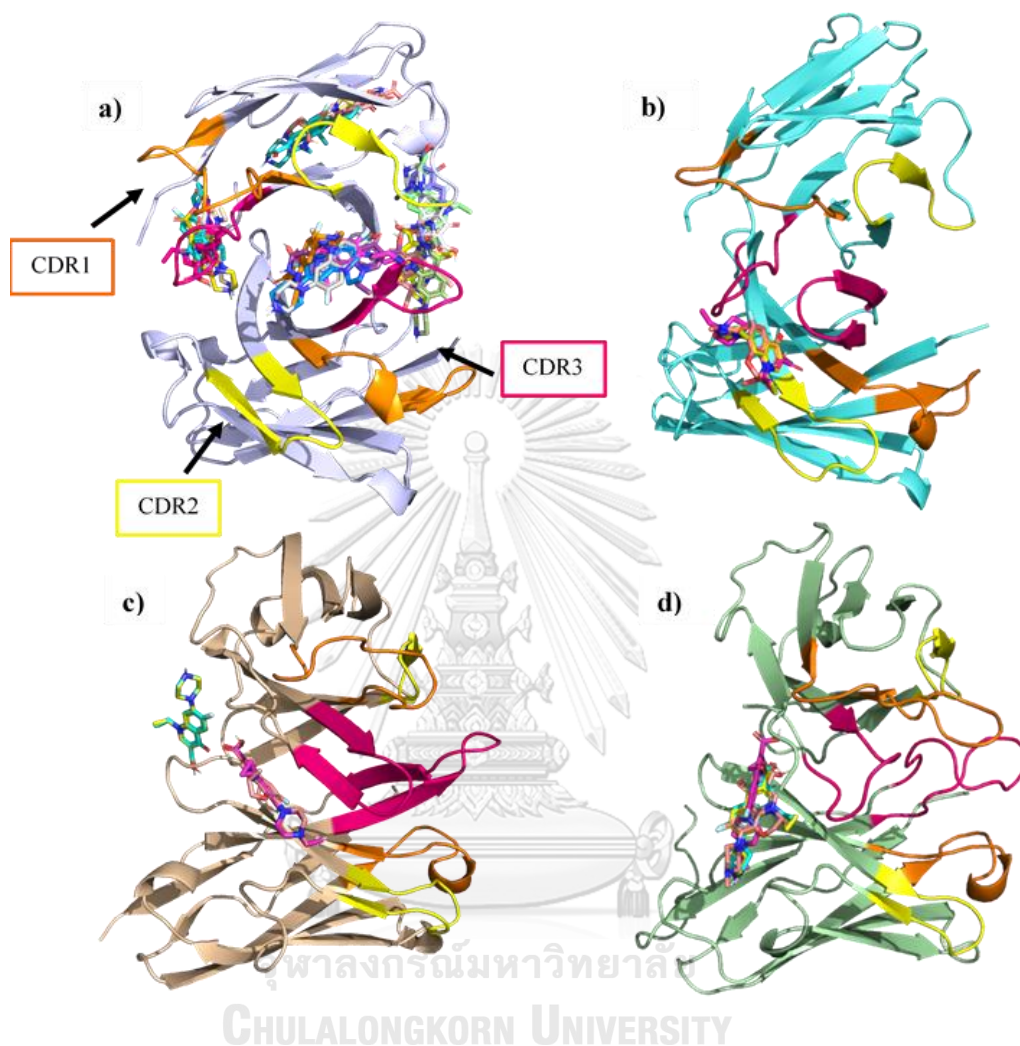


Figure 4.14 Showing the docked FQ molecules include norfloxacin (cyan), enrofloxacin (magenta), ciprofloxacin (yellow), and ofloxacin (salmon pink) with mAbs; a) mAb Nor132, b) mAb Nor155, c) mAb Enro44, and d) mAb Enro48. Image created in PyMOL.

From the docking results, the docked conformation of mAb Nor132 with 4FQs reveal binding energies between  $-7.3$  kcal/mol to  $-7.8$  kcal/mol. As norfloxacin, enrofloxacin, and ciprofloxacin make carbon hydrogen bonds to histidine residue (HIS) at amino acid sequence position 38 of light chain (L:38); HIS (L:38) and ASP (H:100) while ofloxacin makes only single carbon hydrogen bonds to binding site

residue ASP (H:100), and the phenyl group of 4FQs could form  $\pi$ - $\pi$  stacking interactions with TYR (H:99) residues. Additionally, all ligand poses in the area between pocket site HCDR3 and LCDR3, (Figure 4.15). From the result, it can be seen that the binding energies of docking were highly related to the specificity of FQs-mAb for Nor132 observed in icELISA assay except ofloxacin (Table 4.3). As ofloxacin had the binding energy higher than another drugs, probably because ofloxacin bonds with ASP (H:100) residues with the bonding length lesser than 3.45 Å while another drug bond with ASP (H:100) at approximately 3.64 Å of bonding length, which causes the best fitness to mAb Nor132. However, HIS (L:38) and ASP (H:100) residues were probably the major binding site of mAb Nor132. In addition, the docking conformation of mAb Nor155 with a target FQ molecule were examined. All ligands interact with the same residues as conventional hydrogen bonds with binding site residues TYR (H:35), ASN (H:101), and LYS (H:106) and carbon hydrogen bond with ASN (L:92) and ASN (L:93), and other hydrophobic contributors like  $\pi$ - $\pi$  stacking interaction with TYR (H:59) presumably provided better fitting in mAb Nor155 pocket site. Furthermore, the ligand structures are positioned quit similarly in the pocket site HCDR2, HCDR3, and LCDR3 (Figure 4.16).

Comparing mAb Nor132 and mAb Nor155 docking, both mAbs could form bonds with 4FQs into the CDRs pocket site of mAbs. Whereas, mAb Nor155 had more interact with different bonds. It probably concludes that mAb Nor155 was more well fit than mAb Nor132. These reasons could possibly support the different affinities result between mAb Nor132 and mAb Nor155 from SPR assay. Moreover, these results concluded that both mAbs could bind all drug by interaction with several bonds. Basically, interaction of antibody-antigen is hydrogen bond which strong interaction.

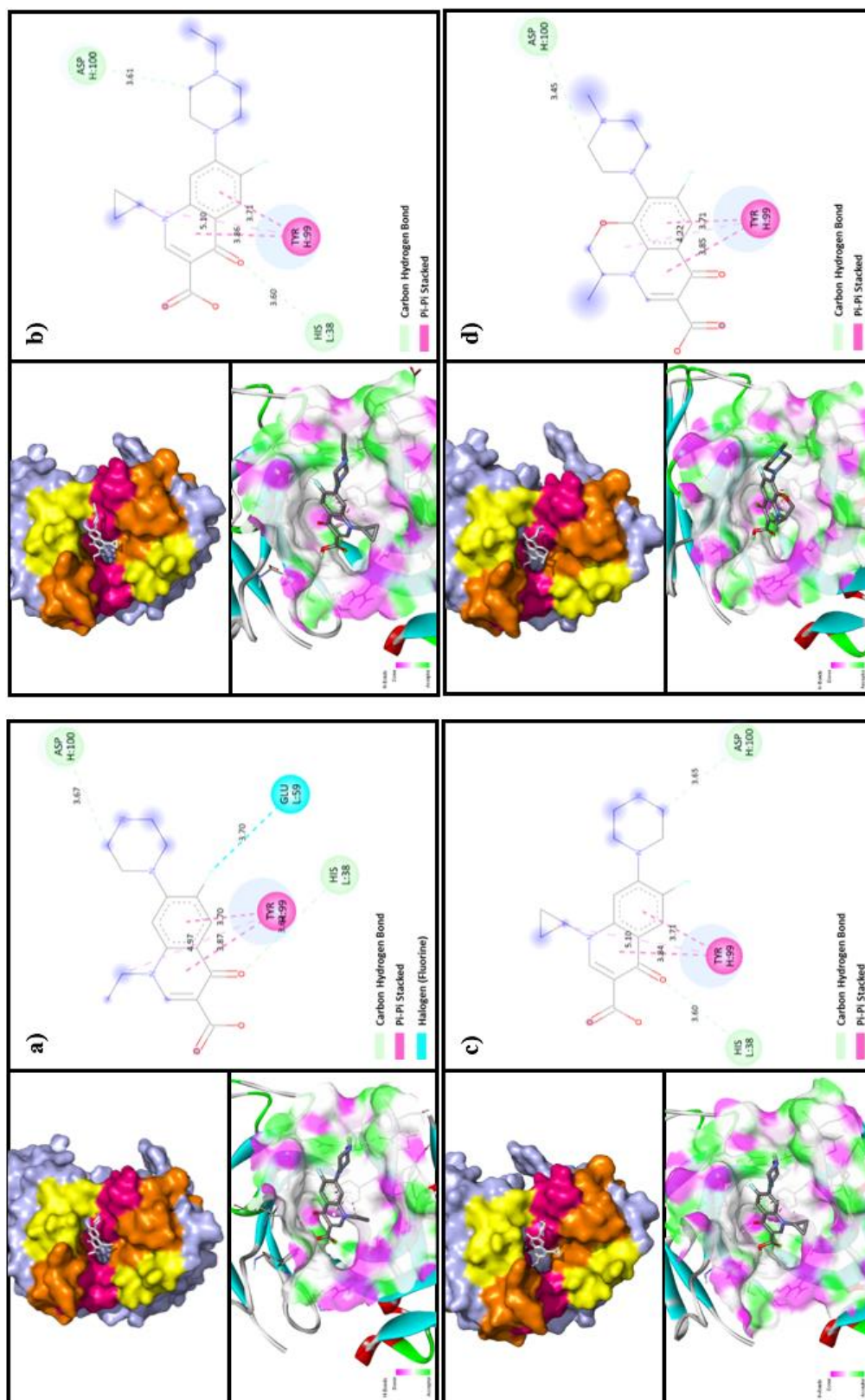


Fig 4.15 Schematic diagram of the binding of mAb Nor132 and a target FQ molecules; a) norfloxacin, b) enrofloxacin, c) ciprofloxacin, and d) ofloxacin.



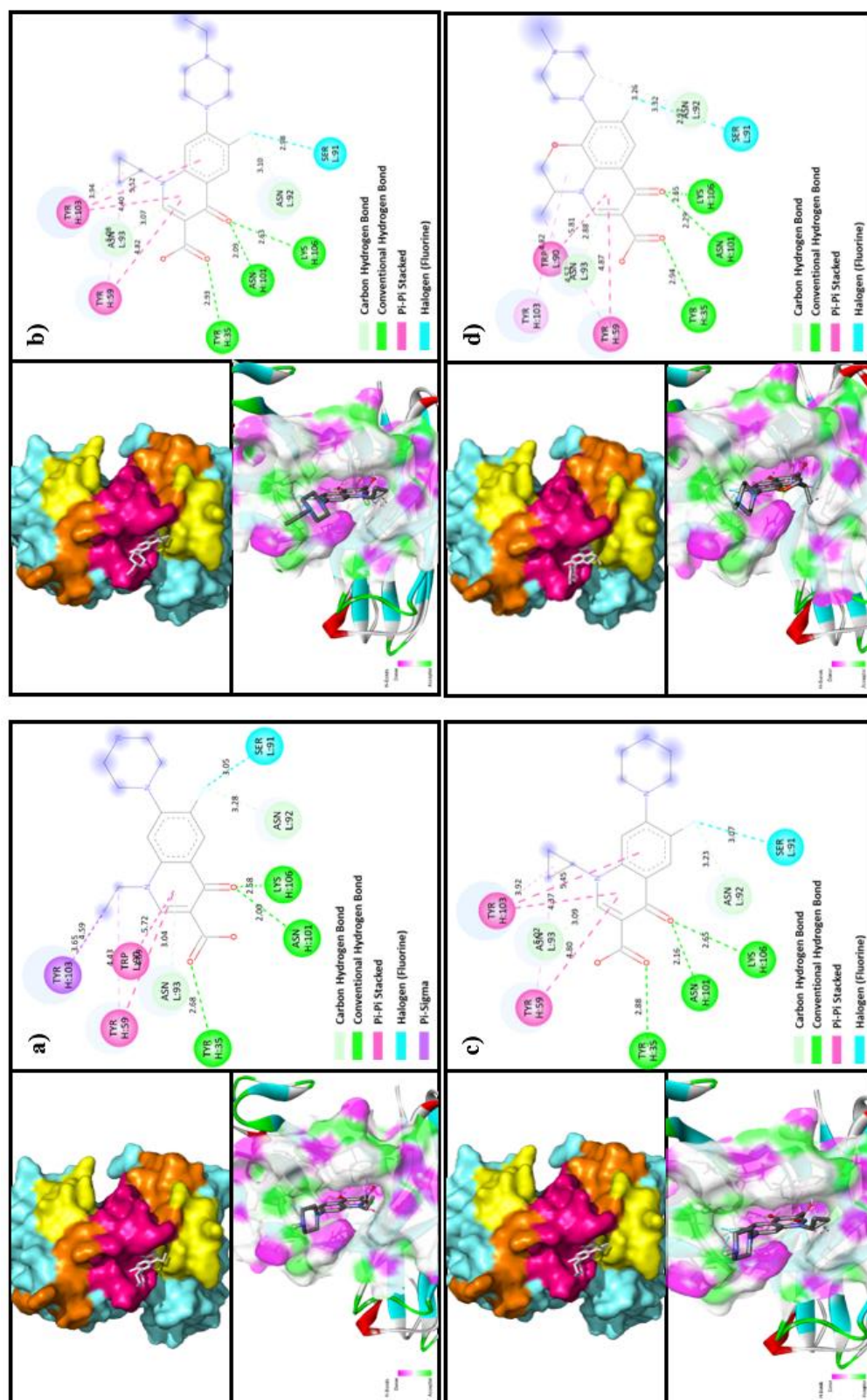
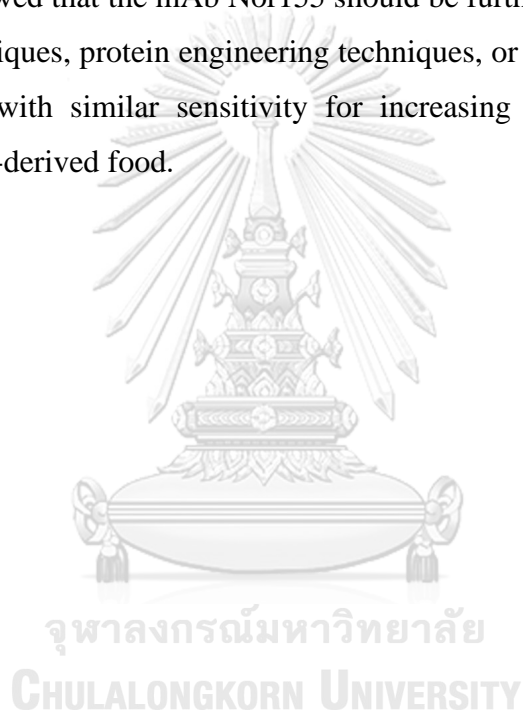


Fig 4.16 Schematic diagram of the binding for mAb Nor155 and a target FQ molecules; a) norfloxacin, b) enrofloxacin, c) ciprofloxacin, and d) ofloxacin.

As for docked pose of ligands with mAb Enro44, the interaction of mAb Enro44 with norfloxacin and ciprofloxacin make conventional hydrogen bond to binding site residues SER (L:8) and GLU (H:42), and carbon hydrogen bond GLY (L:103) which the docked position of both ligands bind outside the area CDRs of mAb Enro44. While enrofloxacin and ofloxacin bind to residues TRP (H:47) and GLY (L:101) as conventional hydrogen bond and carbon hydrogen bond LEU (L:98). The docked conformation of two ligands pose near loop HCDR2 and LCDR3. Nonetheless, hydroxyl moiety of enrofloxacin and ofloxacin structure interact with the same binding residue, the ring parts are pose quit diversely (Figure 4.17). From the Figure 4.17a and 4.17c, the norfloxacin and ciprofloxacin position bonded the other side of CDRs area. In fact, the variable regions ( $V_H$  and  $V_L$ ) will combine with the constant regions. Therefore, the binding couldn't happen since these areas were presumably merged with the constant regions. The interaction of mAb Enro48 and the target FQs showed that when the mAb Enro48 was combined with norfloxacin, GLU (H:65) and ARG (H:40) have conventional hydrogen bond interactions, makes carbon hydrogen bond interactions with GLU (H:46) and LYS (H:61). When the mAb Enro48 was combined with enrofloxacin, which makes single conventional hydrogen bonds to binding site residue SER (L:101), and carbon hydrogen bond with GLU (L:102). The docked conformation of ciprofloxacin, ARG (H:40), GLU (H:65), and GLU (L:102) had conventional hydrogen bond interactions, LYS (H:61) makes carbon hydrogen bond interaction. While conventional hydrogen bonds of ofloxacin bind to ARG (H:40), and carbon hydrogen bond interaction occurred with SER (L:101) and LYS (H:61). Moreover, enrofloxacin and ciprofloxacin make salt bridge to binding site residues GLU (H:46) as Figure 4.18. However, enrofloxacin and ofloxacin ligand pose near the area of CDRs than norfloxacin and ciprofloxacin. In addition, when considering the structure of enrofloxacin and ofloxacin. ofloxacin contain methyl group in piperazine ring like enrofloxacin, and enrofloxacin is the only molecule that has ethyl group in piperazine ring, which is uniquely important for the antibody recognition. Herein, the lowest binding energy ( $\Delta G$ ) and the significant interaction bonds between amino acid residues of mAbs and the target FQ molecules were summarized in Table 4.7.

The blind docking between the mAbs and FQ derivatives shown that mAb Nor155 docking is outstanding. Although mAb Nor155 could bind with the four tested FQs like mAb Nor132, it had stronger binding than mAb Nor132. The FQ drugs posed repeatedly into the CDRs pocket site of mAb Nor155, which oxygen in the carboxylic group and the keto group of drugs could form conventional hydrogen bond with TYR (H:35) of CDR1 and ASN (H:101), LYS (H:106) of CDR3, respectively. Furthermore, fluorine could form halogen bond with SER (L:91) of CDR3 which these bonds probably bind to the main structural areas of FQs group.

The result showed that the mAb Nor155 should be further developed by site direct mutagenesis techniques, protein engineering techniques, or others to get mAb that can bind to all FQs with similar sensitivity for increasing efficiency to detect drug residues in animal-derived food.



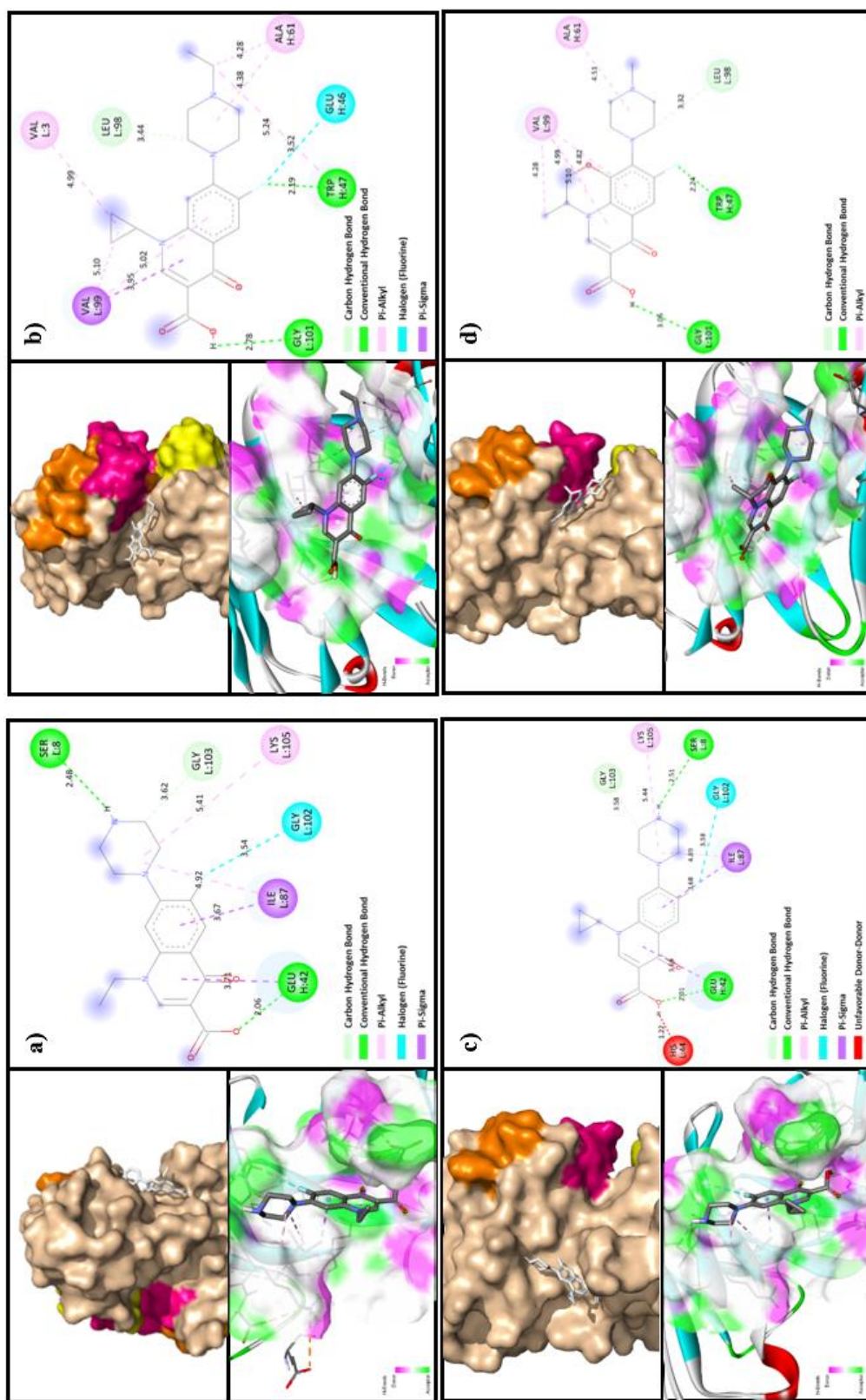


Fig 4.17 Schematic diagram of the binding of mAb Enro44 and a target FQ molecules: a) norfloxacin, b) enrofloxacin, c) ciprofloxacin, and d) ofloxacin.

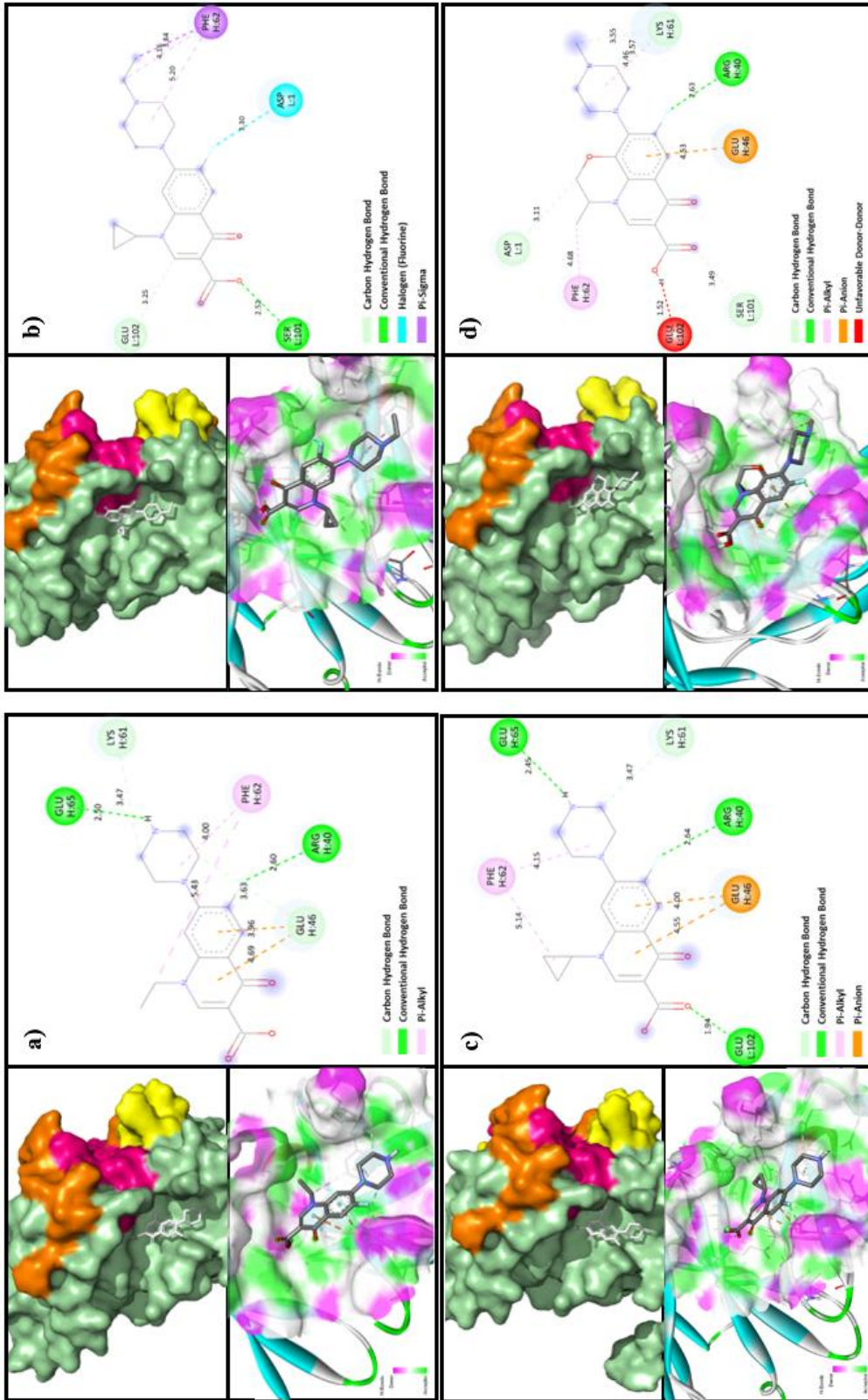


Fig 4.18 Schematic diagram of the binding for mAb Enro48 and a target FQ molecules; a) norfloxacin, b) enrofloxacin, c) ciprofloxacin, and d) ofloxacin.

Table 4.7 Docking scoring function and interaction bonds of mAbs and target fluoroquinolone molecules.

Monoclonal antibody	Ligand	Binding energy ( $\Delta G$ ) (kcal/mol)	Amino acid residue interaction	
			Carbon hydrogen bond	Conventional hydrogen bond
mAb Nor132	Norfloxacin	-7.3	HIS (L:38), ASP (H:100)	-
	Enrofloxacin	-7.5	HIS (L:38), ASP (H:100)	-
	Ciprofloxacin	-7.6	HIS (L:38), ASP (H:100)	-
	Ofloxacin	-7.8	ASP (H:100)	-
mAb Nor155	Norfloxacin	-7.3	ASN (L:92), ASN (L:93)	TYR (H:35), ASN (H:101), LYS (H:106)
	Enrofloxacin	-7.2	ASN (L:92), ASN (L:93)	TYR (H:35), ASN (H:101), LYS (H:106)
	Ciprofloxacin	-7.5	ASN (L:92), ASN (L:93)	TYR (H:35), ASN (H:101), LYS (H:106)
	Ofloxacin	-7.3	ASN (L:92), ASN (L:93)	TYR (H:35), ASN (H:101), LYS (H:106)
mAb Enro44	Norfloxacin	-6.4	SER (L:8), GLU (H:42)	GLY (L:103)
	Enrofloxacin	-6.3	LEU (L:98)	TRP (H:47), GLY (L:101)
	Ciprofloxacin	-6.4	SER (L:8), GLU (H:42)	GLY (L:103)
	Ofloxacin	-6.4	LEU (L:98)	TRP (H:47), GLY (L:101)
mAb Enro48	Norfloxacin	-6.7	GLU (H:46), LYS (H:61)	GLU (H:65), ARG (H:40)
	Enrofloxacin	-7.0	LYS (H:61)	ARG (H:40), GLU (H:65), GLU (L:102)
	Ciprofloxacin	-7.0	GLU (L:102)	SER (L:101)
	Ofloxacin	-6.8	ARG (H:40)	SER (L:101) and LYS (H:61)

## CHAPTER V

### CONCLUSIONS AND SUGGESTION

#### 5.1 Conclusion

Sensitivity, specificity, affinity, and interaction of mAbs to four fluoroquinolones (FQs) including norfloxacin, enrofloxacin, ciprofloxacin and ofloxacin which have closely related chemical structures, were examined by ELISA, SPR, and molecular docking, respectively. Both mAb Nor132 and mAb Nor155 raised against norfloxacin could bind with the four tested antibiotics. However, mAb Nor155 had higher affinity to all FQs than mAb Nor132 did. This could be due to the reason that mAb Nor155 formed conventional hydrogen bond with FQs molecules whereas the bindings of mAb Nor132 with the FQs were without this bond. The binding of mAb Nor155 yielded the highest binding affinity in the pocket between LCDR3 and HCDR3. In case of mAb Enro44 and mAb Enro48 raised against enrofloxacin, these mAbs were highly specific to only enrofloxacin. MAb Enro44 showed the best affinity to enrofloxacin and TRP (H:47) and GLY (L:101) residues were the expected major amino acid sequences of the binding sites. Sensitivity of mAb Nor155 and mAb Nor132 was high enough to generally detect all tested FQs while that of mAb Enro44 and mAb Enro48 was high enough to specifically detect only enrofloxacin at the currently enforced maximum residue limit.

#### 5.2 Suggestions

X-ray crystallography studies should be performed in order to gain more insight and understanding of the affinity binding between the mAbs and the FQs.

Binding of the mAbs with other FQs should be performed to get more information of the major amino acid sequences of the binding sites

## REFERENCES

1. San Martin B, Cornejo J, Iraguen D, Hidalgo H, Anadon A. Depletion study of enrofloxacin and its metabolite ciprofloxacin in edible tissues and feathers of white leghorn hens by liquid chromatography coupled with tandem mass spectrometry. *J Food Prot.* 2007;70(8):1952-7.
2. Yang D, Singh A, Wu H, Kroe-Barrett R. Comparison of biosensor platforms in the evaluation of high affinity antibody-antigen binding kinetics. *Analytical Biochemistry.* 2016;508:78-96.
3. Patel R, Andrien BA, Jr. Kinetic analysis of a monoclonal therapeutic antibody and its single-chain homolog by surface plasmon resonance. *Anal Biochem.* 2010;396(1):59-68.
4. Drescher DG, Selvakumar D, Drescher MJ. Analysis of Protein Interactions by Surface Plasmon Resonance. *Adv Protein Chem Struct Biol.* 2018;110:1-30.
5. Abrigach F, Rokni Y, Takfaoui A, Khoutoul M, Doucet H, Asehraou A, et al. In vitro screening, homology modeling and molecular docking studies of some pyrazole and imidazole derivatives. *Biomedicine & Pharmacotherapy.* 2018;103:653-61.
6. Morris GM, Huey R, Lindstrom W, Sanner MF, Belew RK, Goodsell DS, et al. AutoDock4 and AutoDockTools4: Automated docking with selective receptor flexibility. *Journal of computational chemistry.* 2009;30(16):2785-91.
7. Karthick T, Balachandran V, Perumal S. Spectroscopic investigations, molecular interactions, and molecular docking studies on the potential inhibitor “thiophene-2-carboxylic acid”. *Spectrochimica Acta Part A: Molecular and Biomolecular Spectroscopy.* 2015;141:104-12.
8. Elbegdorj O, Westkaemper RB, Zhang Y. A homology modeling study toward the understanding of three-dimensional structure and putative pharmacological profile of the G-protein coupled receptor GPR55. *Journal of Molecular Graphics and Modelling.* 2013;39:50-60.
9. Uciechowska-Kaczmarzyk U, Chauvot de Beauchene I, Samsonov SA. Docking software performance in protein-glycosaminoglycan systems. *Journal of Molecular Graphics and Modelling.* 2019;90:42-50.



10. Thomsen R, Christensen MH. MolDock: a new technique for high-accuracy molecular docking. *Journal of medicinal chemistry*. 2006;49(11):3315-21.
11. Yu H-W, Halonen MJ, Pepper IL. Chapter 12 - Immunological Methods. In: Pepper IL, Gerba CP, Gentry TJ, editors. *Environmental Microbiology (Third Edition)*. San Diego: Academic Press; 2015. p. 245-69.
12. Yunus G. Chapter 42 - Biosensors: An Enzyme-Based Biophysical Technique for the Detection of Foodborne Pathogens. In: Kuddus M, editor. *Enzymes in Food Biotechnology*: Academic Press; 2019. p. 723-38.
13. Goding JW. 5 - Antibody Structure and Function. In: Goding JW, editor. *Monoclonal Antibodies (Third Edition)*. London: Academic Press; 1996. p. 72-100.
14. Creative Diagnostics. Polyclonal vs. Monoclonal Antibodies 2009 [Available from: <https://www.creative-diagnostics.com/polyclonal-vs-monoclonal-antibodies.htm>].
15. G-BIOSCIENCES. POLYCLONAL ANTIBODY: ADVANTAGE OVER MONOCLONALS 2017, Jan 6 [Available from: <https://info.gbiosciences.com>].
16. Corthell JT. Chapter 5 - Antibodies and Titrations. In: Corthell JT, editor. *Basic Molecular Protocols in Neuroscience: Tips, Tricks, and Pitfalls*. San Diego: Academic Press; 2014. p. 41-6.
17. Goding JW. 7 - Introduction to Monoclonal Antibodies. In: Goding JW, editor. *Monoclonal Antibodies (Third Edition)*. London: Academic Press; 1996. p. 116-40.
18. National Institutes of Health. Fluoroquinolones 2019, July 1 [Available from: <https://livertox.nih.gov/Fluoroquinolones.htm>].
19. Fluoroquinolones. *LiverTox: Clinical and Research Information on Drug-Induced Liver Injury*. Bethesda (MD): National Institute of Diabetes and Digestive and Kidney Diseases; 2012.
20. Ball P, Tillotson G. Tolerability of fluoroquinolone antibiotics. Past, present and future. *Drug safety*. 1995;13(6):343-58.
21. Goldstein EJC. Norfloxacin, a fluoroquinolone antibacterial agent: Classification, mechanism of action, and in vitro activity. *The American Journal of Medicine*. 1987;82(6, Supplement 2):3-17.
22. Moreau R, Elkrief L, Bureau C, Perarnau J-M, Thévenot T, Saliba F, et al. Effects of Long-term Norfloxacin Therapy in Patients With Advanced Cirrhosis.

- Gastroenterology. 2018;155(6):1816-27.e9.
23. Holmes B, Brogden RN, Richards DM. Norfloxacin. *Drugs*. 1985;30(6):482-513.
  24. Papich MG. Enrofloxacin. In: Papich MG, editor. *Saunders Handbook of Veterinary Drugs (Fourth Edition)*. St. Louis: W.B. Saunders; 2016. p. 287-9.
  25. Sherman O, Beizer JL. Possible ciprofloxacin-induced acute cholestatic jaundice. *The Annals of pharmacotherapy*. 1994;28(10):1162-4.
  26. Talan D, Naber K, Palou J, Elkharrat D. Extended-release ciprofloxacin (Cipro XR) for treatment of urinary tract infections. *International journal of antimicrobial agents*. 2004;23 Suppl 1:S54-66.
  27. Jungst G, Mohr R. Side effects of ofloxacin in clinical trials and in postmarketing surveillance. *Drugs*. 1987;34 Suppl 1:144-9.
  28. Blum A. Ofloxacin-induced acute severe hepatitis. *Southern medical journal*. 1991;84(9):1158.
  29. Singh P. Surface plasmon resonance (SPR) based binding studies of refolded single chain antibody fragments. *Biochemistry and Biophysics Reports*. 2018;14:83-8.
  30. Guo X. Surface plasmon resonance based biosensor technique: A review. *Journal of Biophotonics*. 2012;5(7):483-501.
  31. Nguyen HH, Park J, Kang S, Kim M. Surface plasmon resonance: a versatile technique for biosensor applications. *Sensors (Basel, Switzerland)*. 2015;15(5):10481-510.
  32. Pokutta S, Herrenknecht K, Kemler R, Engel J. Conformational changes of the recombinant extracellular domain of E-cadherin upon calcium binding. *Eur J Biochem*. 1994;223(3):1019-26.
  33. Sasahara K, Demura M, Nitta K. Equilibrium and kinetic folding of hen egg-white lysozyme under acidic conditions. *Proteins*. 2002;49(4):472-82.
  34. Litovchick A, Rando RR. Stereospecificity of short Rev-derived peptide interactions with RRE IIB RNA. *RNA*. 2003;9(8):937-48.
  35. Büyükköroğlu G, Dora DD, Özdemir F, Hızal C. Chapter 15 - Techniques for Protein Analysis. In: Barh D, Azevedo V, editors. *Omics Technologies and Bio-Engineering*: Academic Press; 2018. p. 317-51.
  36. Shire SJ. 2 - Analytical tools used in the formulation and assessment of stability of

- monoclonal antibodies (mAbs). In: Shire SJ, editor. *Monoclonal Antibodies*: Woodhead Publishing; 2015. p. 17-44.
37. Davidson B, Fasman GD. The Conformational Transitions of Uncharged Poly-L-lysine.  $\alpha$  Helix-Random Coil- $\beta$  Structure\*. *Biochemistry*. 1967;6(6):1616-29.
  38. Kumagai PS, Araujo APU, Lopes JLS. Going deep into protein secondary structure with synchrotron radiation circular dichroism spectroscopy. *Biophys Rev*. 2017;9(5):517-27.
  39. Tenorio Y, Hernandez-Santoyo A, Altuzar V, Vivanco-Cid H, Mendoza-Barrera C. Protein-Protein and Protein-Ligand Docking. 2013. p. 187.
  40. Huang SY, Zou X. Advances and challenges in protein-ligand docking. *Int J Mol Sci*. 2010;11(8):3016-34.
  41. Sirin S, Apgar JR, Bennett EM, Keating AE. AB-Bind: Antibody binding mutational database for computational affinity predictions. *Protein Sci*. 2016;25(2):393-409.
  42. Pantazes RJ, Maranas CD. MAPs: a database of modular antibody parts for predicting tertiary structures and designing affinity matured antibodies. *BMC Bioinformatics*. 2013;14:168-.
  43. Sela-Culang I, Kunik V, Ofra Y. The structural basis of antibody-antigen recognition. *Front Immunol*. 2013;4:302.
  44. Morris GM, Goodsell DS, Halliday RS, Huey R, Hart WE, Belew RK, et al. Automated docking using a Lamarckian genetic algorithm and an empirical binding free energy function. *Journal of computational chemistry*. 1998;19(14):1639-62.
  45. Goodsell DS, Olson AJ. Automated docking of substrates to proteins by simulated annealing. *Proteins*. 1990;8(3):195-202.
  46. Rarey M, Kramer B, Lengauer T, Klebe G. A fast flexible docking method using an incremental construction algorithm. *J Mol Biol*. 1996;261(3):470-89.
  47. Jones G, Willett P, Glen RC, Leach AR, Taylor R. Development and validation of a genetic algorithm for flexible docking. *J Mol Biol*. 1997;267(3):727-48.
  48. Jones G, Willett P, Glen RC. Molecular recognition of receptor sites using a genetic algorithm with a description of desolvation. *J Mol Biol*. 1995;245(1):43-53.
  49. Abagyan R, Totrov M, Kuznetsov D. ICM—A new method for protein modeling

- and design: Applications to docking and structure prediction from the distorted native conformation. *Journal of computational chemistry*. 1994;15(5):488-506.
50. Bordoli L, Kiefer F, Arnold K, Benkert P, Battey J, Schwede T. Protein structure homology modeling using SWISS-MODEL workspace. *Nature Protocols*. 2009;4(1):1-13.
  51. Arnold K, Bordoli L, Kopp J, Schwede T. The SWISS-MODEL workspace: a web-based environment for protein structure homology modelling. *Bioinformatics*. 2006;22(2):195-201.
  52. Kaever T, Matho MH, Meng X, Crickard L, Schlossman A, Xiang Y, et al. Linear Epitopes in Vaccinia Virus A27 Are Targets of Protective Antibodies Induced by Vaccination against Smallpox. *J Virol*. 2016;90(9):4334-45.
  53. Dyakov YT. Chapter 13 - General and specific aspects of plant and animal immunity. In: Dyakov YT, Dzhavakhiya VG, Korpela T, editors. *Comprehensive and Molecular Phytopathology*. Amsterdam: Elsevier; 2007. p. 351-64.
  54. Kirley TL, Greis KD, Norman AB. Domain unfolding of monoclonal antibody fragments revealed by non-reducing SDS-PAGE. *Biochem Biophys Rep*. 2018;16:138-44.
  55. Becnel Boyd L, Maynard MJ, Morgan-Linnell SK, Horton LB, Sugang R, Hamill RJ, et al. Relationships among Ciprofloxacin, Gatifloxacin, Levofloxacin, and Norfloxacin MICs for Fluoroquinolone-Resistant *Escherichia coli*; Clinical Isolates. *Antimicrobial Agents and Chemotherapy*. 2009;53(1):229.
  56. Higgins P, Fluit AC, Schmitz F. Fluoroquinolones: Structure and Target Sites. *Current drug targets*. 2003;4:181-90.
  57. Wang Z, Zhu Y, Ding S, He F, Beier RC, Li J, et al. Development of a monoclonal antibody-based broad-specificity ELISA for fluoroquinolone antibiotics in foods and molecular modeling studies of cross-reactive compounds. *Anal Chem*. 2007;79(12):4471-83.
  58. Chusri M, Wongphanit P, Palaga T, Puthong S, Sooksai S, Komolpis K. Production and Characterization of a Monoclonal Antibody Against Enrofloxacin. *Journal of microbiology and biotechnology*. 2013;23:69-75.

59. Cooper MA, Williams DH. Kinetic analysis of antibody-antigen interactions at a supported lipid monolayer. *Anal Biochem.* 1999;276(1):36-47.
60. Schasfoort R, Tudos A. *Handbook Of Surface Plasmon Resonance* 2007. 403 p.
61. Hearty S, Leonard P, O'Kennedy R. Measuring antibody-antigen binding kinetics using surface plasmon resonance. *Methods Mol Biol.* 2012;907:411-42.
62. Zhao H, Gorshkova II, Fu GL, Schuck P. A comparison of binding surfaces for SPR biosensing using an antibody-antigen system and affinity distribution analysis. *Methods.* 2013;59(3):328-35.
63. Canziani GA, Klakamp S, Myszka DG. Kinetic screening of antibodies from crude hybridoma samples using Biacore. *Anal Biochem.* 2004;325(2):301-7.
64. Pan M, Li S, Wang J, Sheng W, Wang S. Development and Validation of a Reproducible and Label-Free Surface Plasmon Resonance Immunosensor for Enrofloxacin Detection in Animal-Derived Foods. *Sensors (Basel, Switzerland).* 2017;17(9).
65. Joshi V, Shivach T, Yadav N, Rathore AS. Circular Dichroism Spectroscopy as a Tool for Monitoring Aggregation in Monoclonal Antibody Therapeutics. *Analytical Chemistry.* 2014;86(23):11606-13.
66. Greenfield NJ. Using circular dichroism spectra to estimate protein secondary structure. *Nature protocols.* 2006;1(6):2876-90.
67. Bohm G, Muhr R, Jaenicke R. Quantitative analysis of protein far UV circular dichroism spectra by neural networks. *Protein engineering.* 1992;5(3):191-5.
68. Chelius D, Ruf P, Gruber P, Ploscher M, Liedtke R, Gansberger E, et al. Structural and functional characterization of the trifunctional antibody catumaxomab. *mAbs.* 2010;2(3):309-19.
69. Waterhouse A, Bertoni M, Bienert S, Studer G, Tauriello G, Gumienny R, et al. SWISS-MODEL: homology modelling of protein structures and complexes. *Nucleic Acids Res.* 2018;46(W1):W296-w303.
70. Handoko SD, Ouyang X, Su CT, Kwok CK, Ong YS. QuickVina: accelerating AutoDock Vina using gradient-based heuristics for global optimization. *IEEE/ACM Trans Comput Biol Bioinform.* 2012;9(5):1266-72.
71. Trott O, Olson AJ. AutoDock Vina: improving the speed and accuracy of docking

- with a new scoring function, efficient optimization, and multithreading. *Journal of computational chemistry*. 2010;31(2):455-61.
72. Reverberi R, Reverberi L. Factors affecting the antigen-antibody reaction. *Blood Transfus*. 2007;5(4):227-40.
73. van Oss CJ, Good RJ, Chaudhury MK. Nature of the antigen-antibody interaction. Primary and secondary bonds: optimal conditions for association and dissociation. *J Chromatogr*. 1986;376:111-9.





**APPENDICES**

จุฬาลงกรณ์มหาวิทยาลัย  
**CHULALONGKORN UNIVERSITY**

## APPENDIX A

### Reagents and Buffers

#### 1. Media for hybridoma culture

##### 1.1 Media for hybridoma culture

RPMI 1640 (Roswell Park Memorial Institute)	10.43	g
NaHCO <sub>3</sub>	2	g
L-glutamine	0.1	g
Glucose	2	g
Sodium pyruvate	0.11	g
Distilled water	1000	ml

The medium was sterilized by filter membrane 0.22 µm and stored at 4°C until use.

##### 1.2 Freezing medium (10% v/v DMSO)

Dimethyl sulfoxide (DMSO)	10	ml
RPMI 1640 medium	90	ml

The medium was stored at 4°C until use.

#### 2. Buffer for antibody purification by protein G column

##### 2.1 20 mM sodium phosphate, pH 7.0 (equilibrated buffer)

Na <sub>2</sub> HPO <sub>4</sub> ·12H <sub>2</sub> O	7.16g (dissolved in DDI water 1 L)
NaH <sub>2</sub> PO <sub>4</sub> ·H <sub>2</sub> O	2.76g (dissolved in DDI water 1 L)

Na<sub>2</sub>HPO<sub>4</sub> solution was titrated with NaH<sub>2</sub>PO<sub>4</sub> solution until pH 7.0. The solution was filtered through a 0.2 µm filter membrane and kept at 4 °C until use.

##### 2.2 0.1 M Glycine-HCl buffer, pH 2.7 (eluted buffer)

Glycine	7.5 g
DDI water	1000 ml

Glycine solution was titrated with conc. HCl until pH 2.7. The solution was filtered through a 0.2 µm filter membrane and kept at 4 °C until use.

##### 2.3 1 M Tris-HCl buffer, pH 9.0 (neutralized buffer)

Tris base	121.14 g
DDI water	1000 ml

Tris solution was titrated with conc. HCl until pH 9.0. The solution was



filtered through a 0.2  $\mu\text{m}$  filter membrane and kept at 4  $^{\circ}\text{C}$  until use.

### 3. Buffers and reagents for SDS-PAGE

#### 3.1 10% (w/v) SDS

Sodium dodecyl sulfate (SDS)	10	g
Deionized (DI) water adjusted volume to	100	ml

#### 3.2 10% (w/v) APS

Ammonium persulfate (APS)	1	g
DI water adjusted volume to	10	ml

#### 3.3 1 M Tris-HCl, pH 6.8

Tris base	12.11	g
-----------	-------	---

The reagent was dissolved homogeneously with small volume of DI water and adjusted the pH to 6.8 with 1 N HCl. Then the water was added to reach final volume 100 ml.

#### 3.4 1.5 M Tris-HCl, pH 8.8

Tris base	18.17	g
-----------	-------	---

The reagent was dissolved homogeneously with small volume of DI water and adjusted the pH to 8.8 with 1 N HCl. Then the water was added to reach final volume 100 ml.

#### 3.5 2X Laemmle buffer (SDS-dye) 10 ml

1 M Tris-HCl, pH 6.8	1	ml (final conc. 100 mM)
10% SDS	4	ml (4% v/v)
Glycerol (87%)	2.29	ml (20% v/v)
Bromphenol blue	0.001	g
HPLC water adjusted volume to	10	ml

The solution was stored at -20  $^{\circ}\text{C}$  until use.

#### 3.6 SDS staining dye

2X Laemmli buffer (SDS-dye)	900	$\mu\text{l}$
$\beta$ -mercaptoethanol	100	$\mu\text{l}$

The solution was stored at -20  $^{\circ}\text{C}$  until use.

#### 3.7 10% separating gel (8 ml)

Sterile water	3.436	ml
40% Acrylamide and Bis-acrylamide solution	2	ml

1.5 M Tris-HCl, pH 8.8	2	ml
10% SDS	0.08	ml
10% APS	0.08	ml
TEMED	0.004	ml

### 3.8 5% stacking gel (2 ml)

Sterile water	1.204	ml
40% Acrylamide and Bis-acrylamide solution	0.25	ml
1 M Tris-HCl, pH 6.8	0.504	ml
10% SDS	0.02	ml
10% APS	0.02	ml
TEMED	0.002	ml

### 3.9 5x running buffer for SDS-PAGE

Tris base	15.1	g
Glycine	94	g
SDS	5	g
DI water adjust volume to	1000	ml

For working solution, 1x running buffer was prepared by diluting 100 ml of 5x running buffer to total volume 500 ml using DI water.

### 3.10 Staining solution

Coomassie brilliant blue R-250	2.5	g
Methanol	500	ml
Acetic acid	100	ml
Distilled water adjust volume to	1000	ml

The solution was stored in a dark bottle.

### 3.11 Destaining solution

Destain (30% methanol and 10% acetic acid)		
Methanol	300	ml
Acetic acid	100	ml
DI water adjusted volume to	1000	ml

## 4. Buffers and Reagents for ELISA test kit

### 4.1 0.2 M Phosphate buffer, pH 7.4 (PB stock)

$\text{Na}_2\text{HPO}_4 \cdot 12\text{H}_2\text{O}$	71.63	g (dissolved in DI water 1 L)
--	-------	-------------------------------

$\text{NaH}_2\text{PO}_4 \cdot \text{H}_2\text{O}$  27.60 g (dissolved in DI water 1 L)

$\text{Na}_2\text{HPO}_4$  solution was titrated with  $\text{NaH}_2\text{PO}_4$  solution until pH 7.4. The PB stock solution was mixed and kept at room temperature.

#### 4.2 0.01 M Phosphate buffer saline, pH 7.4 (PBS)

0.2 M Phosphate buffer, pH 7.4	1000	ml
NaCl	175.2	g
DI water adjusted volume to	20	L

#### 4.3 0.05% (v/v) Tween-20 in PBS (PBST; washing buffer)

Tween-20	0.5	ml
PBS	1000	ml

#### 4.4 5% (w/v) skim milk (blocking solution)

Skim milk	5	g
PBS	100	ml

#### 4.5 205 mM potassium citrate buffer, pH 4.0

Citric acid	43.1	g (dissolved in DDI water 1 L)
Potassium citrate	66.5	g (dissolved in DDI water 1 L)

Citric acid solution was titrated with potassium citrate solution until pH 4.0.

The solution was mixed and kept at 4 °C until use.

#### 4.6 TMB substrate solution

3, 3', 5, 5'-Tetramethylbenzidine (TMB)	2.5	mg (dissolved in 250 $\mu\text{l}$ DMF)
205 mM potassium citrate buffer, pH 4.0	10	ml
30% $\text{H}_2\text{O}_2$	3.5	$\mu\text{l}$

#### 4.7 1 M $\text{H}_2\text{SO}_4$ (stop solution)

$\text{H}_2\text{SO}_4$ (95-97%)	102	ml
DI water adjusted volume to	1000	ml

## 5. Buffers and Reagents for SPR

#### 5.1 0.05% (v/v) P20 in PBS (PBS+P20 buffer)

Surfactant P20	0.5	ml
PBS	1000	ml

**5.2 0.05% (v/v) P20 in NaCl (NaCl+P20 buffer)**

Surfactant P20	0.5 ml
NaCl	8.766 g (dissolved in DDI water 1 L)

**5.2 50 mM NaOH (Regeneration buffer)**

NaOH	2 g
DDI water	1000 ml



## APPENDIX B

### 1. Determination of protein concentration of FQ drugs to OVA by BCA protein assay kit

The protein concentrations were calculated from the standard curve of BSA (Figure A.1 and A.2) that was generated from the relation between BSA concentration and the absorbance at 560 nm in Table A.1 and Table A.2.

Table B-1 concentration of standard BSA and absorbance at 560 nm for determination for NOR-OVA and ENRO-OVA concentration

BSA concentration( $\mu\text{g/ml}$ )	Absorbance at 560 nm		
	mean	1	2
0	0.1080	0.1103	0.1057
100	0.2733	0.2701	0.2764
200	0.4632	0.5907	0.3357
400	0.5739	0.7237	0.4240
600	0.8800	0.8861	0.8738
800	1.1536	1.1862	1.1209
1000	1.2715	1.3364	1.2065

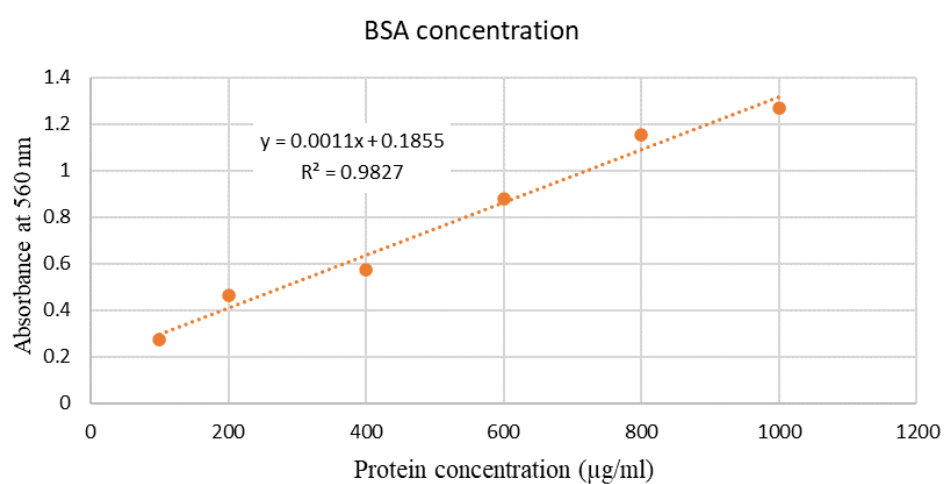


Figure B-1 Standard curve of BSA by BCA protein assay for detection NOR-OVA and ENRO-OVA concentration.

Table B-2 concentration of standard BSA and absorbance at 560 nm for determination for CIPRO-OVA and OFLOX-OVA concentration.

BSA concentration( $\mu\text{g/ml}$ )	Absorbance at 560 nm		
	mean	1	2
0	0.1249	0.1263	0.1234
100	0.2876	0.2798	0.2954
200	0.4665	0.4610	0.4719
400	0.7251	0.6814	0.7687
600	0.9727	0.9821	0.9633
800	1.2054	1.1460	1.2648
1000	1.4228	1.4228	1.4228

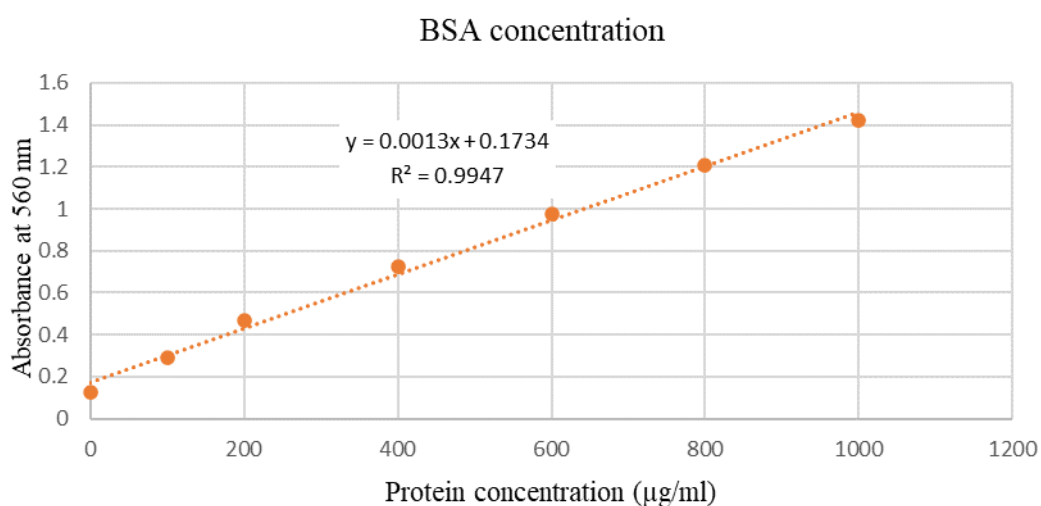


Figure B-2 Standard curve of BSA by BCA protein assay for detection CIPRO-OVA and OFLOX-OVA concentration.

## 2. Determination of Concentration and Molecular Weight of MAbs

Table B-3 concentration and absorbance at 560 nm of BSA standard for the determination of mAbs concentration.

BSA concentration( $\mu\text{g/ml}$ )	Absorbance at 560 nm		
	mean	1	2
0	0.0814	0.0799	0.0828
100	0.2299	0.2270	0.2327
200	0.4449	0.4391	0.4507
400	0.7082	0.6687	0.7477
600	0.9813	0.9780	0.9845
800	1.2492	1.2767	1.2216
1000	1.4311	1.4029	1.4592

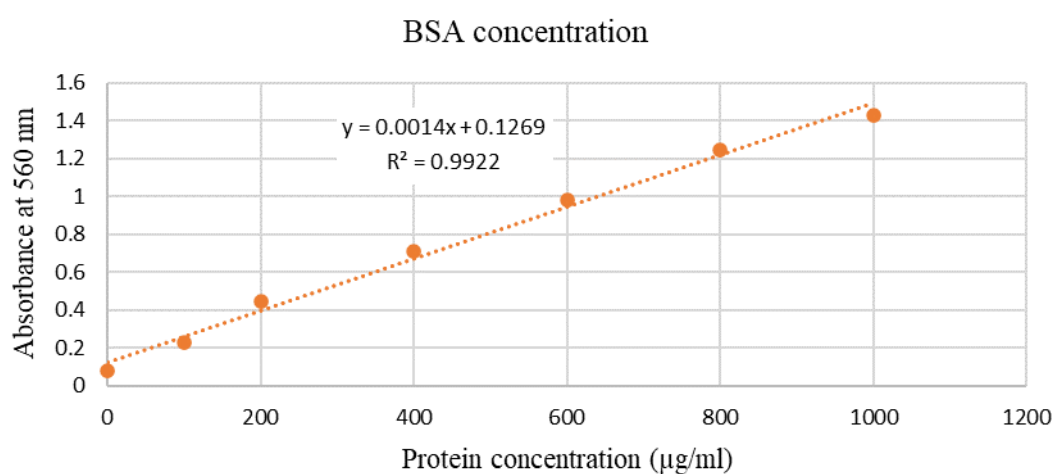


Figure B-3 Standard curve of BSA by BCA protein assay for detection mAbs concentration.

### 3. Grid Boxes used in the thesis

#### Grid box 1

receptor = Nor132VHVL\_H.pdbqt

ligand = norfloxacin\_H.pdbqt

center\_x = 36.519

center\_y = 37.22

center\_z = -4.491

size\_x = 47.25

size\_y = 47.25

size\_z = 47.25

#### Grid box 2

receptor = Nor132VHVL\_H.pdbqt

ligand = Enrofloxacin\_H.pdbqt

center\_x = 36.519

center\_y = 37.22

center\_z = -4.491

size\_x = 47.25

size\_y = 47.25

size\_z = 47.25

#### Grid box 3

receptor = Nor132VHVL\_H.pdbqt

ligand = Ciprofloxacin\_H.pdbqt

center\_x = 36.519

center\_y = 37.22

center\_z = -4.491

size\_x = 47.25

size\_y = 47.25

size\_z = 47.25

#### Grid box 4

receptor = Nor132VHVL\_H.pdbqt

ligand = Ofloxacin\_H.pdbqt

center\_x = 36.519





center\_y = 37.22

center\_z = -4.491

size\_x = 47.25

size\_y = 47.25

size\_z = 47.25

#### **Grid box 5**

receptor = Nor155VHVL\_H.pdbqt

ligand = norfloxacin\_H.pdbqt

center\_x = 37.757

center\_y = 36.377

center\_z = -18.687

size\_x = 32.64

size\_y = 42.432

size\_z = 32.64

#### **Grid box 6**

receptor = Nor155VHVL\_H.pdbqt

ligand = Enrofloxacin\_H.pdbqt

center\_x = 37.757

center\_y = 36.377

center\_z = -18.687

size\_x = 32.64

size\_y = 42.432

size\_z = 32.64

#### **Grid box 7**

receptor = Nor155VHVL\_H.pdbqt

ligand = Ciprofloxacin\_H.pdbqt

center\_x = 37.757

center\_y = 36.377

center\_z = -18.687

size\_x = 32.64

size\_y = 42.432

size\_z = 32.64



จุฬาลงกรณ์มหาวิทยาลัย  
CHULALONGKORN UNIVERSITY

**Grid box 8**

receptor = Nor155VHVL\_H.pdbqt

ligand = Ofloxacin\_H.pdbqt

center\_x = 37.757

center\_y = 36.377

center\_z = -18.687

size\_x = 32.64

size\_y = 42.432

size\_z = 32.64

**Grid box 9**

receptor = Enro44VHVL\_H.pdbqt

ligand = norfloxacin\_H.pdbqt

center\_x = 36.519

center\_y = 37.22

center\_z = -4.491

size\_x = 47.25

size\_y = 47.25

size\_z = 47.25

**Grid box 10**

receptor = Enro44VHVL\_H.pdbqt

ligand = Enrofloxacin\_H.pdbqt

center\_x = 37.757

center\_y = 36.377

center\_z = -18.687

size\_x = 32.64

size\_y = 42.432

size\_z = 32.64

**Grid box 11**

receptor = Enro44VHVL\_H.pdbqt

ligand = Ciprofloxacin\_H.pdbqt

center\_x = 37.757

center\_y = 36.377



center\_z = -18.687

size\_x = 32.64

size\_y = 42.432

size\_z = 32.64

### **Grid box 12**

receptor = Enro44VHVL\_H.pdbqt

ligand = Ofloxacin\_H.pdbqt

center\_x = 37.757

center\_y = 36.377

center\_z = -18.687

size\_x = 32.64

size\_y = 42.432

size\_z = 32.64

### **Grid box 9**

receptor = Enro48VHVL\_H.pdbqt

ligand = norfloxacin\_H.pdbqt

center\_x = 36.519

center\_y = 37.22

center\_z = -4.491

size\_x = 47.25

size\_y = 47.25

size\_z = 47.25



จุฬาลงกรณ์มหาวิทยาลัย  
CHULALONGKORN UNIVERSITY

### **Grid box 10**

receptor = Enro48VHVL\_H.pdbqt

ligand = Enrofloxacin\_H.pdbqt

center\_x = 37.757

center\_y = 36.377

center\_z = -18.687

size\_x = 32.64

size\_y = 42.432

size\_z = 32.64

**Grid box 11**

receptor = Enro48VHVL\_H.pdbqt

ligand = Ciprofloxacin\_H.pdbqt

center\_x = 37.757

center\_y = 36.377

center\_z = -18.687

size\_x = 32.64

size\_y = 42.432

size\_z = 32.64

**Grid box 12**

receptor = Enro48VHVL\_H.pdbqt

ligand = Ofloxacin\_H.pdbqt

center\_x = 37.757

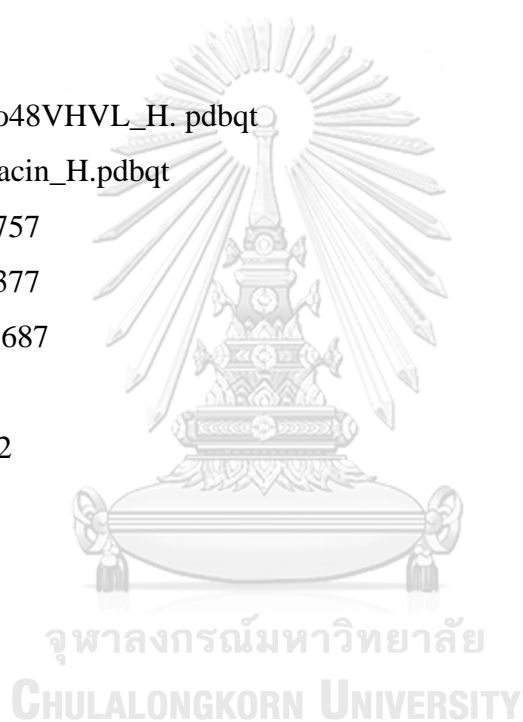
center\_y = 36.377

center\_z = -18.687

size\_x = 32.64

size\_y = 42.432

size\_z = 32.64



**VITA**

<b>NAME</b>	Patamalai Boonserm
<b>DATE OF BIRTH</b>	28 February 1995
<b>PLACE OF BIRTH</b>	Phra Nakhon Si Ayutthaya
<b>INSTITUTIONS ATTENDED</b>	Program in Biotechnology, Faculty of Science, Chulalongkorn University
<b>PUBLICATION</b>	Kinetics of Binding Interaction between Norfloxacin and Monoclonal Antibody Using Surface Plasmon Resonance
<b>AWARD RECEIVED</b>	best oral presentation award



จุฬาลงกรณ์มหาวิทยาลัย  
CHULALONGKORN UNIVERSITY